



Plains CO₂ Reduction (PCOR) Partnership
Energy & Environmental Research Center (EERC)

BELL CREEK TEST SITE – SIMULATION REPORT

Plains CO₂ Reduction (PCOR) Partnership Phase III Task 9 – Deliverable D66, Update 3

Originally Submitted: August 2011; Update 1 Submitted: August 2012; Update 2 Submitted: August 2013

Prepared for:

William Aljoe

National Energy Technology Laboratory
U.S. Department of Energy
626 Cochran Mill Road
PO Box 10940
Pittsburgh, PA 15236-0940

DOE Cooperative Agreement No. DE-FC26-05NT42592

The information and results presented within this annually updated report represent work performed by the EERC as part of the PCOR Partnership Program. The content represents the authors' views and interpretations at the time the report was written. However, in keeping with the EERC's adaptive management approach, the geologic model and simulations are iteratively updated as new information becomes available. As a result, future versions of Deliverable D66 may contain new data and interpretations that may supersede the information within this report.

Prepared by:

Guoxiang Liu
Jason R. Braunberger
Hui Pu
Panqing Gao
Charles D. Gorecki
Jun Ge
Robert C.L. Klenner
Terry P. Bailey
Neil W. Dotzenrod
Nicholas W. Bosshart
Scott C. Ayash
John A. Hamling
Edward N. Steadman
John A. Harju

Energy & Environmental Research Center
University of North Dakota
15 North 23rd Street, Stop 9018
Grand Forks, ND 58202-9018

2018-EERC-05-08

August 2014
Approved

EERC DISCLAIMER

LEGAL NOTICE This research report was prepared by the Energy & Environmental Research Center (EERC), an agency of the University of North Dakota, as an account of work sponsored by the U.S. Department of Energy (DOE) National Energy Technology Laboratory (NETL). Because of the research nature of the work performed, neither the EERC nor any of its employees makes any warranty, express or implied, or assumes any legal liability or responsibility for the accuracy, completeness, or usefulness of any information, apparatus, product, or process disclosed or represents that its use would not infringe privately owned rights. Reference herein to any specific commercial product, process, or service by trade name, trademark, manufacturer, or otherwise does not necessarily constitute or imply its endorsement or recommendation by the EERC.

ACKNOWLEDGMENTS

This work was performed under the DOE NETL Cooperative Agreement No. DE-FC26-05NT42592. The EERC would like to thank Denbury Resources Inc. (Denbury) for providing necessary data to perform this work. Special thanks go to the members of Denbury's Bell Creek team for their valuable input and fruitful discussions.

DOE DISCLAIMER

This report was prepared as an account of work sponsored by an agency of the United States Government. Neither the United States Government, nor any agency thereof, nor any of their employees, makes any warranty, express or implied, or assumes any legal liability or responsibility for the accuracy, completeness, or usefulness of any information, apparatus, product, or process disclosed, or represents that its use would not infringe privately owned rights. Reference herein to any specific commercial product, process, or service by trade name, trademark, manufacturer, or otherwise does not necessarily constitute or imply its endorsement, recommendation, or favoring by the United States Government or any agency thereof. The views and opinions of authors expressed herein do not necessarily state or reflect those of the United States Government or any agency thereof.

TABLE OF CONTENTS

| | |
|--|------------|
| LIST OF FIGURES | ii |
| LIST OF TABLES | iv |
| EXECUTIVE SUMMARY | v |
| INTRODUCTION | 1 |
| PURPOSE..... | 5 |
| BACKGROUND | 6 |
| SCOPE OF WORK..... | 7 |
| 3-D Geologic Modeling | 8 |
| PNL Model and Updated Structural Framework..... | 8 |
| Reference Model..... | 10 |
| Reservoir Simulation..... | 11 |
| Phase 1 Area Reservoir Simulation | 12 |
| Phase 2 Area Reservoir Simulation | 19 |
| SUMMARY | 32 |
| LIMITATIONS..... | 33 |
| ONGOING WORK..... | 34 |
| V3 3-D Geologic Model..... | 34 |
| Fluid Model and Reservoir Simulation | 34 |
| EOS and Relative Permeability Curves | 34 |
| History Matching of CO ₂ Flood..... | 35 |
| Integrated History Matching of Phases 1 and 2..... | 35 |
| 3-D Mechanical Earth Model..... | 35 |
| CONCLUSIONS | 36 |
| REFERENCES | 36 |
| RESERVOIR SIMULATION RESULTS: PHASE 1 | Appendix A |
| RESERVOIR SIMULATION RESULTS: PHASE 2 | Appendix B |

LIST OF FIGURES

| | | |
|----|---|----|
| 1 | Map depicting the location of the Bell Creek oil field in relation to the PRB and the completed pipeline route to the site from the Lost Cabin gas plant..... | 2 |
| 2 | Local stratigraphy of the Bell Creek development area..... | 3 |
| 3 | Study area of the Bell Creek oil field showing the nine phases of scheduled injection..... | 4 |
| 4 | Project elements of the Bell Creek CO ₂ storage and EOR project | 5 |
| 5 | Map of wells showing where baseline and monitor pass PNLs were collected in relation to the Bell Creek oil field..... | 9 |
| 6 | Injection well: reference track, gamma ray log, resistivity log, CO ₂ saturation, oil saturation, water saturation, facies, perforations, effective porosity, shale volume, and horizontal permeability | 10 |
| 7 | Production well: reference track, gamma ray log, resistivity log, CO ₂ saturation, oil saturation, water saturation, facies, perforations, effective porosity, shale volume, and horizontal permeability | 11 |
| 8 | Zoomed-in image of wells in the Phase 1 area..... | 13 |
| 9 | Incremental oil recovery vs. time for Cases 1–5 in the Phase 1 area | 15 |
| 10 | Incremental oil recovery vs. HCPVI for Cases 1–5 in the Phase 1 area | 15 |
| 11 | Oil rate for all cases in the Phase 2 area..... | 16 |
| 12 | Cumulative CO ₂ utilization factors for all cases in the Phase 1 area | 16 |
| 13 | Actual injected CO ₂ volume as a percentage of proposed CO ₂ injection for Phase 1 | 17 |
| 14 | Comparison of cumulative equivalent volume injection in the Phase 1 area..... | 18 |
| 15 | Gas/water ratio for WAG cases in the Phase 1 area..... | 18 |
| 16 | Stored CO ₂ for all scenarios in the Phase 1 area | 19 |
| 17 | Map showing geologic model boundary, dynamic model boundary, and their relation to the planned Bell Creek project development phases | 20 |

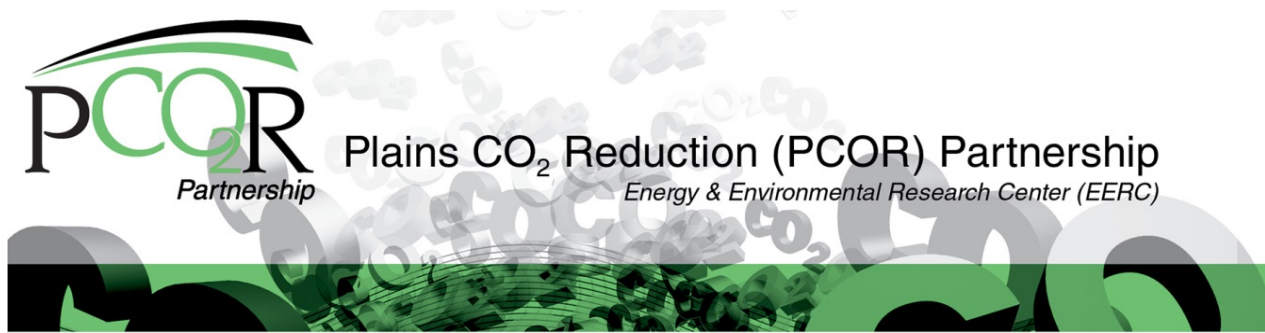
Continued. . .

LIST OF FIGURES (continued)

| | | |
|----|--|----|
| 18 | History-matching results for field oil production rate, where the circles represent the field data and the solid line represents the simulation results..... | 21 |
| 19 | History-matching results for simulated and actual water cut of the field, where the circles represent the field data and the solid line represents the simulation results..... | 21 |
| 20 | History-matching results for field gas production rate, where the circles represent the field data and the solid line represents the simulation results..... | 22 |
| 21 | Average reservoir pressure over the reservoir's history, where the circles represent the field data and the solid line represents the simulation results..... | 22 |
| 22 | Map showing the dynamic model outline of the Phase 2 area | 24 |
| 23 | Potential barrier between Wells 33-15 and 33-16 in the Phase 2 area | 25 |
| 24 | Incremental oil recovery vs. time for Cases 1–5 in the Phase 2 area | 27 |
| 25 | Incremental oil recovery vs. HCPVI for Cases 1–5 in the Phase 2 area | 27 |
| 26 | Oil rates for all cases in the Phase 2 area | 28 |
| 27 | Cumulative CO ₂ utilization factors in the Phase 2 area | 28 |
| 28 | Actual injected CO ₂ volume as a percentage of proposed CO ₂ injection for Phase 2 | 29 |
| 29 | Comparison of cumulative equivalent volume injection in the Phase 2 area..... | 29 |
| 30 | CO ₂ /water injectivity ratio for two WAG cases in the Phase 2 area..... | 30 |
| 31 | Stored CO ₂ for all scenarios in the Phase 2 area | 30 |

LIST OF TABLES

| | | |
|---|--|----|
| 1 | Simulation Parameters for Each Investigatory Case in the Phase 1 Area | 13 |
| 2 | Simulation Results for CO ₂ Stored and Produced and Injected Water and CO ₂ for 6 HCPVI in the Phase 1 Area..... | 14 |
| 3 | Simulation Results for Produced Hydrocarbons and Flood Performance for 6 HCPVI in the Phase 1 Area..... | 14 |
| 4 | CO ₂ Breakthrough for Each Investigatory Case in the Phase 1 Area | 14 |
| 5 | Simulation Parameters for Each Investigatory Case in the Phase 2 Area | 26 |
| 6 | Simulation Results for CO ₂ Stored and Produced and Injected Water and CO ₂ for 6 HCPVI in the Phase 2 Area | 26 |
| 7 | Simulation Results for Produced Hydrocarbons and Flood Performance for 6 HCPVI in the Phase 2 Area | 26 |
| 8 | CO ₂ Breakthrough for Each Investigatory Case in the Phase 2 Area..... | 26 |



BELL CREEK TEST SITE – SIMULATION REPORT

EXECUTIVE SUMMARY

The Plains CO₂ Reduction (PCOR) Partnership is working with Denbury Resources Inc. (Denbury) to evaluate the effectiveness of large-scale injection of carbon dioxide (CO₂) into the Bell Creek oil field for CO₂ enhanced oil recovery (EOR) and to study long-term associated CO₂ storage. Discovered in 1967, the Bell Creek oil field in southeastern Montana has undergone primary production (solution gas drive), waterflooding, and two micellar–polymer pilot tests. Approximately 37.7% of the estimated 353 million barrels (MMbbl) of original oil in place has been produced to date, and it is anticipated that 40–50 MMbbl of additional oil will be produced through CO₂ EOR in this field.

With the goal of providing a comprehensive assessment of associated CO₂ storage behavior, the PCOR Partnership has initiated a modeling and numerical simulation effort as part of its adaptive management approach to program development. The modeling and simulation program includes 1) characterizing and modeling the study area using advanced geologic modeling workflows; 2) developing a robust pressure, volume, and temperature model to predict the miscibility behavior of the CO₂–Bell Creek crude system and to aid in compositional simulation; 3) history-matching the constructed dynamic reservoir models; and 4) running predictive simulations to aid in monitoring long-term behavior of injected CO₂.

This report encompasses the modeling and simulation work completed since the August 2013 Bell Creek Simulation report and includes 1) the incorporation of 33 baseline and seven repeat pulsed-neutron logs (PNLs) to improve the static and dynamic geocellular models, 2) history-matching and predictive simulations of the Phase 2 area of the Bell Creek Field, and 3) additional predictive simulations of the Phase 1 area of the Bell Creek Field.

In order to better evaluate different injection scenarios, five simulation cases for both Phases 1 and 2 (ten cases total) were performed to evaluate water alternating gas (WAG) and continuous CO₂ injection (CCI) at two injection bottomhole pressure constraints and varying WAG cycle lengths. The results indicate that WAG is more effective at yielding a faster oil recovery and better sweep efficiency than CCI in Phase 1 and Phase 2, while CCI results in more CO₂ being stored.

The estimated associated CO₂ storage potential varied from 3.37 million tons (Mt) of CO₂ with 6 hydrocarbon pore volumes (HCPVs) of CCI to 1.68 Mt of CO₂ with 6 HCPV (3 HCPV of CO₂) of WAG injection in Phase 1. In Phase 2, the estimated associated CO₂ storage potential varied from 3.21 Mt of CO₂ with CCI to 2.11 Mt for WAG injection. The CO₂ utilization factor ranged from 2.60 to 8.75 thousand standard cubic feet (Mscf)/bbl in Phase 1 and varies from 4.85 to 7.53 Mscf/bbl in Phase 2, depending on the scenario (Table ES-1).

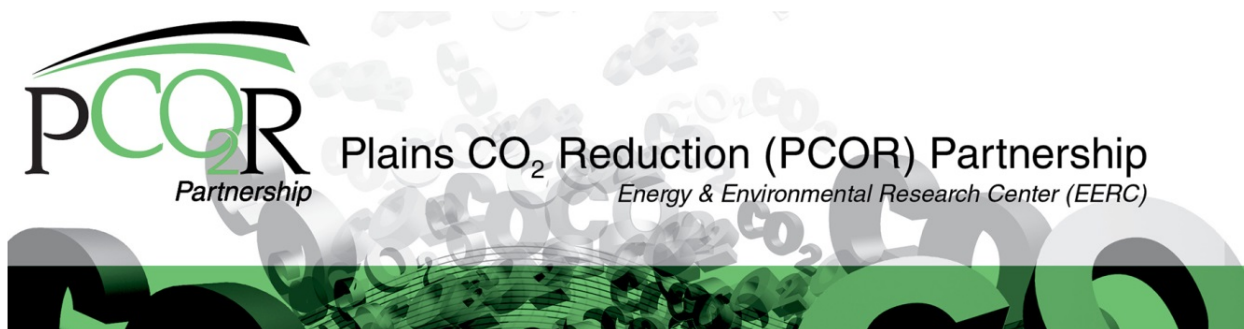
For the Phase 1 area, the earliest CO₂ breakthrough at a production well during simulation occurred 2 months after the start of CO₂ injection for the continuous CO₂ flooding scenario, while the earliest CO₂ breakthrough for WAG occurred after 2.5 months. The simulation results also indicated that the injected CO₂ in this phase is expected to reach Observation Well 05-06 OW about 6 months after injection for both scenarios. In Phase 2, the earliest CO₂ breakthrough at a production well occurred after about 4 months after the start of CO₂ injection for the continuous CO₂ flooding scenario, increasing to 5 months for WAG cases.

Ongoing modeling and simulation work in the Bell Creek oil field includes refining the Version 3 geocellular model using newly acquired 3-D seismic data, additional repeat PNLs, and log and core data. The Version 3 model will be integrated with a comprehensive reference model for geomechanical modeling, as well as Phases 1 and 2 combined simulations, to improve the understanding of long-term storage of CO₂ associated with EOR in the Bell Creek Field. Moreover, relative permeability curves are being revised using special core analysis conducted by Core Labs. These results will be incorporated into the next iteration of the simulation activities to finely tune CO₂ EOR efficiency. Finally, recent data recorded from the ongoing CO₂ flooding in the Bell Creek oil field will be matched to the dynamic simulation results.

Table ES-1. Phases 1 and 2 CO₂ Storage and Utilization Factor Results for All Cases

| Case No. | Flood Type | Injector Pressure, psi | Producer Pressure, psi | Phase 1 | Phase 1 | Phase 2 | Phase 2 Utilization Factor, Mscf/bbl |
|----------------|------------|------------------------|------------------------|-----------------------------|------------------------------|-----------------------------|--------------------------------------|
| | | | | Stored CO ₂ , Mt | Utilization Factor, Mscf/bbl | Stored CO ₂ , Mt | |
| 1 (hysteresis) | WAG | 2700 | 2300 | 2.24 | 5.01 | 2.15 | 5.17 |
| 2 | WAG | 2700 | 2300 | 1.77 | 3.09 | 2.11 | 4.85 |
| 3 | WAG | 2900 | 2300 | 1.68 | 2.60 | 2.22 | 4.96 |
| 4 | CCI | 2700 | 2300 | 3.37 | 8.75 | 3.21 | 7.53 |
| 5 | CCI | 2900 | 2300 | 3.18 | 8.05 | 3.18 | 7.51 |

The information and results presented within this annually updated report represent work performed by the EERC as part of the PCOR Partnership Program. The content represents the authors' views and interpretations at the time the report was written. However, in keeping with the EERC's adaptive management approach, the geologic model and simulations are iteratively updated as new information becomes available. As a result, future versions of Deliverable D66 may contain new data and interpretations that may supersede the information within this report.



BELL CREEK TEST SITE – SIMULATION REPORT

INTRODUCTION

The Plains CO₂ Reduction (PCOR) Partnership, led by the Energy & Environmental Research Center (EERC), is working with Denbury Resources Inc. (Denbury) to determine the effect of large-scale injection of carbon dioxide (CO₂) into a deep clastic reservoir for the purpose of CO₂ enhanced oil recovery (EOR) and to monitor associated CO₂ storage at the Bell Creek oil field, which is operated by Denbury Onshore LLC. A technical team that includes Denbury, the EERC, and others will conduct a variety of activities to determine the baseline reservoir characteristics, including predictive simulations of CO₂ injection. This will facilitate assessment of various potential injection schemes, guide monitoring strategies, and determine the ultimate fate of injected CO₂. Denbury will carry out the injection and production operations, while the EERC will provide support for site characterization, modeling and simulation, and risk assessment and will aid in the development of the monitoring, verification, and accounting (MVA) plan to address key technical subsurface risks (Gorecki and others, 2012).

The Bell Creek oil field in southeastern Montana is a subnormally pressured reservoir with significant hydrocarbon charge that lies near the northeastern boundary of the Powder River Basin (PRB) (Figure 1). Exploration and production activities for mineral and energy resources in the area over the last 55 years have yielded a significant amount of information about the geology of southeastern Montana and the northern PRB, which has been cataloged in a literature review. Decades of oil and gas production through primary and secondary recovery (waterflood and polymer flood pilot tests) have resulted in reservoir decline and have led to the planned implementation of a CO₂ injection-based tertiary oil recovery project. CO₂ is being delivered to the site via the 232-mile Greencore Pipeline from the ConocoPhillips Lost Cabin natural gas-processing plant and from Exxon Mobil's Shute Creek gas-processing plant in LaBarge, Wyoming, via a tie-in to the Greencore Pipeline (Figure 1). Currently, around 50 million standard cubic feet (MMscf) of CO₂ a day is delivered to the field for CO₂ operations.

CO₂ is being injected into the oil-bearing sandstone reservoir in the Lower Cretaceous Muddy (Newcastle) Formation at a depth of approximately 4500 feet (1372 meters) (Figure 2). Nine stages of injection are scheduled to occur across the field (Figure 3). It is expected that the reservoir is suitable for miscible flooding conditions, with an incremental oil production target of 40–50 million barrels (MMbbl). The activities at the Bell Creek oil field will inject an estimated 1 million tons (Mt) of purchased CO₂ annually, much of which will be permanently stored at the end of the EOR project.

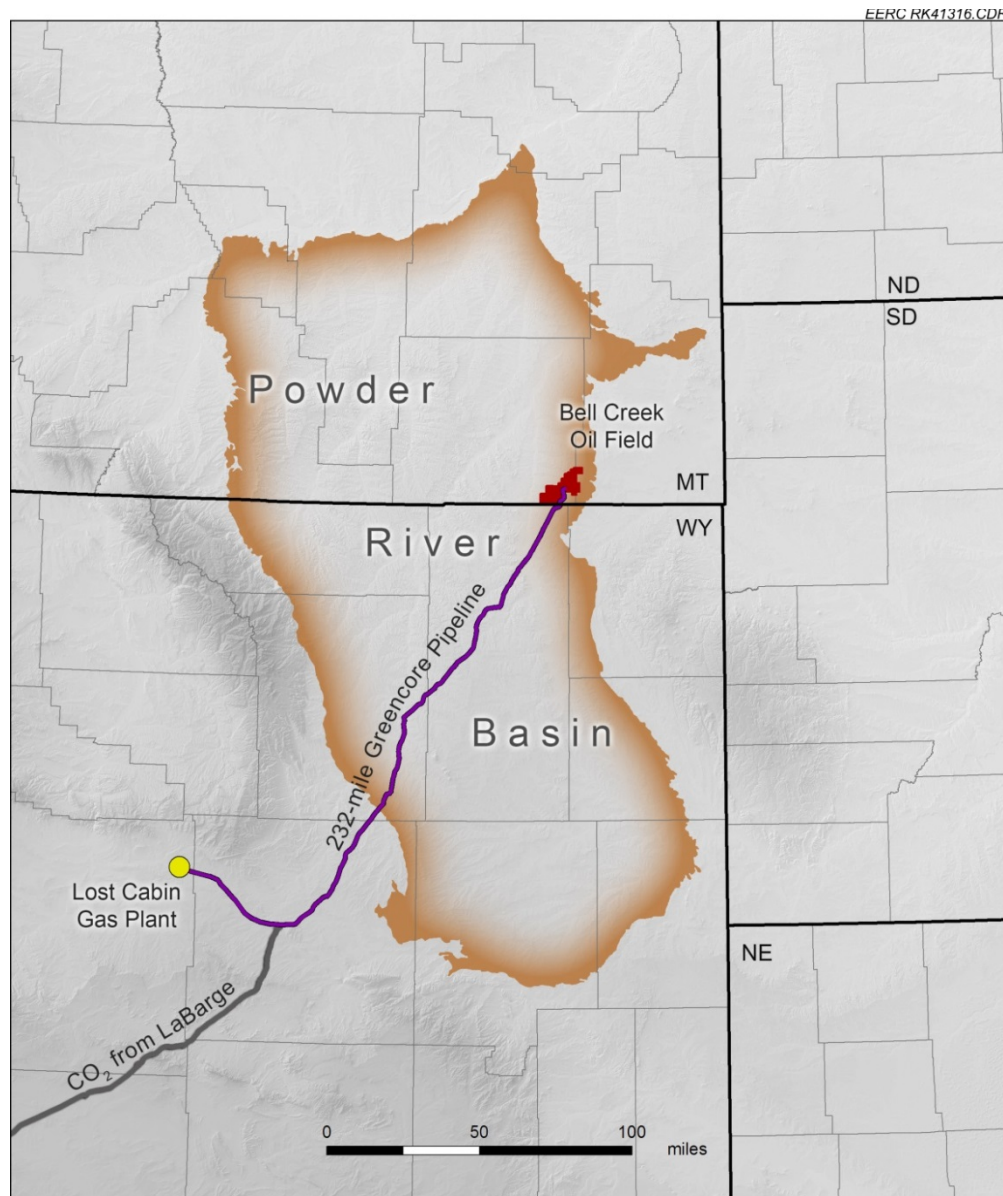


Figure 1. Map depicting the location of the Bell Creek oil field in relation to the PRB and the completed pipeline route to the site from the Lost Cabin gas plant.

Within the Bell Creek oil field, the Muddy Formation is dominated by high-porosity (25%–35%), high-permeability (150–1175 mD) sandstones deposited in a nearshore marine environment (Saini and others, 2012). The initial reservoir pressure was approximately 1200 psi, which is significantly lower than the regional hydrostatic pressure regime (2100 psi at 4500 feet). The oil field is located structurally on a shallow monocline with a 1°–2° dip to the northwest and with an axis trending southwest to northeast for a distance of approximately 20 miles. Stratigraphically, the Muddy Formation in the Bell Creek oil field features an updip sand facies pinchout into shale facies serving as a trap. The barrier bar sand bodies of the Muddy Formation

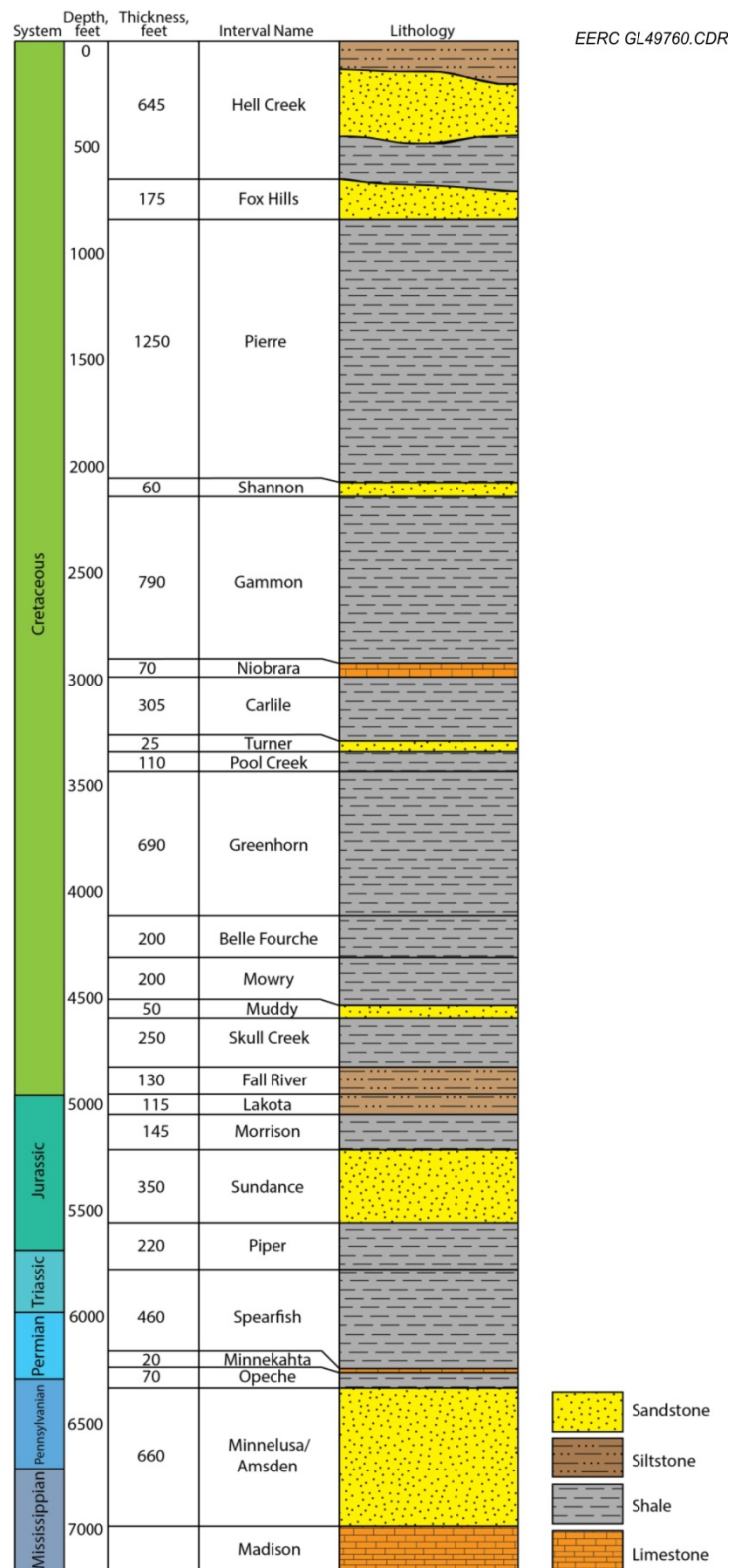


Figure 2. Local stratigraphy of the Bell Creek development area. Structural tops have been updated using pulsed-neutron log (PNL) data from the Hell Creek Formation down to the base of the Muddy Formation.

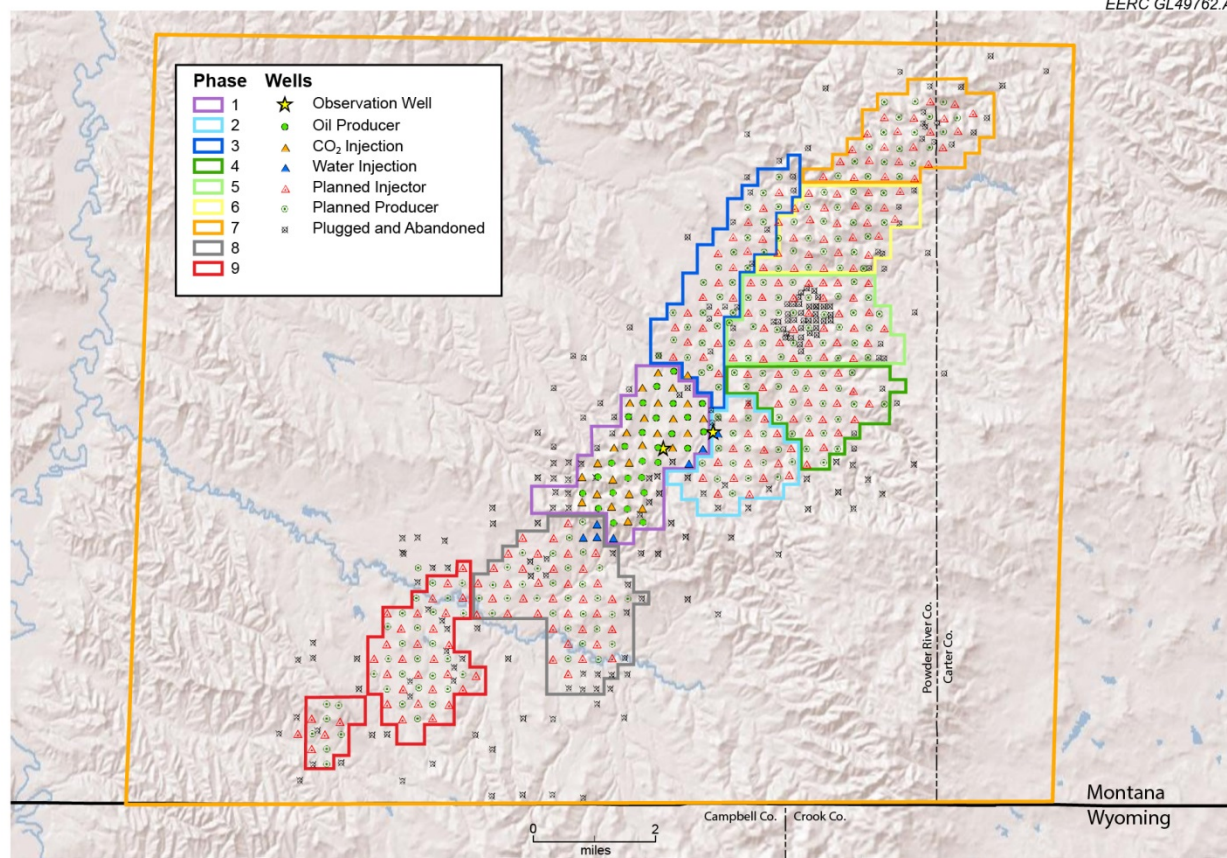


Figure 3. Study area of the Bell Creek oil field showing the nine phases of scheduled injection.

strike southwest to northeast and lie on a regional structural high, which represents a local paleodrainage deposition. A deltaic siltstone overlaps the sandstone on an erosional barrier bar surface and, finally, is partially dissected and somewhat compartmentalized by intersecting shale-filled, incisive erosional channels.

The overlying Lower Cretaceous Mowry Formation provides the primary seal, preventing fluid migration to overlying aquifers and to the surface. On top of the Mowry Formation are several thousand feet of low-permeability formations, including the Belle Fourche, Greenhorn, Niobrara, and Pierre Formation, which will provide redundant layers of protection in the unlikely event that the primary seal fails to prevent upward fluid migration fieldwide (Figure 2).

To facilitate these activities, a detailed static geologic model (Version [V] 2 model) was constructed by representing a 200-square-mile study area centered on Phase 1 as reported in Deliverable (D) 66 PCOR Partnership Phase III Task 9, Update 2, 2013. The simulation activities during this reporting period were mostly focused on the Phases 1 and 2 areas for history-matching production/injection and pressure records and various predictive simulations. The simulation work will provide valuable data to support the design and implementation of a monitoring program to track the injected CO₂ in the Bell Creek Field.

PURPOSE

The PCOR Partnership is developing an adaptive management approach for large-scale CO₂ storage projects consisting of four main components: site characterization; modeling and simulation; risk assessment; and MVA. Each component is continually evaluated and updated throughout the lifetime of a project. The results of each evaluation then serve as input for the remaining components (Figure 1). This iterative cycle is repeated throughout all project phases, from feasibility study through postclosure monitoring. The PCOR Partnership's adaptive management approach allows the site-specific nature of any carbon capture and storage project to be taken into account and creates a dynamic environment where monitoring strategies, for example, can be adjusted to an evolving risk and operational profile. Thus the MVA techniques deployed will always target relevant technical risks and ensure that the most cost-effective, technically viable, site-specific strategies will be used throughout the life of a project. This integrated process will be refined through each incremental stage of the project, from initial planning, to injection, and through postclosure.

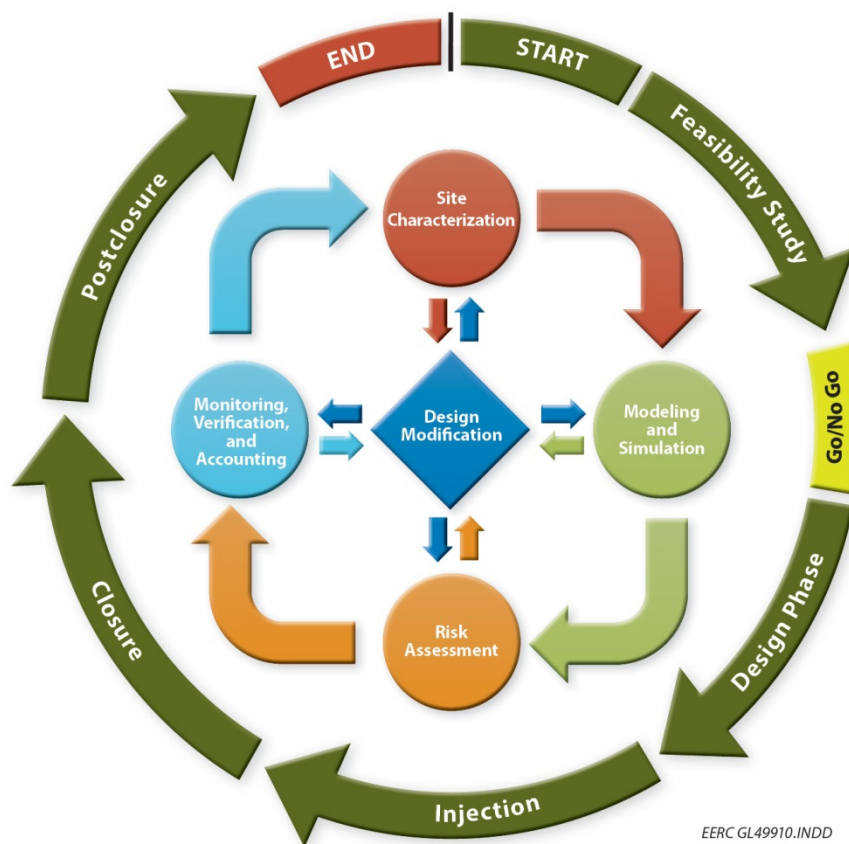


Figure 4. Project elements of the Bell Creek CO₂ storage and EOR project. Each of these elements feeds into another, iteratively improving results and efficiency of evaluation (modified from Gorecki and others, 2012).

The EERC's geologic modeling of the subsurface assists in understanding and predicting the behavior of the injected CO₂ and reservoir fluids over the injection and postinjection period. To aid in the validation of the reservoir model, history matching is performed on a numerically tuned dynamic reservoir model that is constructed using a completed 3-D static geologic model. This is followed by simulation work, which is a valuable tool for assessing scenarios of fluid migration within the reservoir and the potential for out-of-zone fluid migration. Additionally, simulation activities provide a means to evaluate the sweep and storage efficiency and the applicability of various monitoring activities related to both associated CO₂ storage and CO₂ EOR in different scenarios.

Performing geologic characterization, geocellular modeling, and numerical simulation is essential input for risk identification and to guide MVA. This approach lays the foundation for a project-specific, risk-based, goal-oriented MVA plan. The goal of the MVA plan is to effectively monitor the behavior of the injected CO₂ and reservoir fluids in the subsurface throughout the project life. Predictive simulations allow for targeted deployment of MVA data acquisitions at optimal geographic locations and time intervals to maximize the knowledge gained and minimize expenditures. The results and experience gained at the Bell Creek oil field will provide insight and knowledge that can be directly and readily applied to similar projects within the PCOR Partnership region and throughout the world (Steadman and others, 2011; Hamling and others, 2013).

BACKGROUND

Following the adaptive management philosophy developed by the PCOR Partnership (Figure 4), modeling and simulation activities have been updated annually based on available site characterization data and field injection/production records to improve risk identification and the MVA plan. All elements have been integrated into an iterative process to produce meaningful results for large-scale CO₂ storage and EOR projects. To date, three versions of the modeling and simulation reports have been produced to cover the highlights of activities since 2011. A brief description of each report follows:

- **Bell Creek Test Site Simulation Report: PCOR Partnership Phase III Task 9 Deliverable D66, 2011, approved (Pu and others, 2011)**

The V1 3-D geologic model was developed based on the available site characterization data at the time and was focused on the Phase 1 area. A generalized lithology and stratigraphic framework in the Bell Creek oil field were interpreted that include four distinct lithofacies, "Springen Ranch shale," "coastal plain," "Bell Creek sand," and "Rozet shale" in the Muddy Formation. The structure and properties were populated based on the 154 wells within the study boundary. Available data were analyzed, interpreted, and incorporated into the 3-D static geologic and dynamic reservoir models to represent geologic and reservoir properties in order to provide a solid groundwork for simulation activities.

The PVT (pressure, volume, and temperature) data from three fluid samples were analyzed and lumped as seven components that matched the laboratory data. The results indicate that miscibility for oil samples can be achieved at approximately 2800 psi.

- **Bell Creek Test Site Simulation Report: PCOR Partnership Phase III Task 9 Deliverable D66, 2012, approved (Saini and others, 2012)**

A 1-D compositional simulation of the experimental slim-tube tests was performed to ensure the robustness of the seven-component Peng–Robinson (PR) equation of state (EOS) developed in 2011. The minimum miscibility pressure (MMP) estimated from slim-tube simulation is about 2750 psia at 108°F, which agrees with the experimental results.

The constructed geologic model was validated through history matching of oil rate, water cut, and gas/oil ratio and was used for various predictive simulation scenarios for the Phase 1 area. A total of 12 cases based on a five-spot, a quarter five-spot, and the entire Phase 1 pattern were designed to address associated CO₂ storage and CO₂ breakthrough at the monitoring well, 05-06 OW, from a CO₂ water alternating gas (WAG) injection scenario.

- **Bell Creek Test Site Simulation Report: PCOR Partnership Phase III Task 9 Deliverable D66, 2013, pending approval (Braunberger and others, 2013)**

A detailed 3-D static geocellular model of the Bell Creek oil field area (V2 model) was constructed utilizing pertinent reservoir characterization data gathered in an extensive literature review and current core analysis work for the entire Bell Creek oil field and surrounding area. Seven hundred forty-eight wells with wireline logs and many with core data were analyzed, interpreted, and incorporated into the 3-D static geocellular and dynamic reservoir models to represent geologic stratigraphy, petrophysical facies, and reservoir properties for simulation activities.

The seven-component PR EOS model was tuned and matched to both original oil and depleted oil from slim-tube test and laboratory data. This produced an acceptable EOS for both matching historic production/injection and for performing predictive simulations.

The Phase 1 area and immediately adjacent area were clipped from the V2 model and matched to production and injection historical records for a total of 46 years to validate the model and to get a good estimate of the current saturations and pressures in the model. Five predictive simulation cases were run to evaluate WAG and continuous CO₂ injection (CCI) at two injection bottomhole pressure (BPH) constraints and varying WAG cycle lengths.

SCOPE OF WORK

In order to evaluate the efficiency of large-scale CO₂ injection for CO₂ EOR and to monitor the associated CO₂ storage in the Muddy Formation at the Bell Creek oil field, several iterations of a 3-D geologic model coupled with dynamic simulation work were completed as submitted in the previous three D66 reports (2011, 2012, and 2013). This report documents the modeling and simulation activities completed over the course of the past year (August 2013–August 2014),

which include 1) geological interpretation based on the newly acquired PNL and other available data from seismic survey and core descriptions. Well logging was performed through casing from the surface to reservoir to primarily identify changes in fluid saturations of CO₂, water, and oil for fluid movement monitoring and characterization in, above, and below the reservoir. These data also help to identify geologic formation breaks, which are critical to understanding the local stratigraphy of the Bell Creek Field from the reservoir to the surface, by introducing a 3-D seismic data set with high lateral resolution (~82 feet); 2) history-matching field records including production/injection and reservoir pressure data in the Phase 2 area for 46 years; 3) predictive simulations in both Phases 1 and 2 with various scenarios to address the WAG and CCI schemes for associated CO₂ storage, oil recovery, and CO₂ utilization factor, ultimately improving risk identification and MVA strategies; and 4) ongoing work for another iteration of modeling and simulation activities, which has been integrated into the PCOR Partnership's adaptive management plan (Figure 4).

3-D Geologic Modeling

PNL Model and Updated Structural Framework

A PNL campaign was launched for the Bell Creek Field to assist with monitoring CO₂ breakthrough between production and injection wells. This campaign will expand MVA efforts as well as advance awareness of sweep efficiency, effective storage capacity, and flow directions (vertically and laterally) of injected CO₂. The campaign comprises two parts with different objectives. The first is to obtain baseline logs within the current development phase before CO₂ is injected, thus providing a clear picture of baseline fluid saturations in the reservoir. These saturation properties are obtained by processing a combination of both Sigma and inelastic capture (IC) logs using a probabilistic model in Techlog. In addition to the Sigma and IC logs, there are also gamma ray, neutron porosity, and temperature logs associated with each logging run. The baseline logging was performed successfully on 33 wells from November 2012 to June 2013. These data have allowed for the creation of a more detailed stratigraphic column from the ground surface to the reservoir, which is the basis for the new structural framework (Figure 2). The second part of the PNL campaign is to collect multiple rounds of monitor passes which are acquired after CO₂ injection has started. The same probabilistic model is used to process the data, thus allowing for a direct comparison of fluid saturations between the baseline and monitor passes. The first round of monitor passes was completed on seven wells from August 2013 to January 2014 (Figure 5). The processed monitor logs, when compared to the baseline logs, showed evidence of CO₂ being present in the near-wellbore environment of both the injection and production wells that have observed CO₂ breakthrough (Figures 6 and 7). The injection wells show dewatering of the pores along the wellbore by exhibiting a decrease in water saturation. The production wells show preferential CO₂ migration into the reservoir depending on facies and reservoir properties (Braunberger and others, 2014).

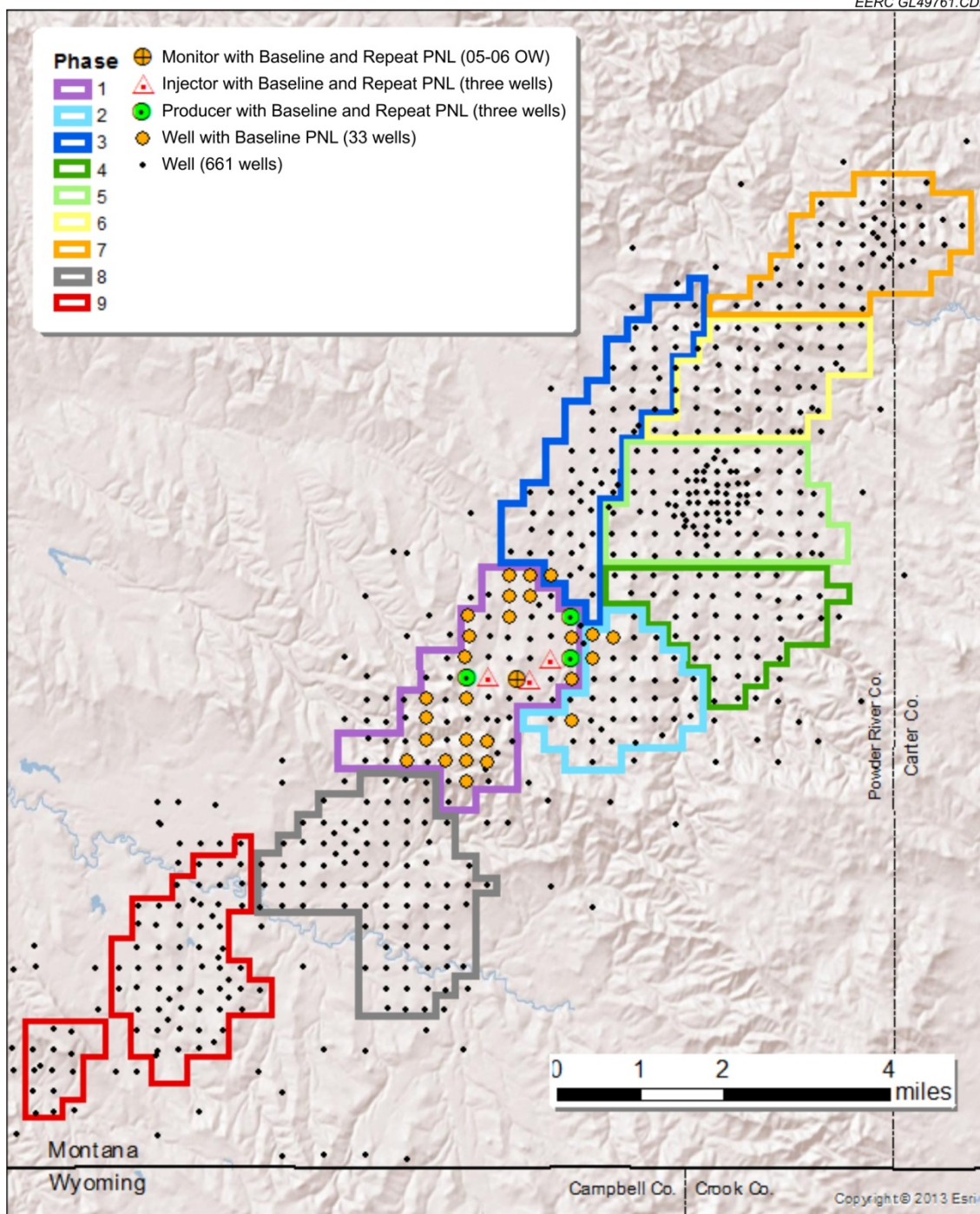


Figure 5. Map of wells showing where baseline and monitor pass PNLs were collected in relation to the Bell Creek oil field.

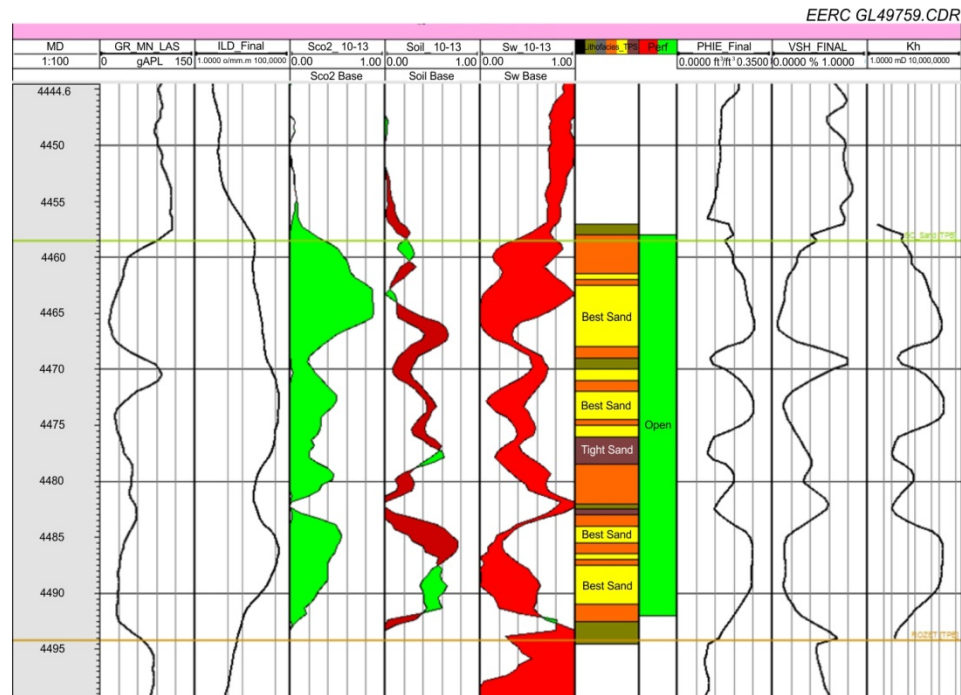


Figure 6. Injection well (left to right): reference track (measured depth in feet), gamma ray log, resistivity log, CO₂ saturation, oil saturation, water saturation, facies, perforations, effective porosity, shale volume, and horizontal permeability. For the saturations, a fill of green means there was an increase in saturation when comparing the monitor pass to the baseline pass, while the red means there was a decrease in saturation. Interval tops shown are Bell Creek sand and Rozet (image from Braunberger and others, 2014).

Reference Model

A reference model has been built in Petrel to house the collection of V1 and V2 geologic models, the PNL model, and the geomechanical model. The associated data include 751 wells including field and processed logs, core analysis, structural tops, cultural surface boundaries, and completed simulation results. The goal of creating a reference model is to provide a central location for all pertinent data and allow easy access to the diverse team when building new and updating comprehensive regional and localized models. The data undergo a routine quality check to keep the data up to date and provide an efficient way to convey geo-based data sets. The 3-D reference model has already been used to provide quicker data sharing and transfer while starting new Petrel projects for the V3 geologic models and geomechanical models.

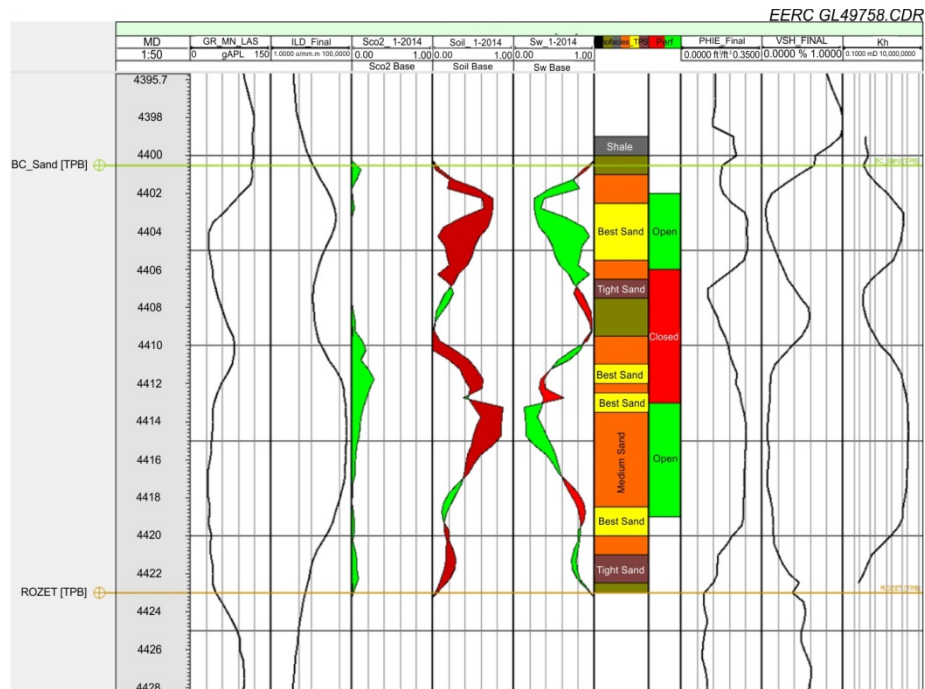


Figure 7. Production well (left to right): reference track (measured depth in feet), gamma ray log, resistivity log, CO₂ saturation, oil saturation, water saturation, facies, perforations, effective porosity, shale volume, and horizontal permeability. For the saturations, a fill of green means there was an increase in saturation when comparing the monitor pass to the baseline pass, while the red means there was a decrease in saturation. Interval tops shown are Bell Creek sand and Rozet (image from Braunberger and others, 2014).

Reservoir Simulation

While the geologic model provides a framework for dynamic simulation activities, the dynamic reservoir model incorporates a variety of additional reservoir data to accurately simulate the reservoir's pressure and fluid mobilization response to injection and/or production processes. The static geologic model realizations with the mean original oil in place (OOIP) value were exported to Computer Modelling Group Ltd.'s (CMG's) Builder software to construct a reservoir simulation model. The PVT data, relative permeability data, and well production and injection history were brought into Builder to begin the process of building the dynamic reservoir model.

Fluid flow simulations were performed using CMG's GEM, a general compositional and unconventional reservoir simulator. These flow simulation studies allowed the validation of the geologic model and the fine tuning of model parameters to match reservoir production, pressure, and injection responses through history matching. After a history match was performed, the predictive simulations with CCI and CO₂ WAG injections were run to evaluate CO₂ storage capacity, sweep efficiency and recovery factor, and CO₂ utilization for oil recovery, ultimately to improve long-term risk identification and MVA strategies.

Phase 1 Area Reservoir Simulation

The dynamic reservoir model used for history matching and predictive simulations covers the Phase 1 area and a small portion of the surrounding areas, which were clipped from the fieldwide geologic model (V2) (Figure 3). Following a satisfactory history match detailed in the 2013 D66 report, predictive simulations were performed to evaluate the effects of various CO₂ injection schemes on movement of injected CO₂ in the reservoir over time.

Updated Predictive Simulations and Results

According to the CO₂ injection plan, a total of 26 active injection wells and 26 active production wells were included in the predictive simulation model (Figure 8). The CO₂ injection rate was specified to be 50 MMscf/day. In all cases, a minimum bottomhole flowing pressure of 2300 psi was specified for the production wells as the operating constraint. The CO₂ injection wells were controlled by CO₂ injection rates and limited by maximum BHP constraints of either 2700 or 2900 psi. The history-matching results were used as the initial condition for predictive simulation model input to develop the reservoir-monitoring strategies.

A total of five cases were run with varying injection BHP constraints, CO₂ injection rates, the use or not of relative permeability hysteresis for the gas phase, and CCI and WAG (1:1 injection ratio) processes (Table 1). Cases 1–3 were WAG injection scenarios with a 3-month WAG cycle. Case 1 was designed to test the effect of hysteresis on CO₂ flooding by including relative permeability hysteresis for the gas phase, characterized by the Land model, which describes the amount of nonwetting phase trapped after a drainage cycle (Land, 1968; Joekear-Niasar and others, 2013). Case 3 varied the injection BHPs from 2700 to 2900 psi to analyze the sensitivity of this variable to fluid movement of the system. Cases 4 and 5 tested CCI but changed injection BHPs from 2700 to 2900 psi. The production BHPs for all of the cases were fixed at 2300 psi. BHP constraints were chosen based on the development plan, field practice, and the pressure required to produce from the field without a pump unit. The CO₂ injection rate was 2.7 MMscf/well/day, and the water injection rate for WAG cases was 1080 bbl/day/well. WAG is a 3-month 1:1 cycle for water and CO₂ injection. Under the aforementioned CO₂ and/or water injection rates, it takes approximately 3.1 years for 1 hydrocarbon pore volume of injection (HCPVI). The results are summarized in Tables 2–4 and detailed in Figures A-1–A-27 in Appendix A.

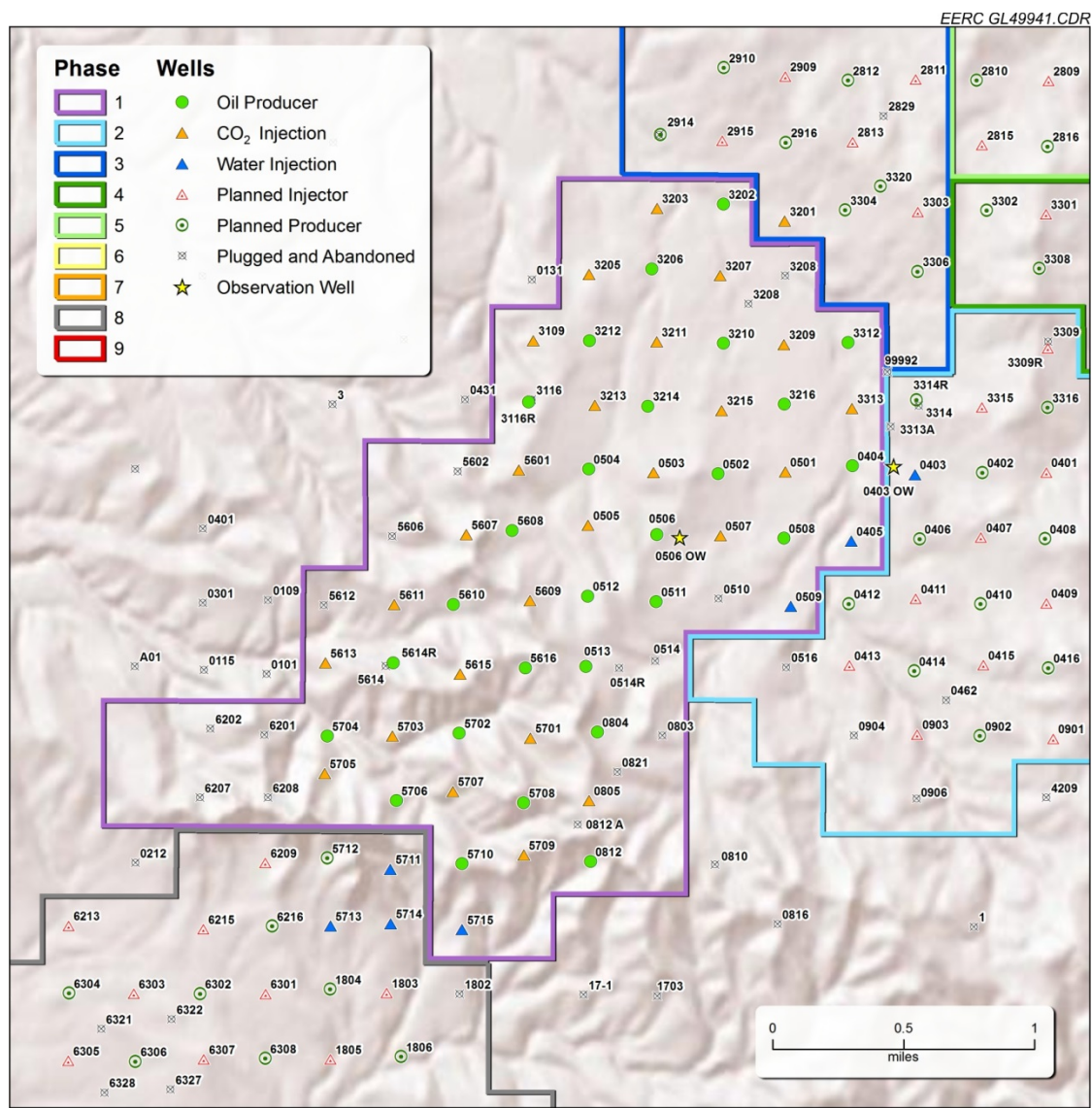


Figure 8. Zoomed-in image of wells in the Phase 1 area.

Table 1. Simulation Parameters for Each Investigatory Case in the Phase 1 Area

| Case No. | Flood Type | Injector Pressure, psi | Producer Pressure, psi | Total Volume Injected, HCPV | Proposed CO ₂ Injected, HCPV | Actual CO ₂ Injected, HCPV | Cycle Length |
|----------------|------------|------------------------|------------------------|-----------------------------|---|---------------------------------------|--------------|
| 1 (hysteresis) | WAG | 2700 | 2300 | 6 | 3 | 2.33 | 3-month 1:1 |
| 2 | WAG | 2700 | 2300 | 12 | 6 | 5.08 | 3-month 1:1 |
| 3 | WAG | 2900 | 2300 | 12 | 6 | 5.52 | 3-month 1:1 |
| 4 | CCI | 2700 | 2300 | 6 | 6 | 5.58 | – |
| 5 | CCI | 2900 | 2300 | 6 | 6 | 5.81 | – |

Table 2. Simulation Results for CO₂ Stored and Produced and Injected Water and CO₂ for 6 HCPVI in the Phase 1 Area

| Case No. | 6 HCPVI End Date | Cumulative CO ₂ Injected, Bscf ¹ | Cumulative Water Injected, MMbbl | Cumulative CO ₂ Produced, Bscf | Cumulative Water Produced, MMbbl | Associated CO ₂ Stored, Bscf | Associated CO ₂ Stored, Mt |
|-------------------|-------------------------|---|---|--|---|--|--|
| 1 (hysteresis) | 12/2031 (3 HCPVI) | 177 | 36.7 | 135 | 42 | 42 | 2.24 |
| 2 | 12/2041 | 295 | 65.8 | 261 | 65 | 33 | 1.77 |
| 3 | 11/2036 | 266 | 78.7 | 235 | 76 | 32 | 1.68 |
| 4 | 12/2031 | 424 | – | 360 | 19 | 64 | 3.37 |
| 5 | 12/2031 | 445 | – | 385 | 21 | 60 | 3.18 |

¹ Billion standard cubic feet.**Table 3. Simulation Results for Produced Hydrocarbons and Flood Performance for 6 HCPVI in the Phase 1 Area**

| Case No. | Peak Oil Production Rate, bbl/day | Cumulative Oil Production, million bbl | Average Reservoir Pressure, psi | Recovery Factor, % | Utilization Factor, Mscf ¹ /bbl |
|----------------|---|--|---------------------------------------|--------------------------|--|
| 1 (hysteresis) | 2254 | 7.85 | 2619 | 16.98 | 5.01 |
| 2 | 2307 | 9.53 | 2598 | 20.58 | 3.09 |
| 3 | 3417 | 10.79 | 2700 | 23.33 | 2.60 |
| 4 | 2300 | 6.86 | 2523 | 14.84 | 8.75 |
| 5 | 3130 | 7.02 | 2534 | 15.17 | 8.05 |

¹ Thousand standard cubic feet.**Table 4. CO₂ Breakthrough for Each Investigatory Case in the Phase 1 Area**

| Case No. | Flood Type | Injector Pressure, psi | Producer Pressure, psi | Breakthrough Time at the First Production Well, month | Breakthrough at Monitoring Well 05-06 OW | Cycle Length |
|----------------|---------------|------------------------------|------------------------------|---|---|--------------|
| 1 (hysteresis) | WAG | 2700 | 2300 | 3.5 | 6.5 | 3-month 1:1 |
| 2 | WAG | 2700 | 2300 | 2.5 | 5.5 | 3-month 1:1 |
| 3 | WAG | 2900 | 2300 | 2.5 | 5.5 | 3-month 1:1 |
| 4 | CCI | 2700 | 2300 | 2.5 | 5.5 | – |
| 5 | CCI | 2900 | 2300 | 2.0 | 5.5 | – |

Discussion of Incremental Oil Recovery, Utilization Factor, and Oil Production

The incremental oil recoveries versus time and HCPVI for all cases are shown in Figures 9 and 10, respectively. Overall, Cases 1–3 with the WAG process yield higher oil recovery than those with CCI in Cases 4 and 5 (Figures 9–11). Case 1, considering the effect of relative permeability hysteresis for the gas phase, is slightly lower than that of Cases 2 and 3 without hysteresis. The highest incremental oil recovery is from Case 3 with 2900 psi of injection BHP.

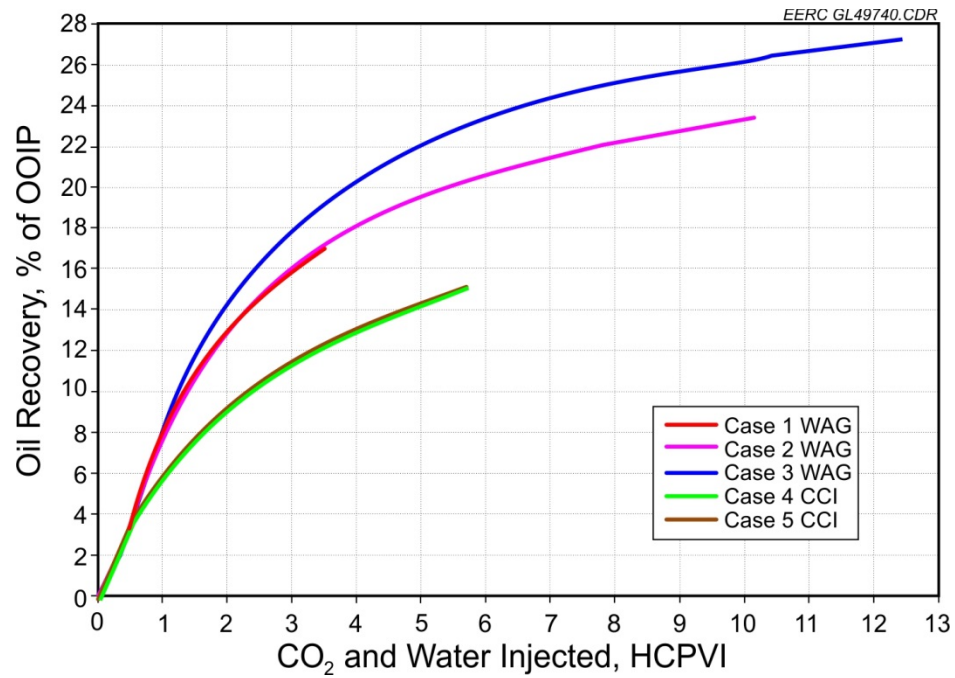


Figure 9. Incremental oil recovery vs. time for Cases 1–5 in the Phase 1 area.

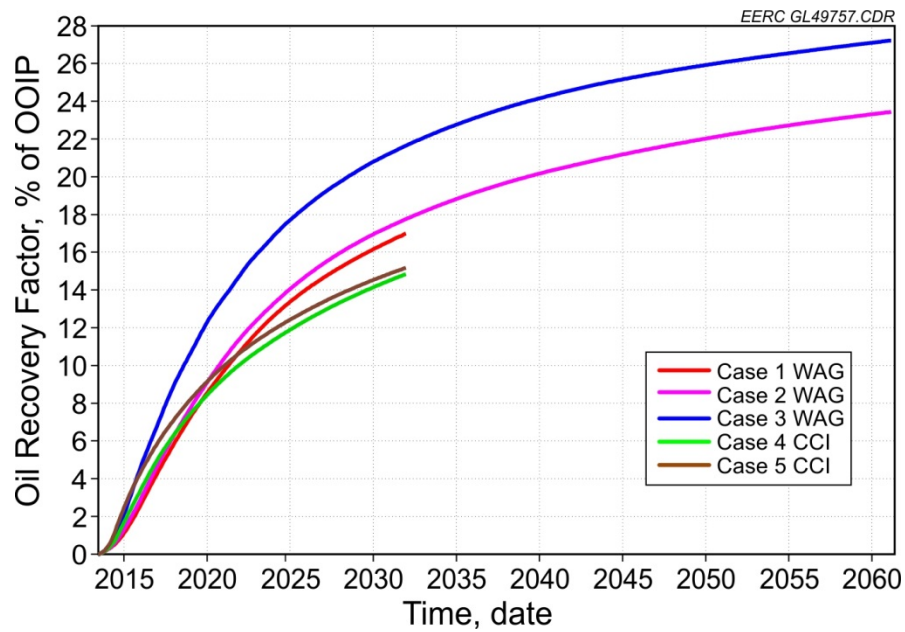


Figure 10. Incremental oil recovery vs. HCPVI for Cases 1–5 in the Phase 1 area.

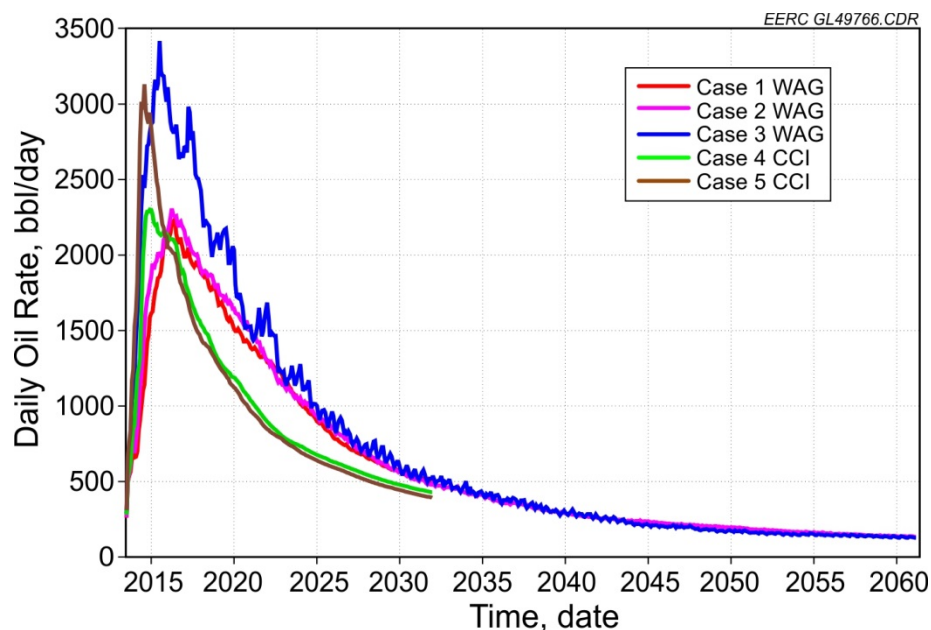


Figure 11. Oil rate for all cases in the Phase 2 area.

The CO₂ utilization factors for the five cases are shown in Table 3. WAG processes have CO₂ utilization factors of 2.60–5.01 Mscf/bbl for various operating pressures and injection volumes, while the CCI gave higher CO₂ utilization factors in the range of 8.05–8.75 Mscf/bbl because of the fact that only CO₂ is replacing the produced fluids in these two scenarios (Figure 12).

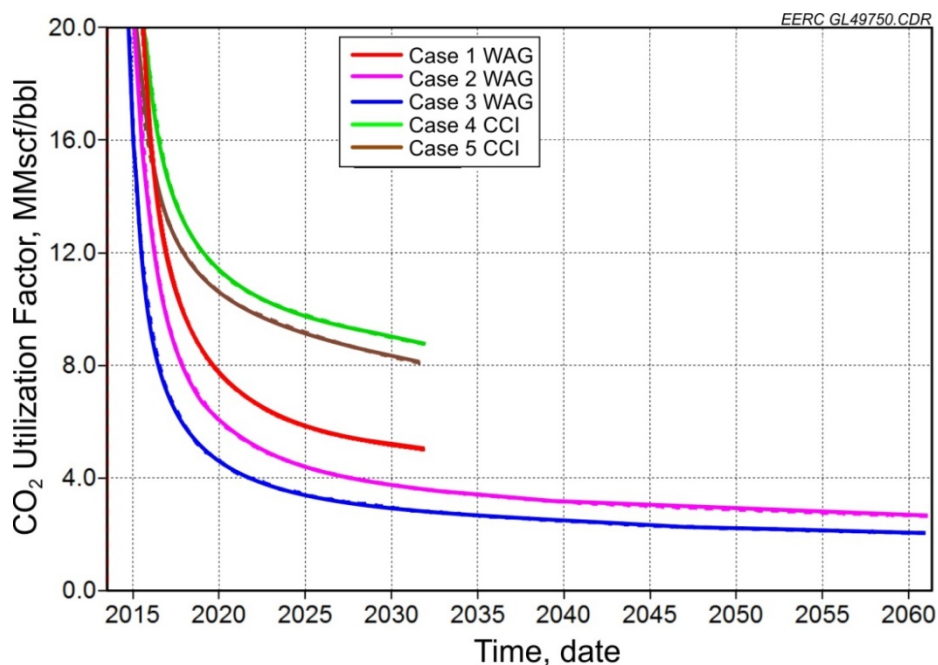


Figure 12. Cumulative CO₂ utilization factors for all cases in the Phase 1 area.

With regard to cumulative oil production, the results with WAG injection in Cases 1–3 are higher than those with CCI in Cases 4 and 5 (Figures 9–11). The hysteresis effect decreases cumulative oil production slightly compared to Cases 1 and 2. The peak oil rates of cases with an operating BHP of 2900 psi have much higher peak oil rates than those with a BHP constraint of 2700 psi. The detailed plots and images of CO₂ and water injection, oil production, and CO₂ storage for all cases are shown in Figures A-3–A-27 in Appendix A.

Effect of Injection Mode

WAG simulations were performed using 3 HCPV of CO₂ and 3 HCPV of water for Case 1 and 6 HCPV of CO₂ and 6 HCPV of water for the other two cases, whereas CCI used 6 HCPV of CO₂ for both cases. For the CCI process, the daily CO₂ injection rate was 67.5 MMscf/day, which was distributed to 26 injection wells. For the WAG processes, the daily CO₂ injection rate was 33.8 MMscf/day, which was distributed to 13 injection wells, and the daily water injection rate of 14,040 bbl was divided and distributed to the other 13 injection wells (Figures 13 and 14). The incremental oil recovery for Case 1 (WAG with hysteresis) is 16.98% OOIP after 6 HCPVI, while the oil recovery is 14.84% OOIP for Case 5 (Table 3, Figures 9 and 10). Besides a higher peak oil rate, Case 3 (without hysteresis) also shows an overall higher oil rate and faster recovery rate than that of Case 5 (Figures 9–11). However, the gas/water ratio of WAG cases varies between Cases 1 and 2 generally (Figure 15).

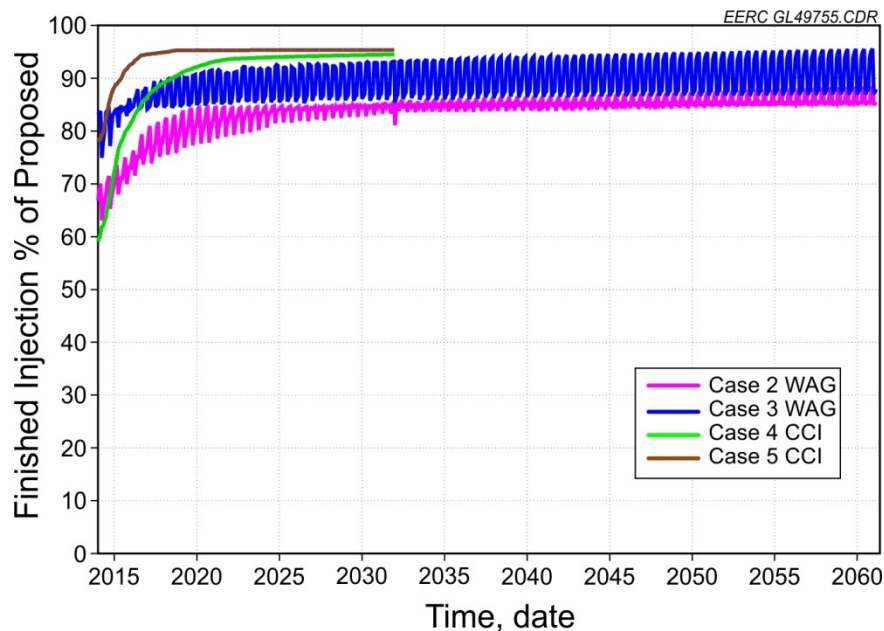


Figure 13. Actual injected CO₂ volume as a percentage of proposed CO₂ injection for the cases in the Phase 1 area.

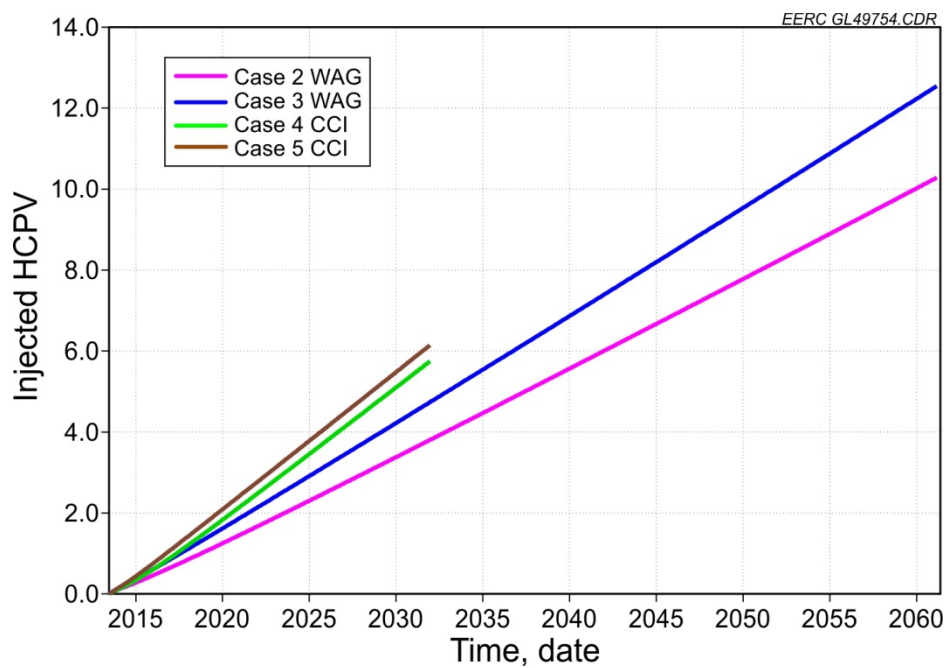


Figure 14. Comparison of cumulative equivalent volume injection in the Phase 1 area.

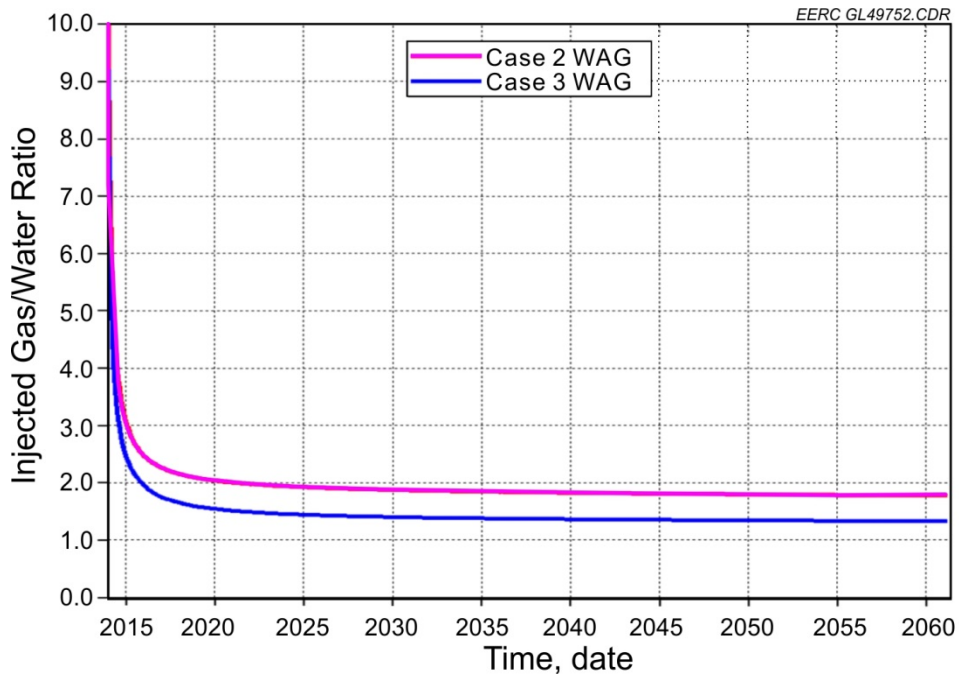


Figure 15. Gas/water ratio for WAG cases in the Phase 1 area.

CO₂ Stored

The stored CO₂ for the WAG processes varies from 1.68 to 2.24 Mt with varying injection volumes, while the stored CO₂ for the CCI processes was about 3 Mt (Figure 16). This discrepancy is the result of doubling the volume of cumulative CO₂ injected for the CCI cases compared to the WAG cases and the fact that only CO₂ is being injected in the CCI cases to replace the produced fluid, whereas in the WAG cases, injected water can also replace the produced oil and water. The earliest CO₂ breakthrough occurred 2 months after the start of CO₂ injection for the continuous CO₂ flooding scenario, while the earliest CO₂ breakthrough with WAG occurred after 2.5 months in Phase 1.

The simulation results also indicated that injected CO₂ in this phase is expected to reach the observation well, 05-06 OW, about 6 months after injection for both the continuous CO₂ flooding and WAG scenarios. The results of each injection case, which illustrate the amount of CO₂ injected (HCPVI) versus the associated CO₂ storage that may occur as part of normal EOR operations and their movement, are shown in Figures A-23–A-27 in Appendix A.

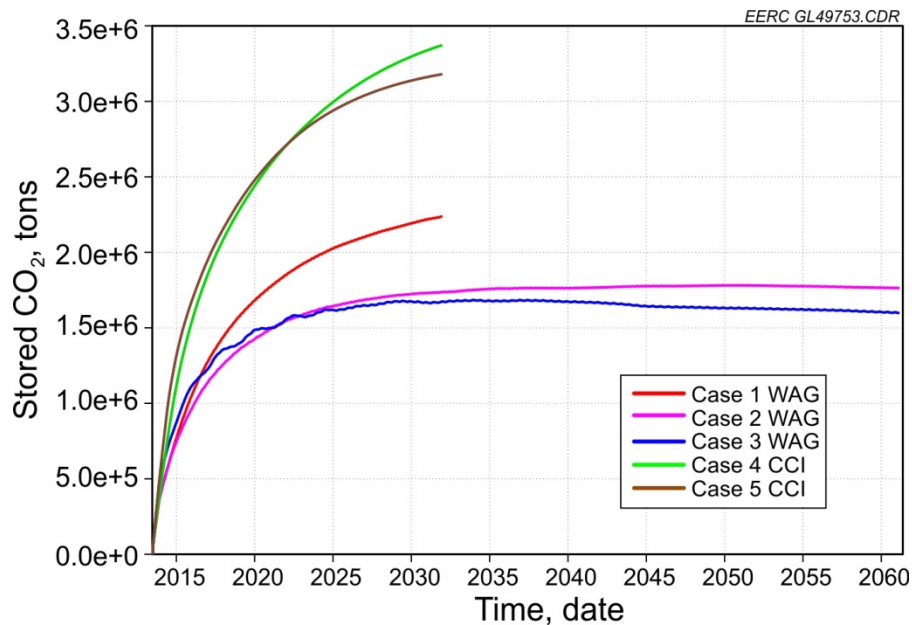


Figure 16. Stored CO₂ for all scenarios in the Phase 1 area.

Phase 2 Area Reservoir Simulation

The dynamic model was clipped from the Bell Creek Field model (V2), which covers both Phase 1 and Phase 2 areas with a total of 859,362 cells, by gridding $259 \times 158 \times 21$. Most of the Phase 1 area was set as an inactive cell in the current Phase 2 simulation activities but will be active in the next step for combined Phases 1 and 2 simulations (Figures 17). A total of 42 vertical wells were included in the Phase 2 simulation model, which includes 32 production wells and ten injection wells.

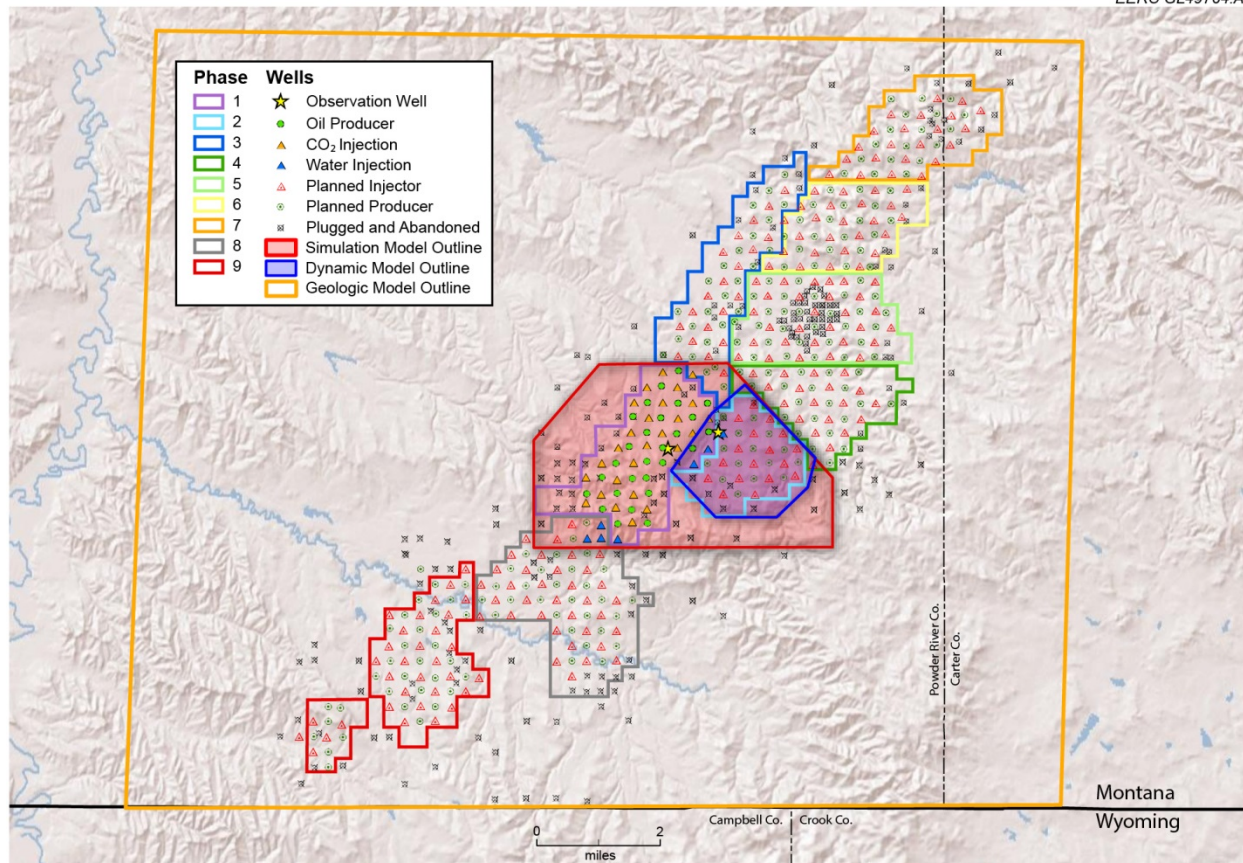


Figure 17. Map showing geologic model boundary (orange), dynamic model boundary (blue), and their relation to the planned Bell Creek project development phases.

History Matching and Results

History matching is a method of adjusting reservoir properties/parameters within a simulation model to match historical field data (production/injection records and/or pressure data) through an iterative trial-and-error process. This process varies parameters and properties within an accepted range of the realistic engineering and geologic inputs. In this way, the resulting properties and parameters still accurately reflect the original hard data. History matching reduces the geologic uncertainties, which will allow for more accurate prediction of future reservoir performance. Simulations aimed at matching the reservoir's oil and water production during primary depletion and waterflooding were run using CMG's CMOST tool and GEM simulator. The history-matching process was performed and matched the field production and injection records spanning 1968 to 2013, a total of 46 years.

Phasewise History-Matching and Results

After a number of history-matching runs, a relatively close match was achieved between the observed oil rates, water cut, gas rate, average reservoir pressure data, and simulation outputs (Figures 18–21).

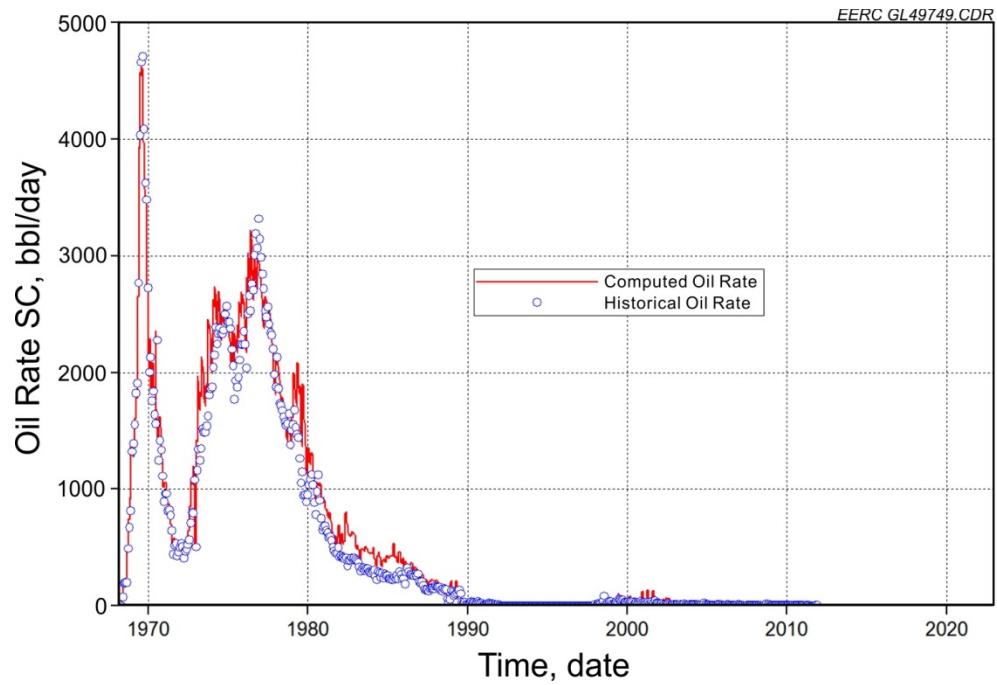


Figure 18. History-matching results for field oil production rate, where the circles represent the field data and the solid line represents the simulation results (SC is standard condition).

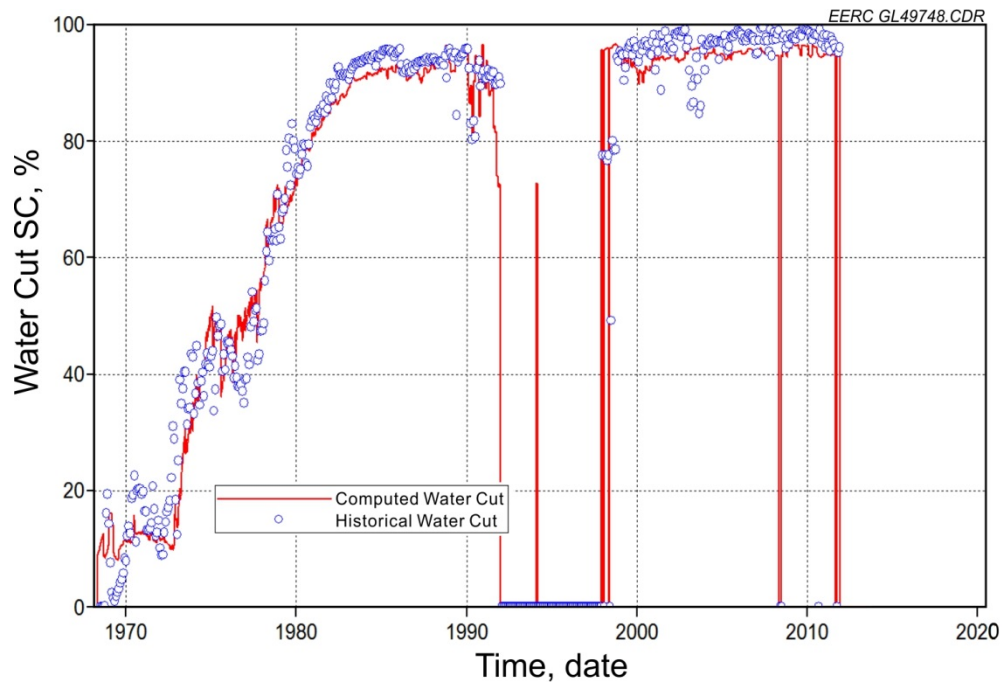


Figure 19. History-matching results for simulated and actual water cut of the field, where the circles represent the field data and the solid line represents the simulation results.

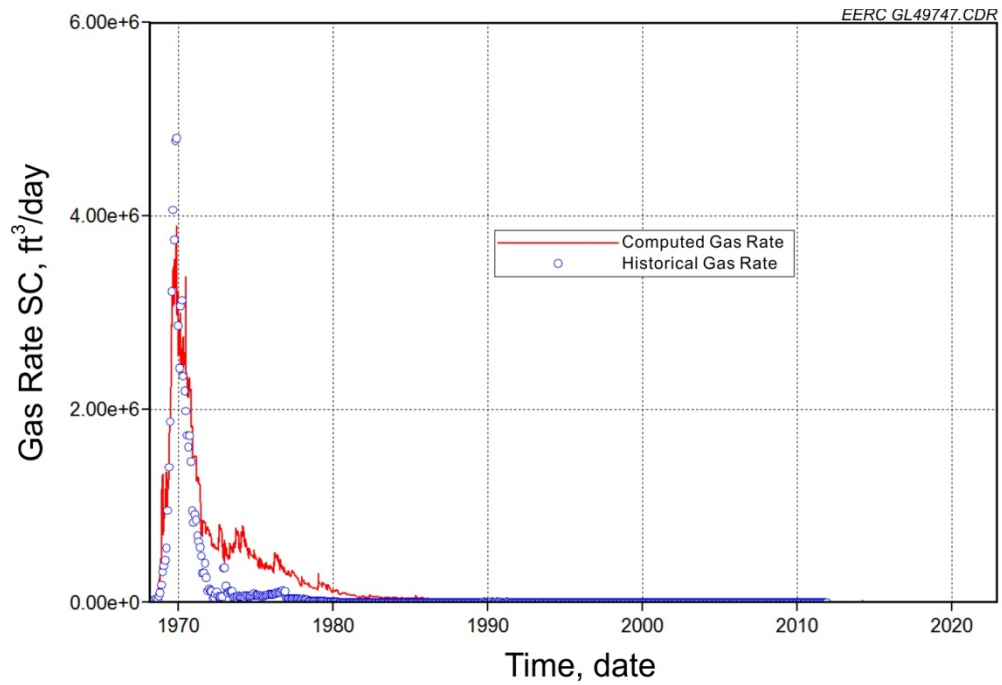


Figure 20. History-matching results for field gas production rate, where the circles represent the field data and the solid line represents the simulation results.

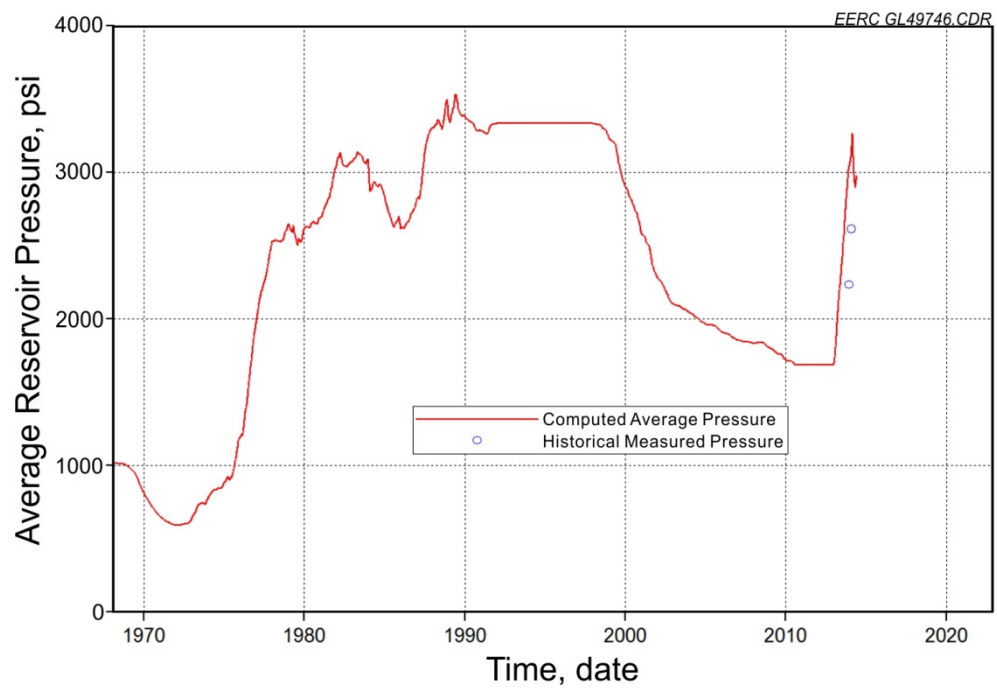


Figure 21. Average reservoir pressure over the reservoir's history, where the circles represent the field data and the solid line represents the simulation results.

According to the gas production record, the gas rate initially increased rapidly and then dropped during primary depletion (Figure 20). The early stage of production at Bell Creek was through solution gas drive. Because of the limited pressure data during the early and middle production stages, the matched pressure results with a few scattered points could only be used for tracking the trend of average reservoir pressure (Figure 21).

Individual Well History-Matching Results

Because of the uneven injection and production in the Phase 2 area, the primary target of history matching for individual wells was the timing of water breakthrough. These results showed that the water cuts for 25 of 32 individual wells are in good agreement with historical records. The rest of the wells without fair match were completed in the possible water zone, and these wells have relatively short production history as well. Results for 18 wells are provided in Appendix B (Figures B-6–B-11).

History-Matching Discussion

After a comprehensive analysis of the field production/injection data, models, and history-matching efforts in both the Phases 1 and 2 areas, there were several discussions to help better understand the reservoir behavior in this study area.

Long period of uneven injection and production – As in the Phase 1 area of the field, primary production was through solution gas drive, and based on the analysis of historical production data, water injection in the Phase 2 area started in 1972. During the first 3 years of waterflooding, an injection/production ratio of about 0.7 was maintained, which resulted in a decrease in reservoir pressure after primary depletion. In the mid-1970s, the water injection built up a driveline to push the oil bank from downdip northwest to updip southeast, also increasing the injection/production ratio. A significant pressure gradient against gravity was constructed and kept for 15 years (1975–1990) (Figure 21).

Fluid communication with neighboring phases – Based on history-matching results, there is fluid communication with neighboring phases. This is evident around Well 33-15, which is critical in understanding the fluids exchange between phases. There is a barrier to flow in the northern portion of the Phase 2 area adjacent to Phase 4, which is confirmed by dryhole wells drilled in this area early in the development of the field. Correspondingly, the injected water from Well 33-15 has three potential directions to move. Two of them can be determined by the timing of water breakthrough of nearby wells. History matching indicates that a considerable amount of injected water from Well 33-15 (Figure 22) flowed into the Phase 1 area. Comparing the water injection history of all wells, both the injection volume and injection duration of Well 33-15 dominate the secondary recovery of the Phase 2 area.

The production of the updip area of Phase 2 after 1983 was restricted by low pressure caused by uneven injection and production from downdip to updip, which resulted in a liquid shortage in the simulation model with a closed boundary. By analyzing the injection record of Well 03-01 (in the Phase 4 area) and near producers, there was more than likely a certain amount of injected water from the Phase 4 area flowing into the Phase 2 area to support the liquid around the Well 03-10 area.

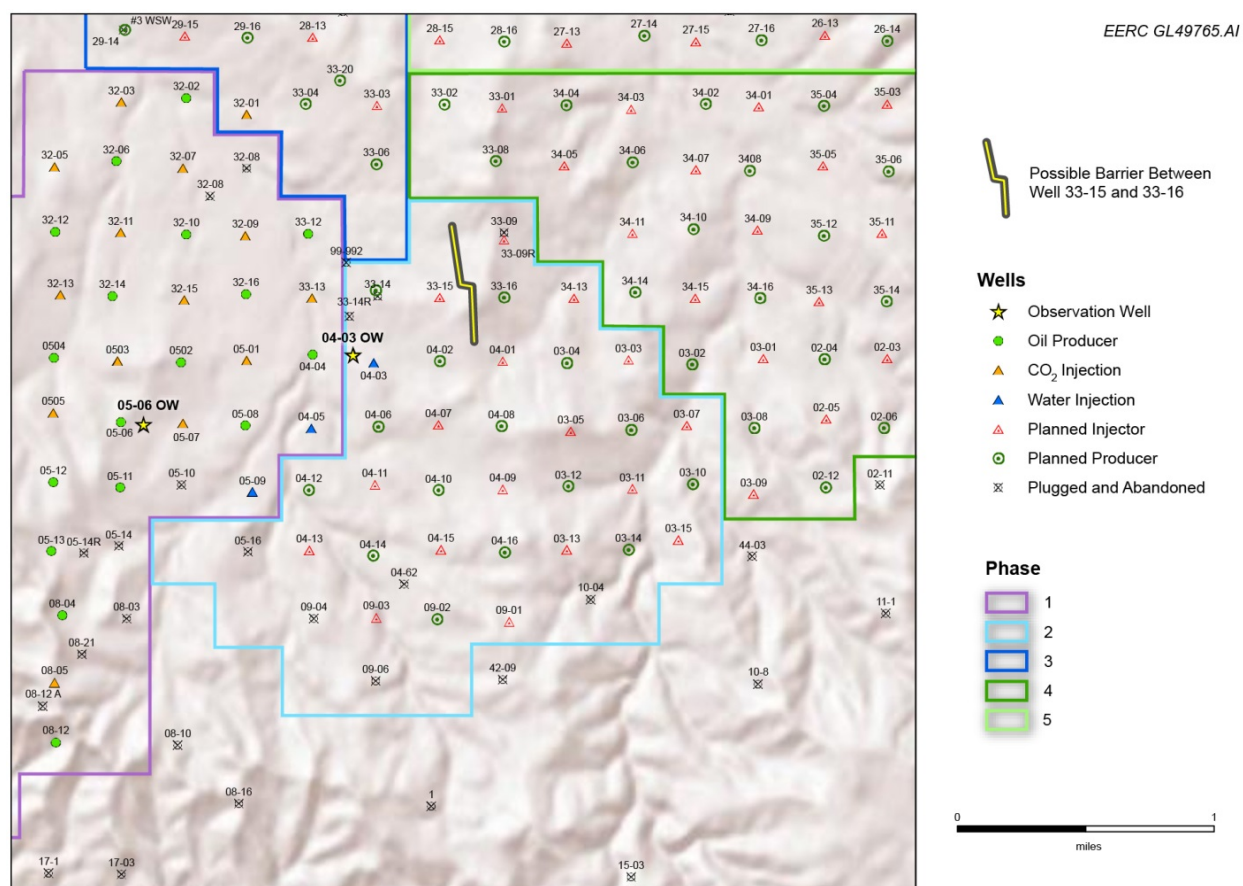


Figure 22. Potential barrier between Wells 33-15 and 33-16 in the Phase 2 area.

Possible internal barrier around the dominant water injection well – As discussed previously, the split of injected water from Well 33-15 is important to maintain the material balance in Phase 2 production and history match. Well 33-15 is the main water injector for most of the nearby producers. With the water breakthrough and water cut reasonably matched for most producers, Well 33-16 has a very early breakthrough in the model. Since there was no liquid exchange in Phase 4 around the area, history matching of the water cut trend for Well 33-16 indicates a barrier between Wells 33-15 and 33-16 (Figure 22).

Possible water zone downdip of the Phase 2 area – The production records of six wells (04-03, 04-11, 04-12, 04-13, 04-14, 09-03) downdip of the Phase 2 area showed very early stage waterflooding (Figure 23). According to the geologic model, most of the cells in this area hold good reservoirs (high permeability, high porosity, and high oil saturation). A J-function-based saturation model above the oil–water contact (OWC) indicated an originally oil rich zone in the area. Early geological explanations from operators indicated that there is another OWC in the Phase 2 area, which is at about 670 feet (elevated). By checking perforation intervals of wells with early water, the lowest bottom was 650 feet, which did not take into account the possibility of a new OWC causing early water production.

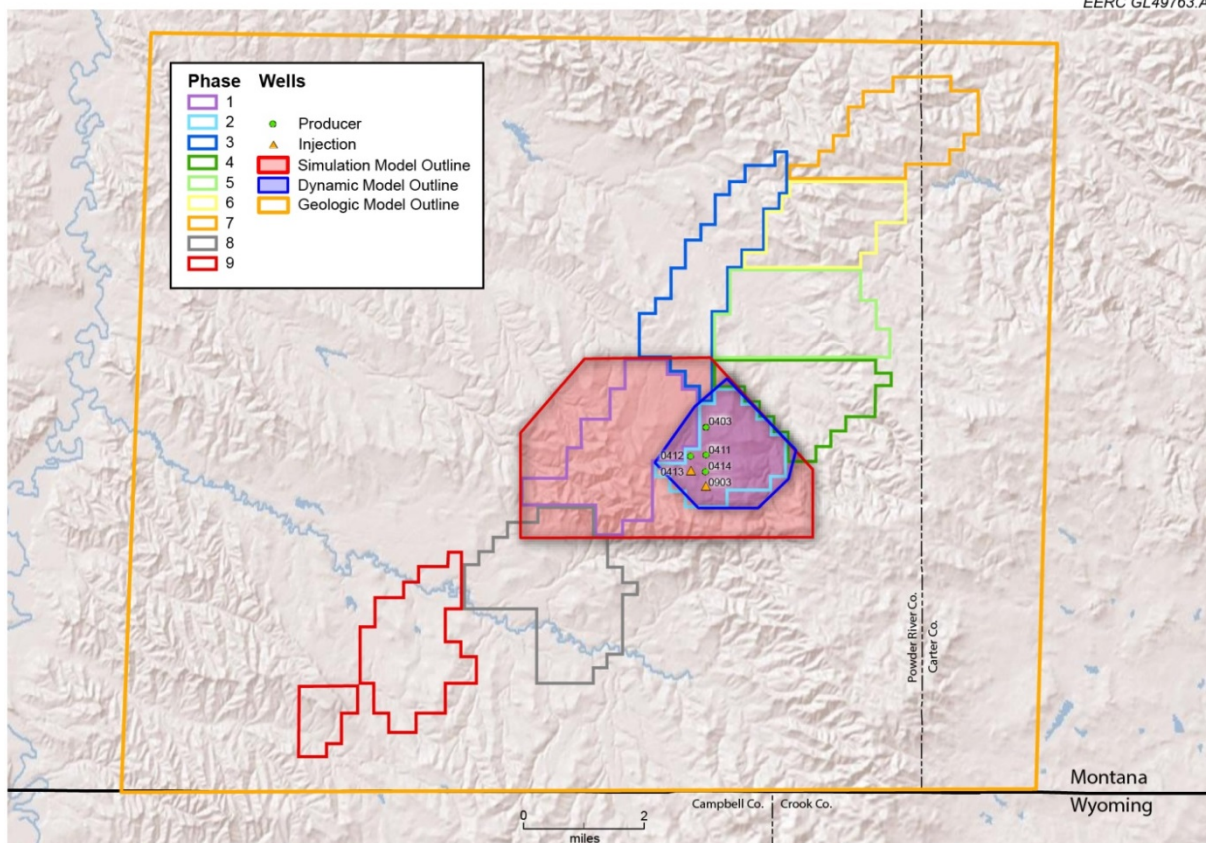


Figure 23. Map showing the six well locations in the Phase 2 area.

Predictive Simulations and Results

Once a satisfactory history match was obtained, predictive simulations were performed to evaluate the effects of various CO₂ injection schemes on movement of injected CO₂ in the reservoir over time. Continuous miscible CO₂ flooding and CO₂ WAG were chosen as tertiary EOR processes, and both were used to evaluate various future production and injection scenarios in the predictive simulations. The detailed designs are similar to the prediction for the Phase 1 area (Table 1).

According to the CO₂ injection plan, a total of 21 active injection wells and 15 active production wells are included in the predictive simulation model. The CO₂ injection rate is specified for individual wells to be 2.7 MMscf/well/day. In all cases, a minimum bottomholeflowing pressure of 2300 psi is specified for the production wells as the operating constraint. The CO₂ injection wells were controlled by CO₂ injection rates and secondarily constrained by maximum BHPs of either 2700 or 2900 psi.

The same five scenarios as the Phase 1 area were run to investigate the effect of CO₂ injection on the EOR process based on different injection and production schemes and HCPVs of injected fluids (Table 5). The results are summarized in Tables 5–8 and Figures 23–30. Figure 31 shows the total CO₂ stored associated with all the simulated EOR scenarios for Phase 2.

Table 5. Simulation Parameters for Each Investigatory Case in the Phase 2 Area

| Case | Flood Type | Injector Pressure, psi | Producer Pressure, psi | Total HCPVI | Proposed CO ₂ HCPVI | Actual CO ₂ HCPVI | Cycle Length |
|----------------|------------|------------------------|------------------------|-------------|--------------------------------|------------------------------|--------------|
| 1 (hysteresis) | WAG | 2700 | 2300 | 6 | 3 | 4.9 | 3-month |
| 2 | WAG | 2700 | 2300 | 6 | 3 | 4.8 | 3-month |
| 3 | WAG | 2900 | 2300 | 6 | 3 | 5 | 3-month |
| 4 | CCI | 2700 | 2300 | 6 | 6 | 6 | – |
| 5 | CCI | 2900 | 2300 | 6 | 6 | 6 | – |

Table 6. Simulation Results for CO₂ Stored and Produced and Injected Water and CO₂ for 6 HCPVI in the Phase 2 Area

| Case No. | 6 HCPVI End Date | Cumulative CO ₂ , Injected Bscf | Cumulative Water Injected, MMbbl | Cumulative Water Produced, MMbbl | Cumulative Gas Produced, Bscf | Associated CO ₂ Storage, Bscf | Associated CO ₂ Storage, Mt |
|----------|------------------|--|----------------------------------|----------------------------------|-------------------------------|--|--|
| 1 | 05/2100 | 330 | 31.8 | 36.1 | 229 | 40.8 | 2.15 |
| 2 | 05/2100 | 320 | 32.5 | 36.1 | 293 | 40.0 | 2.11 |
| 3 | 05/2082 | 337 | 28.4 | 33.1 | 301 | 42.1 | 2.22 |
| 4 | 08/2055 | 419 | – | 12.5 | 369 | 60.8 | 3.21 |
| 5 | 06/2044 | 419 | – | 12.3 | 358 | 60.3 | 3.18 |

Table 7. Simulation Results for Produced Hydrocarbons and Flood Performance for 6 HCPVI in the Phase 2 Area

| Case No. | Peak Oil Production Rate, bbl/day | Cumulative Oil Production, million bbl | Average Reservoir Pressure, psi | Ultimate Recovery Factor, % | Utilization Factor, Mscf/bbl |
|----------------|-----------------------------------|--|---------------------------------|-----------------------------|------------------------------|
| 1 (hysteresis) | 1050 | 7.63 | 2405 | 22.96 | 5.17 |
| 2 | 1150 | 8.31 | 2400 | 24.98 | 4.85 |
| 3 | 1465 | 8.44 | 2420 | 25.39 | 4.96 |
| 4 | 1675 | 8.00 | 2400 | 24.06 | 7.53 |
| 5 | 2340 | 8.00 | 2430 | 24.06 | 7.51 |

Table 8. CO₂ Breakthrough for Each Investigatory Case in the Phase 2 Area

| Case No. | Flood Type | Injector Pressure, psi | Producer Pressure, psi | Breakthrough Time at the First Production Well, month | Cycle Length |
|----------------|------------|------------------------|------------------------|---|--------------|
| 1 (hysteresis) | WAG | 2700 | 2300 | 8.0 | 3-month |
| 2 | WAG | 2700 | 2300 | 6.5 | 3-month |
| 3 | WAG | 2900 | 2300 | 5.0 | 3-month |
| 4 | CCI | 2700 | 2300 | 5.5 | – |
| 5 | CCI | 2900 | 2300 | 4.3 | – |

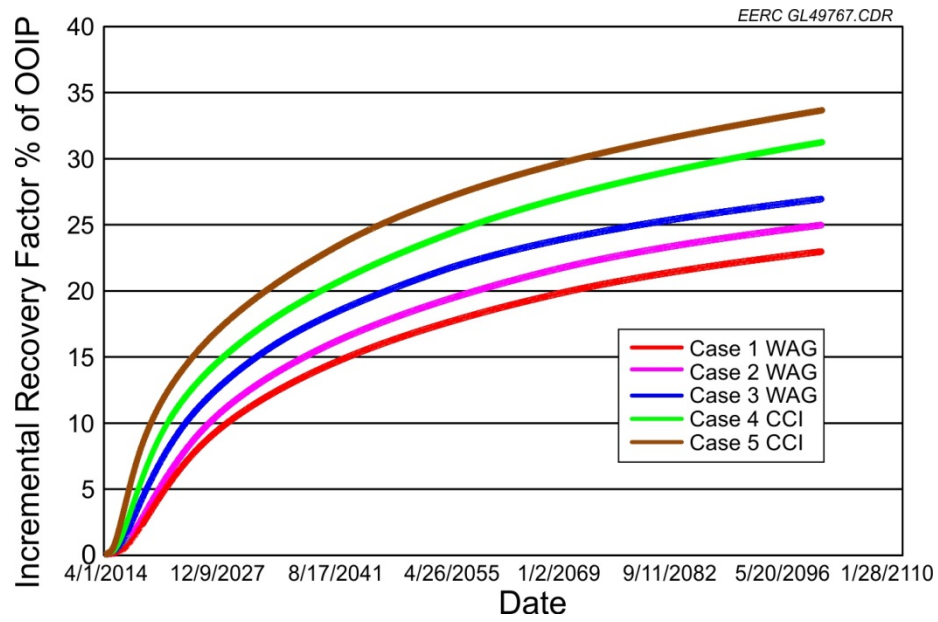


Figure 24. Incremental oil recovery vs. time for Cases 1–5 in the Phase 2 area.

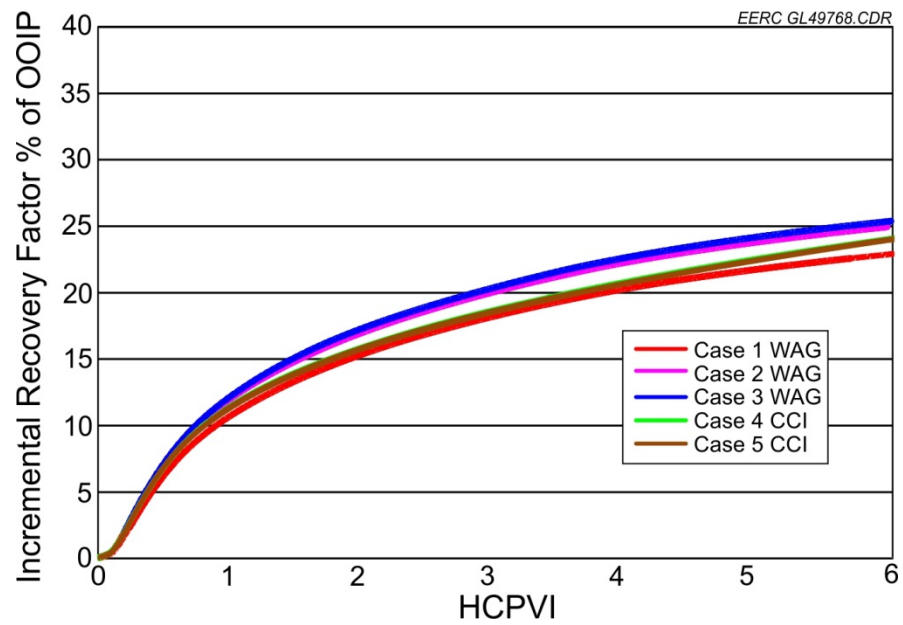


Figure 25. Incremental oil recovery vs. HCPVI for Cases 1–5 in the Phase 2 area.

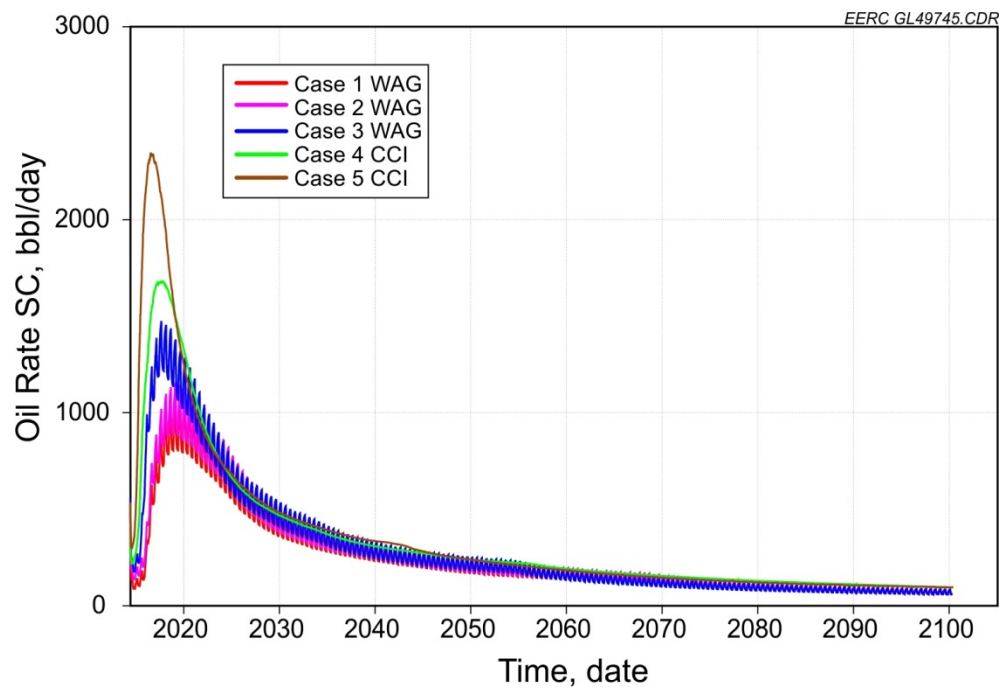


Figure 26. Oil rates for all cases in the Phase 2 area.

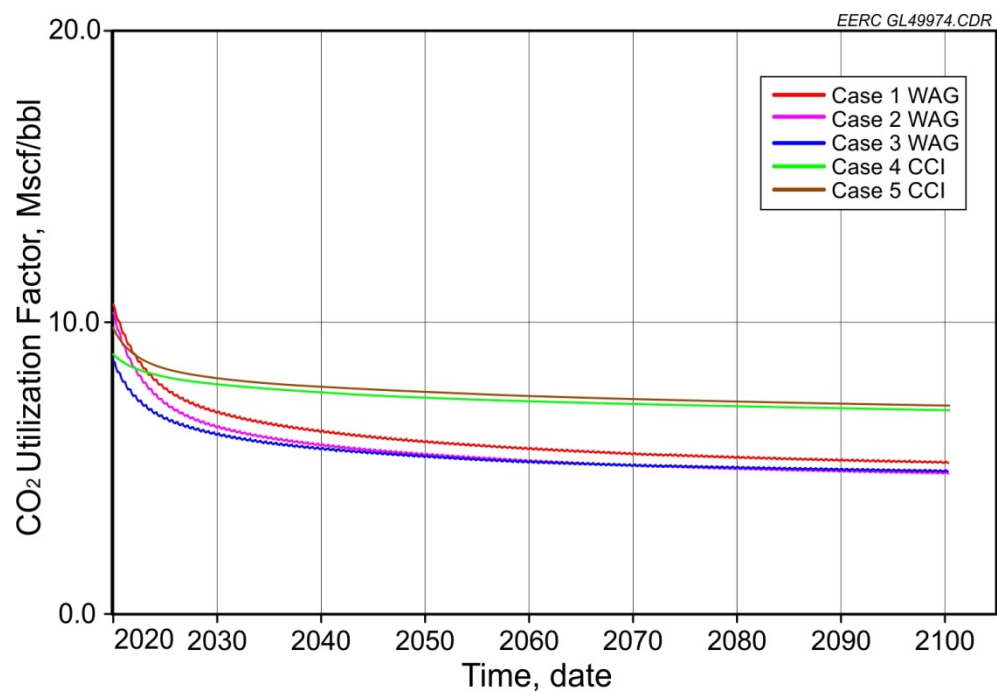


Figure 27. Cumulative CO₂ utilization factors in the Phase 2 area.

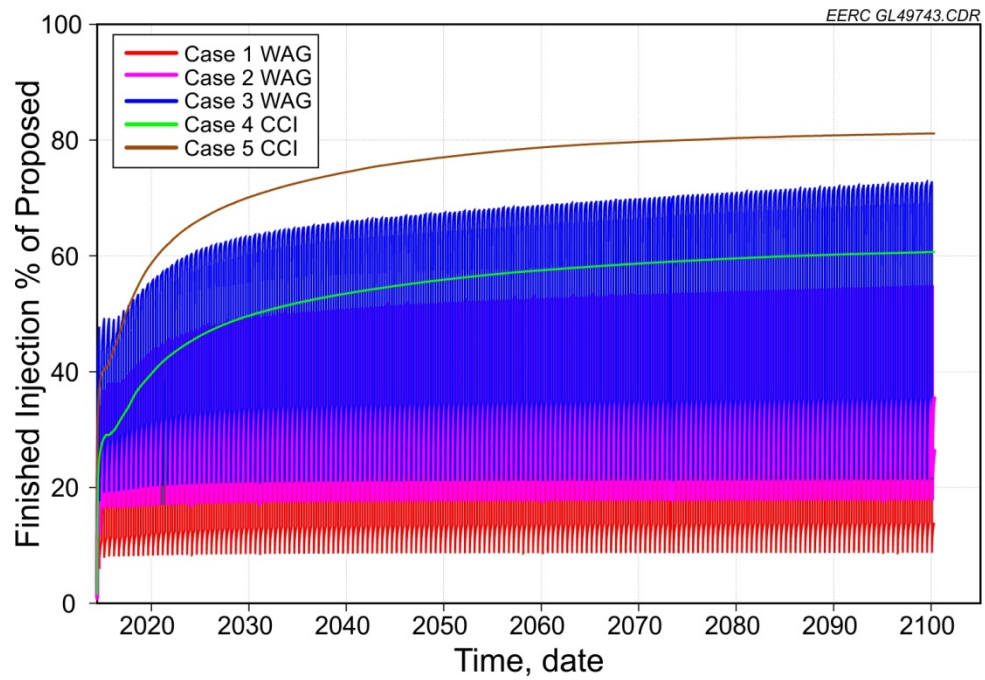


Figure 28. Actual injected CO₂ volume as a percentage of proposed CO₂ injection for Phase 2.

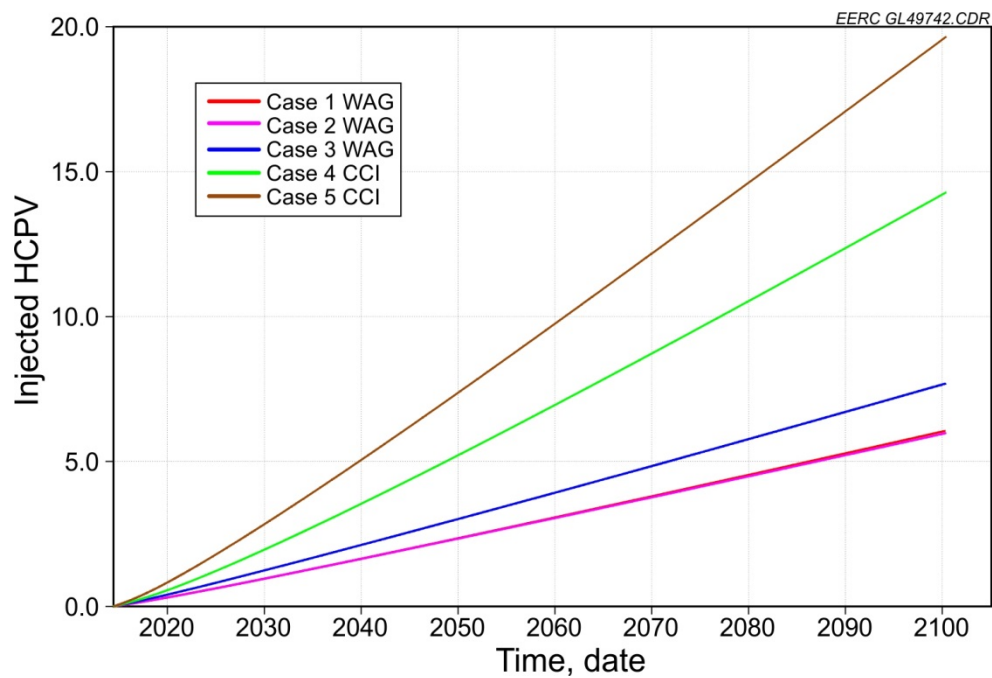


Figure 29. Comparison of cumulative equivalent volume injection in the Phase 2 area.

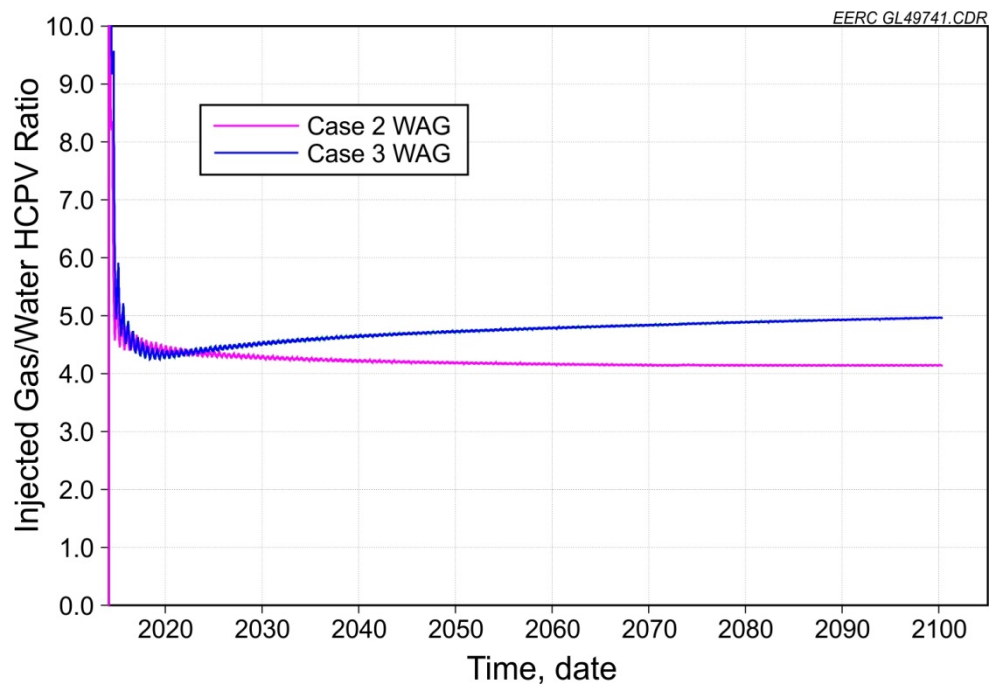


Figure 30. CO₂/water injectivity ratio for two WAG cases in the Phase 2 area.

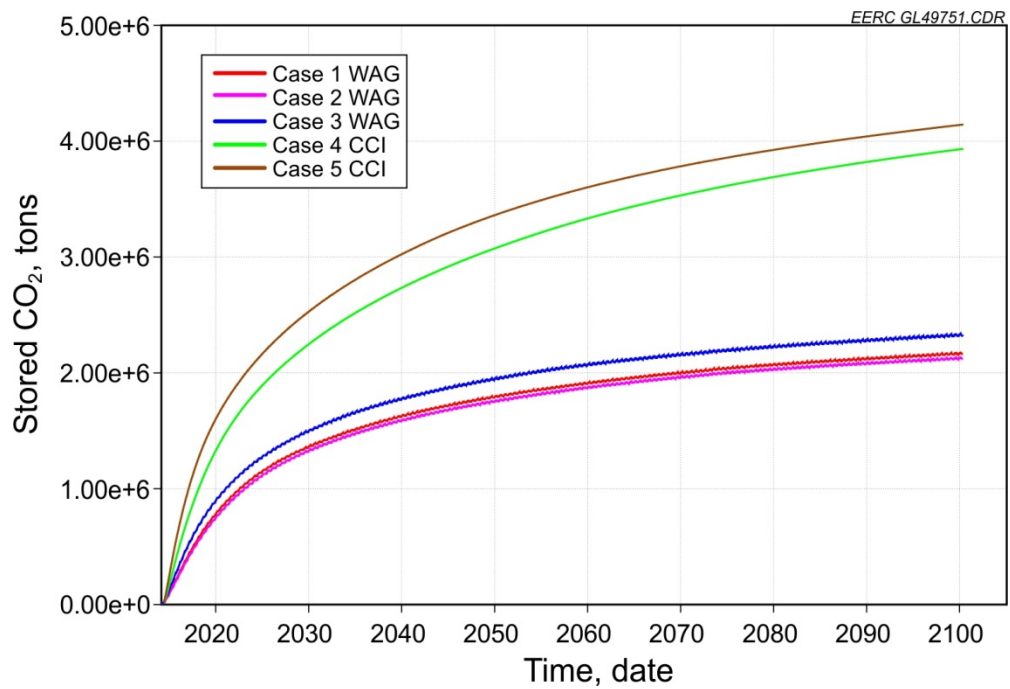


Figure 31. Stored CO₂ for all scenarios in the Phase 2 area.

Discussion of Incremental Oil Recovery, Utilization Factor, and Oil Production

The incremental oil recoveries versus time and HCPVI for all cases are shown in Figures 24 and 25, respectively. Among the five predictive scenarios, Case 3 with WAG at an operating injection pressure of 2900 psi yields the highest oil recovery with equivalent injection volume. Comparing the oil recoveries of Case 1 (WAG with hysteresis), the value is lowest even compared to cases with CCI. Overall, the oil recovery percentages in Cases 4 and 5 are similar, although the produced oil rates are different with the same HCPVIs (Figures 25 and 26).

The CO₂ utilization factors for Cases 1–5 are shown in Table 7 and Figure 27. WAG scenarios (Cases 1–3) have CO₂ utilization factors ranging from 4.85 to 5.17 Mscf/bbl for various operating injection pressures, while the CCI shows a higher CO₂ utilization factor of about 7.52 Mscf/bbl on average. With hysteresis considered in the model, the utilization factor indicates that Case 1 could store more CO₂ than other WAG cases.

Compared with Phase 1, Phase 2 CO₂ injectivity is relatively lower, which is primarily the result of the injection/production ratio under BHP constraints. In the Phase 1 model, the injection/production ratio is 26:26, which is much lower than the 21:15 ratio in the Phase 2 model.

With regard to cumulative oil production, the results are higher with WAG injection in Cases 2 and 3 than with CCI in Cases 4 and 5 at the same injected HCPVIs. Hysteresis decreases cumulative oil production slightly, as shown in a comparison of Cases 1 and 2. The peak rate of CCI is better than in the WAG scenarios, which is different from Phase 1 results (Figures 24–26).

Effect of Injection Mode

For injection wells, injection pressure constraints of 2700 and 2900 psi were used in the predictive simulation cases (Table 5). In addition to geologic transmissivity, the predictive results show that the injection pressure significantly affects the actual amount of injected CO₂, and all cases experienced injection rates lower than the targeted 2.7 MMscf/well/day. Overall, approximately 50% of the CO₂ and 15% of the water were injected in Case 3 with 2900 psi of injection BHP. The number is even lower for the rest of the WAG cases (Table 6). The cases with CCI followed the same trend, and the total injected fluids were at least 20% lower than the targeted values (Figure 28). A comparison of cumulative equivalent volume injected and ratio of injected CO₂ and water among the scenarios is plotted in Figures 29 and 30. The ratio of injected CO₂/water for all scenarios is much higher than the proposed value of 1:1 (Figure 30).

With regard to the proposed WAG ratio of 1:1 for 3 HCPV CO₂ and 3 HCPV water, the daily CO₂ injection rate was 26.5 MMscf/day, which was distributed among 11 injection wells, and the daily water injection rate of 12,210 bbl/day was distributed among the other 11 injection wells. The ultimate recovery for Case 1 (WAG with hysteresis) was 22.96% of OOIP after 6 HCPVI, while the oil recovery was 24.06% of OOIP for Case 5 (Table 7, Figures 24 and 25).

CO₂ Stored

The stored CO₂ for the WAG scenarios varied from 2.11 to 2.22 Mt, while the stored CO₂ for the CCI scenarios was about 3.20 Mt. This discrepancy is caused by doubling the volume of cumulative CO₂ injected for the CCI cases compared to the WAG cases. The results for each injection case are illustrated in Figure 31. The earliest CO₂ breakthrough occurred about 4 months after the start of CO₂ injection for the continuous CO₂ flooding scenario, while the earliest CO₂ breakthrough with WAG occurred in the Phase 2 area after 5 months.

SUMMARY

During the last year, modeling and simulation activities for the Bell Creek CO₂ EOR and storage project were updated, including development of the reference model, the baseline and repeat PNL campaign, history matching the Phase 2 model, and predictive simulation in both Phases 1 and 2. Multiple simulation scenarios for both phases were developed and tested in order to estimate associated CO₂ storage potential for the Bell Creek Field as well as to better understand factors that affect CO₂ EOR, such as sweep efficiency, recovery factor, and CO₂ utilization. Additionally, these results will assist with risk assessment and MVA planning for long-term storage. Key highlights and results of the current simulation activities include the following:

- Thirty-three baseline PNLs and seven repeat PNLs provided confidence in updating the local stratigraphic column and thicknesses in the area of investigation from reservoir to ground surface. Moreover, changes in fluid saturations of CO₂, water, and oil were also identified through the repeat logs on certain injection and production wells. These results have been integrated into the ongoing modeling and simulation activities.
- A reference model was built in Petrel to house all modeling and characterization data. The model includes both V1 and V2 geologic models, PNLs, and both historic and newly acquired logs and core data.
- A Phase 2 area model was created from the V2 fieldwide 3-D geologic model and was validated by history-matching oil, water, and gas production; water injection; and scattered reservoir pressure data.
- Both Phases 1 and 2 history-matched models were used for predictive simulations. Five scenarios for each phase (ten cases total) were designed to address reservoir fluid movement through continuous miscible CO₂ flooding and CO₂ WAG schemes.
- Given the same HCPVI, WAG scenarios yielded a higher oil recovery overall than CCI in both Phase 1 and Phase 2. Cases including relative permeability hysteresis for the gas phase resulted in slightly lower oil recovery than the cases without hysteresis. The highest incremental oil recovery was seen in cases with higher injection BHPs.
- Associated storage of CO₂ in WAG scenarios is higher for cases considering the effect of relative permeability hysteresis for the gas phase. However, associated CO₂ storage

for WAG scenarios is lower in all cases than those with continuous miscible CO₂ flooding. This results in lower CO₂ utilization factors for WAG than CCI.

- In WAG cases, the cumulative equivalent volume and ratio of injected water and CO₂ in the Phase 2 area are much higher than those in the Phase 1 area, primarily because of the injection/production ratio: 26:26 in Phase 1 and 21:15 in Phase 2. The unbalanced injection/production ratio in the Phase 2 area resulted in a quick decrease in injectivity.
- BHP value for injection wells plays a significant role in fluid injection and production. The cases with higher BHPs result in higher oil production and CO₂ and/or water injection in both WAG and CCI scenarios. However, because of the higher production, stored CO₂ in these cases is lower than other cases in both schemes that ultimately result in higher recovery factors and lower CO₂ utilization factors.
- Generally, the trends of oil recovery factor, CO₂ stored, and CO₂ utilization for Phases 1 and 2 are similar, although the area, well numbers, injectivity, and productivity are quite different between them.

LIMITATIONS

Although meaningful simulation results have been presented here, they are primarily based on the V2 geologic model. This version, while still useful, does not contain certain data that have been collected in the past year. As a result, a V3 model is currently under development that will further reduce uncertainty by incorporating petrographics, outcrop fieldwork, VSP (vertical seismic profile) surveys, 3-D seismic survey, PNLs, and additional core characterization data. The following improvements will be made: 1) the petrophysical facies will be correlated to both core and petrographic descriptions, 2) PNLs will provide a better stratigraphic and structural framework as well as monitor changes in reservoir fluid volumes and ensure CO₂ containment, and 3) VSP and 3-D seismic survey data will provide a detailed structural framework with geobody representation and inversion values for reservoir properties that will be cokriged to the existing petrophysically derived properties.

Although several scattered reservoir pressure data points were matched, a limitation of this dynamic simulation work is still the history matching of average reservoir pressure, since only the initial and limited average pressures are available. More historical reservoir pressure data would lead to more accurate calculated pressure; however, these data are not available.

During the predictive simulation of CO₂ flooding, the relative permeability hysteresis and CO₂ solubility in the aqueous phase were considered for only select cases, so the estimated incidental CO₂ storage capacity values for different cases may appear to be on the lower side overall. The WAG ratio of 1:1 was used in all of the simulation cases, but in future predictive simulation, other injection ratios may be evaluated for their effects on associated CO₂ storage and incremental oil recovery.

ONGOING WORK

V3 3-D Geologic Model

Ongoing characterization and monitoring efforts have created large data sets, including PNLs, structural and seismic interpretation, core analysis, and history-matching results, that have important roles in improving the structural, petrophysical, and saturation models of the Bell Creek Field. All of these data will serve as the basis for a V3 model that will build upon V2 to reduce uncertainty in the geologic interpretations.

The V3 structural model will update surfaces created from the results of the PNLs and 3-D seismic survey interpretation and enhance the lateral structural resolution between wells. This enhanced resolution will provide a more accurate calculation of pore volumes and help identify structural features and thickness uncertainties that may inhibit flow throughout the reservoir as well as above and below to ensure CO₂ containment.

An integrated approach will be used to create a facies and associated petrophysical model using results from the seismic survey, PNLs, and core descriptions as well as recent core analysis and interpretation. The seismic survey will highlight areas that may be geologically similar, termed “geobodies.” These geobodies typically have similar seismic amplitudes or attributes and can be a direct correlation for the facies model.

Once the core, seismic, and log data are integrated and processed, a detailed facies model will be created using multipoint statistics (MPS). This approach is a pixel-based modeling algorithm that resembles object modeling by capturing the geologic heterogeneity of a depositional system. The MPS algorithm uses a training image (TI) that captures the geometries of the depositional environment and uses the statistics of the hard and soft data sets from those geometries to populate the model. For the V3 Bell Creek model, this will include the use of the soft probabilities calculated from the seismic and identified geobodies. Additionally, the core descriptions and well logs will also serve as control points for guiding the MPS algorithm. The results of the facies model will provide a facies distribution similar to that seen in a modern-day depositional environment. Porosity, permeability, fluid saturation, and other key rock properties are then populated based on field tests and the PNLs. An upscaling process will be followed to prepare an appropriate simulation model.

Fluid Model and Reservoir Simulation

EOS and Relative Permeability Curves

Through the special core analysis being conducted by Core Labs, the relative permeability curves will be updated and the revised versions used in the next cycle of activities. The new version simulation model may have up to five sets of relative permeability curves. The new measured relative permeability curves will provide additional insight into CO₂ EOR efficiency, which will be used to improve predictive scenarios.

History Matching of CO₂ Flood

The manual history-matching method used for the current dynamic simulation was obtained by running simulations for the historical period, comparing results to actual field data, and adjusting simulation input to improve match. This process is very onerous and time-consuming. Automatic history-matching techniques, e.g., CMG's CMOST, automatically vary reservoir parameters until criteria are achieved and a history match of field performance is obtained. Computer-aided history matching by CMOST, which minimizes the global objective function error, e.g., the difference between observed reservoir performance and simulation results, is planned for the future round of dynamic simulations.

The production and injection history of the CO₂ flood from the start of CO₂ injection to April 16, 2014, was added to the previously history matched simulation model, and the history matching work of newly added CO₂ injection is under way. After a satisfactory history match of CO₂ flood is achieved, the matched model will be used for the predictive simulation of other CO₂ injection scenarios.

Integrated History Matching of Phases 1 and 2

Simulation efforts will be recombined to achieve an integrated model covering both the Phases 1 and 2 areas. The experience derived from the history matching of each individual phase will be used to ensure the quality of the combined model and speed up the history-matching process. In addition to the regular indices to be matched, the combined model will partially focus on the fluid communications between phases.

3-D Mechanical Earth Model

In order to assess the state of stresses and reservoir mechanical properties (e.g., rock strength, pore pressure, in situ stress, and elastic properties) caused by injection and production, a 3-D mechanical earth model (MEM) is currently being created for the Bell Creek Field. The 3-D MEM will aid in the understanding of reservoir response to various stress states, assisting with the prediction of formation deformation, permeability variation, and the maximum injection rate and pressure that can be used without compromising the integrity of the reservoir and confining units.

The 3-D MEM is being created based on the existing 1-D MEM, while incorporating several additional wells with geomechanical property logs, wells with PNLs run to the near-surface, and 3-D seismic data. The 3-D MEM will contain a combination of stress states, geologic structure, seismic inversion-derived lithofacies, and reservoir elastic properties. All of the geomechanical properties will be populated into the whole field by the petrophysical modeling process in Petrel, with the 3-D seismic property as the secondary data.

Once completed, this fieldwide 3-D MEM will be used to conduct geomechanical simulations. The dynamic simulations of the rock mechanical properties and reservoir conditions will provide more accurate support for the prediction of wellbore instability, fault reactivation, and potential leakage of CO₂ during injection, production, and long-term storage.

CONCLUSIONS

Over the past year, Bell Creek modeling and simulation activities have included a PNL campaign, creation of a reference model, history matching of the production/injection data and selected available reservoir pressures, and predictive simulations including WAG and CCI schemes with various BHPs for both Phases 1 and 2.

The PNL campaign with 33 baseline PNL and seven repeat logs provided confidence in identifying the stratigraphic column and thicknesses in the area of investigation from reservoir to ground surface. Moreover, fluid saturations of CO₂, water, and oil were also identified through the repeat logs on certain injection and production wells. These results have been integrated into a reference model along with other updated data from wells and are being used to track the presence of CO₂, directly benefitting the monitoring and risk assessment activities for the project.

The Phase 2 area model was clipped from the 3-D full-field geologic model (V2), validated by matching the historical production/injection and reservoir pressure data and, finally, used for various predictive CO₂ injection simulation scenarios. Predictive simulation using WAG scenarios yielded a higher oil recovery overall than CCI for both Phases 1 and 2. Cases including relative permeability hysteresis for the gas phase resulted in slightly lower oil recovery than the cases without hysteresis. The highest incremental oil recovery was seen in cases with higher injection BHPs. Cumulative oil production and recovery factor follow the same trend as oil recovery; however, the cases with CCI resulted in more CO₂ stored than the WAG cases. This results in higher CO₂ utilization factors for the CCI than WAG cases. The time required for CO₂ breakthrough at the first production well in Phase 1 is less than in Phase 2 because the well ratio in Phase 1 is 26:26, compared to 21:15 for Phase 2. This also resulted in different volume ratios of injected water and CO₂ for each phase. Simulation results from these activities will be incorporated into the overall iterative management approach for the project and used to refine site characterization and MVA activities, if necessary.

REFERENCES

- Braunberger, J.R., Hamling, J.A., Gorecki, C.D., Steadman, E.N., Harju, J.A., Miller, H., Rawson, J., Walsh, F., Pasternack, E., Rowe, W., and Butsch, R., 2014, Characterization and time-lapse monitoring utilizing pulsed-neutron well logging at an incidental CO₂ storage demonstration: Paper to be presented at the 12th International Conference on Greenhouse Gas Technologies (GHGT-12), Austin, Texas, October 5–9, 2014.
- Braunberger, J.R., Pu, H., Gorecki, C.D., Bailey, T.P., Bremer, J.M., Peck, W.D., Gao, P., Ayash, S.C., Liu, G., Hamling, J.A., Steadman, E.N., Harju, J.A., 2013, Bell Creek Test Site – Simulation Report: Plains CO₂ Reduction (PCOR) Partnership Phase III, Task 9 – Deliverable D66, Update 2, Technical report to U.S. Department of Energy National Energy Technology Laboratory, August.
- Gorecki, C., Hamling, J., Klapperich, R., Steadman, E., and Harju, J., 2012, Integrating CO₂ EOR and CO₂ storage in the Bell Creek oil field: Presented at Carbon Management Technology Conference, Paper 151476.

- Hamling, J.A., Gorecki, C.D., Klapperich, R.J., Saini, D., and Steadman, E.N., 2013, Overview of the Bell Creek combined CO₂ storage and CO₂ enhanced oil recovery project: *Energy Procedia*, v. 37, p. 6402–6411.
- Joekar-Niasar, V.F., Doster, R., Armstrong, T., Wildenschild, D., and Celia, M.A., 2013, Trapping and hysteresis in two-phase flow in porous media—a pore-network study: *Water Resources Research*, v. 49, p. 4244–4256, doi:10.1002/wrcr.20313.
- Land, C.S., 1968, Calculation of imbibition relative permeability for two- and three-phase flow from rock properties: *Journal of the Society of Petroleum Engineers*, v. 8, no. 2, p. 149–156; *Trans., AIME*, 243, SPE-1942-PA, doi: 10.2118/1942-PA.
- Pu, H., Hamling, J.A., Bremer, J.M., Bailey, T.P., Braunberger, J.R., Ge, J., Saini, D., Sorensen, J.A., Gorecki, C.D., Steadman, E.N., and Harju, J.A., 2011, Bell Creek Test Site – Simulation Report, Plains CO₂ Reduction (PCOR) Partnership Phase III, Task 9 – Deliverable D66, Technical report to U.S. Department of Energy National Energy Technology Laboratory, August.
- Saini, D., Braunberger, J.R., Pu, H., Bailey, T.P., Ge, J., Crotty, C.M., Liu, G., Hamling, J.A., Gorecki, C.D., Steadman, E.N., and Harju, J.A., 2012, Bell Creek Test Site – Simulation Report: Plains CO₂ Reduction (PCOR) Partnership Phase III, Task 9 – Deliverable D66, Update 1, Technical report to U.S. Department of Energy National Energy Technology Laboratory, August.
- Steadman, E.N., Anagnost, K.K., Botnen, B.W., Botnen, L.S., Daly, D.J., Gorecki, C.D., Harju, J.A., Jensen, M.D., Peck, W.D., Romuld, L., Smith, S.A., Sorensen, J.A., and Votava, T.J., 2011, The Plains CO₂ Reduction (PCOR) Partnership—developing carbon management options for the central interior of North America: *Energy Procedia*, v. 4, p. 6061–6068.

APPENDIX A

RESERVOIR SIMULATION RESULTS: PHASE 1

RESERVOIR SIMULATION RESULTS: PHASE 1

This appendix contains the detailed results of five predictive simulations based on the dynamic simulation model in Phase 1 (Figure A-1), which was clipped from the 3-D field model (Figure A-2). Injected and produced oil, CO₂, and water over the simulation period varied with total amount of hydrocarbon pore volume (HCPV) associated with water cut, gas-to-oil ratio (GOR), and average reservoir pressure profiles, shown in Figures A-3–A-17. The stored CO₂ for five cases is plotted in Figures A-18–A-22 for storage comparison over the various conditions. The CO₂ plumes with 1, 3, and 6 HCPV injected (HCPVI) are tracked for each case to monitor the fluid movement during the water alternating gas (WAG) and continuous CO₂ injection (CCI) scenarios in Figures A-23–A-27.

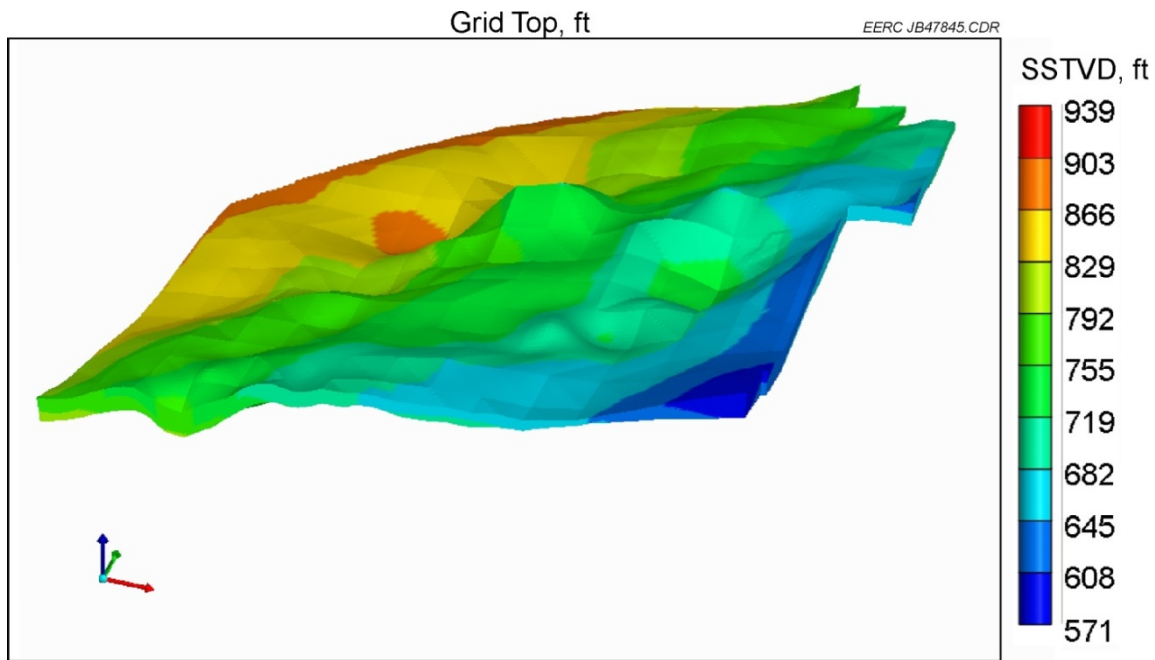


Figure A-1. 3-D view of Phase 1 simulation model (SSTVD is subsea true vertical depth).

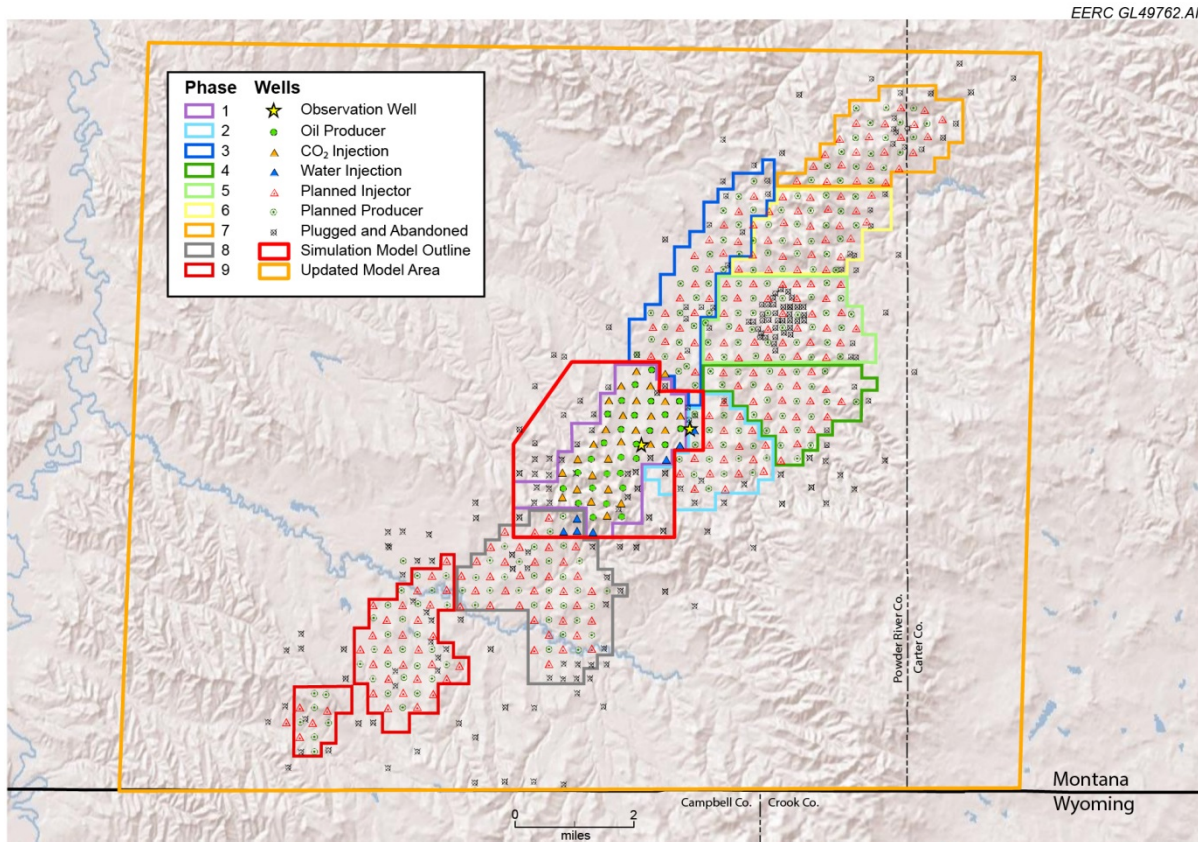


Figure A-2. Map of Phase 1 model area in field region.

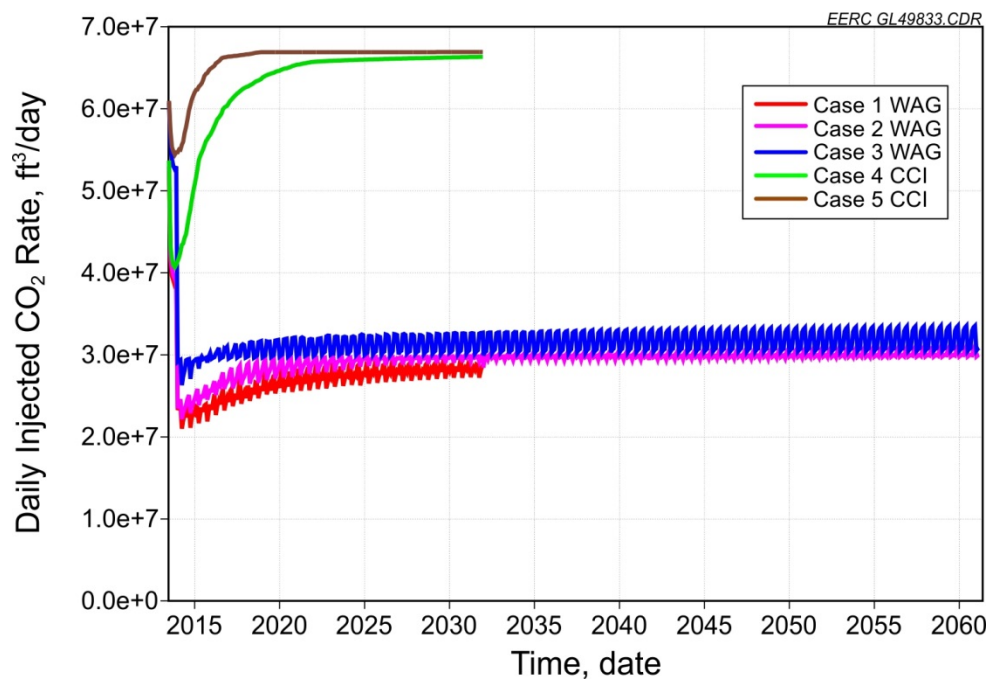


Figure A-3. Daily injected CO₂ for all five cases.

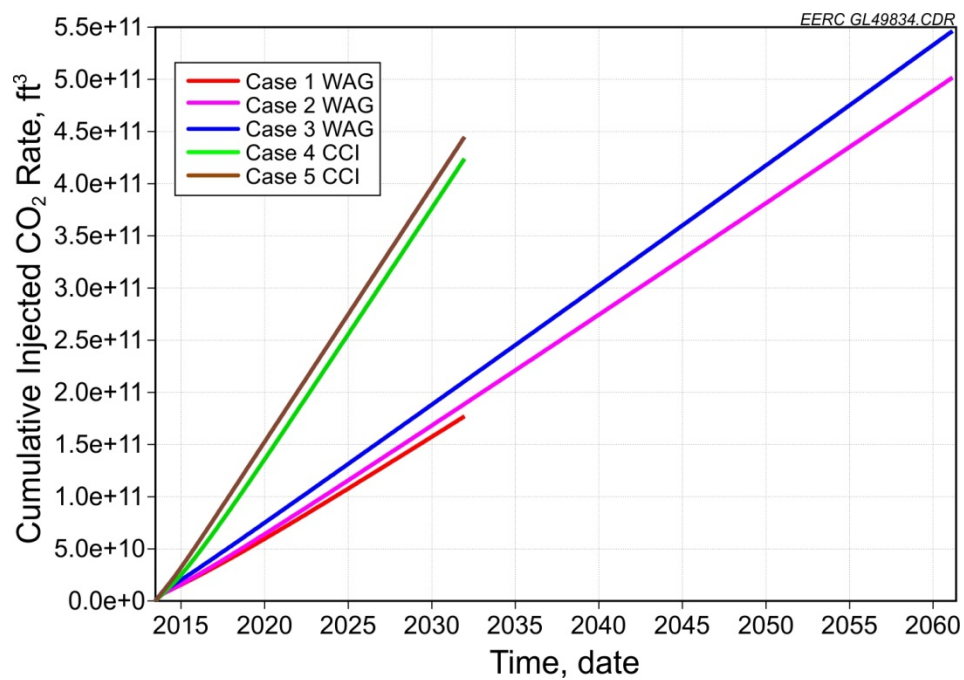


Figure A-4. Cumulative injected CO₂ for all five cases.

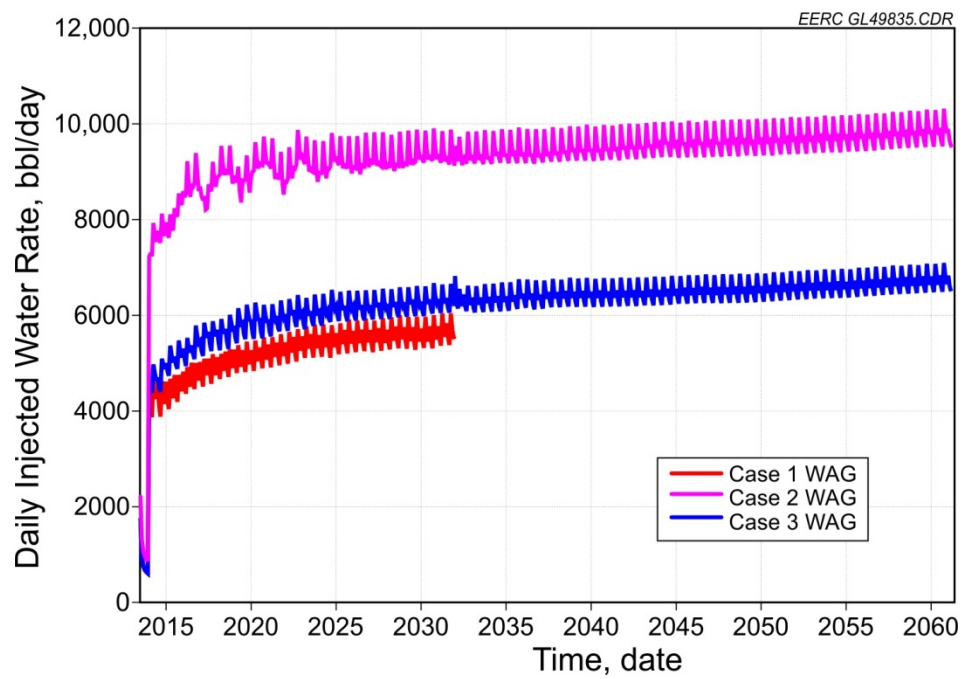


Figure A-5. Daily injected water for WAG cases.

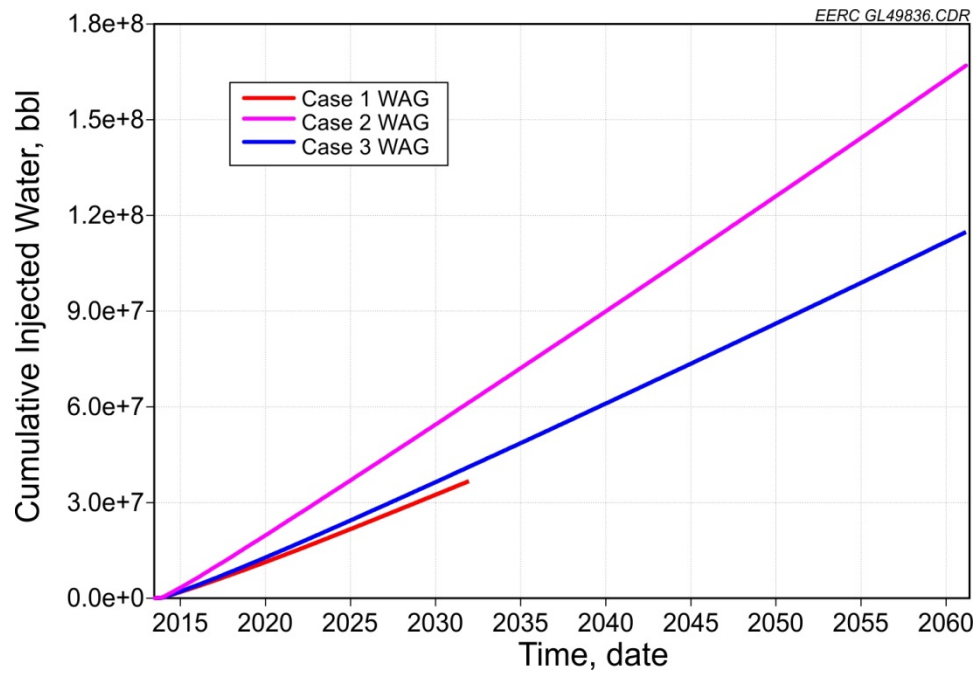


Figure A-6. Cumulative injected water for WAG cases.

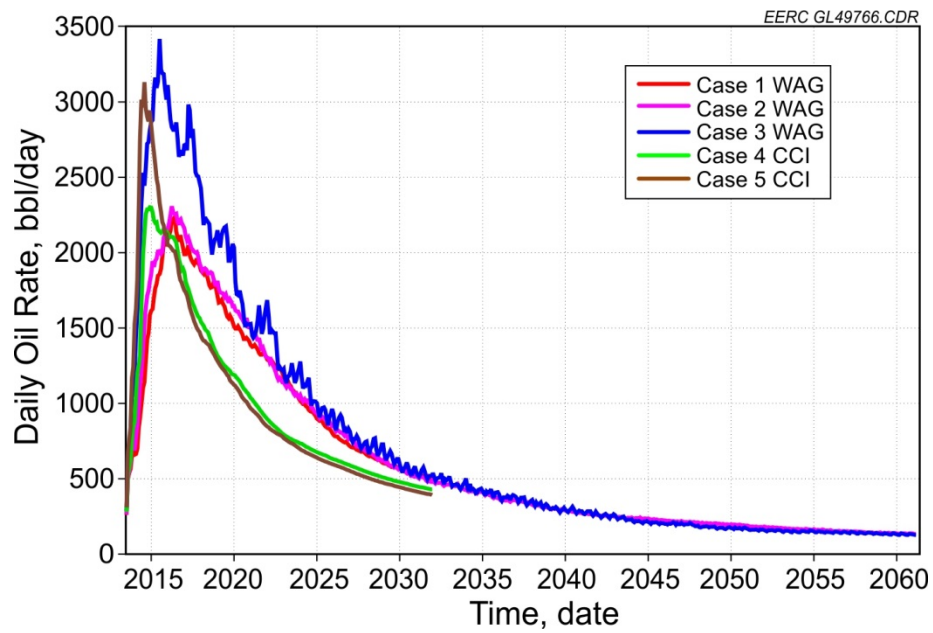


Figure A-7. Daily oil production for all five cases.

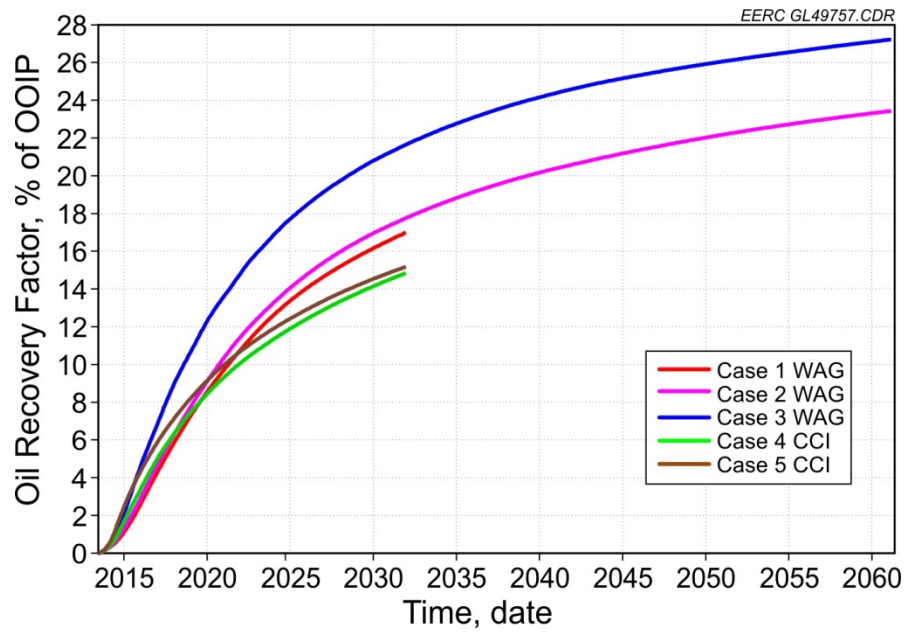


Figure A-8. Cumulative oil production for all five cases.

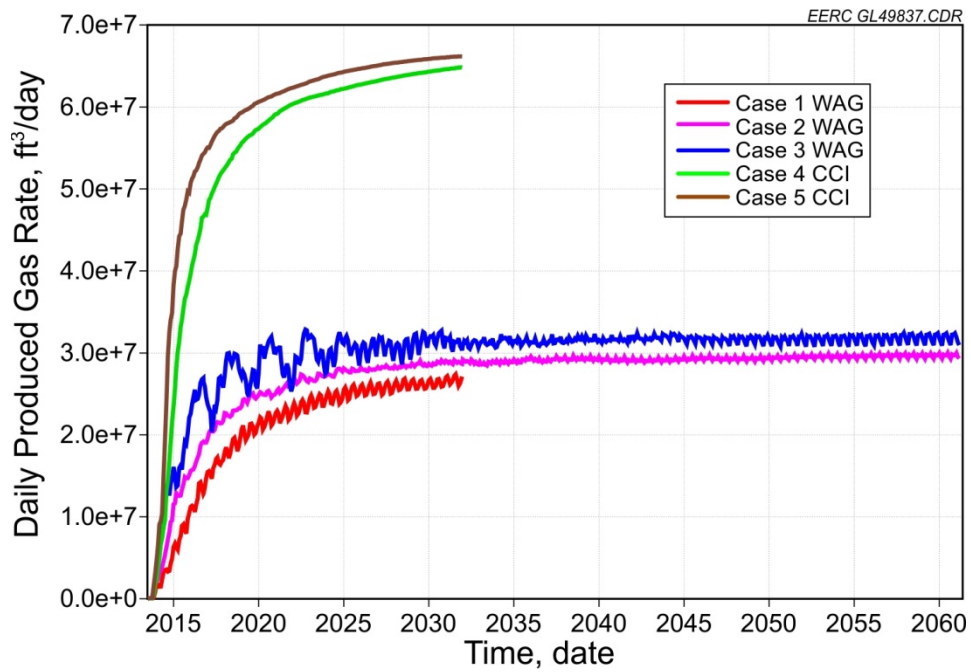


Figure A-9. Daily gas production for all five cases.

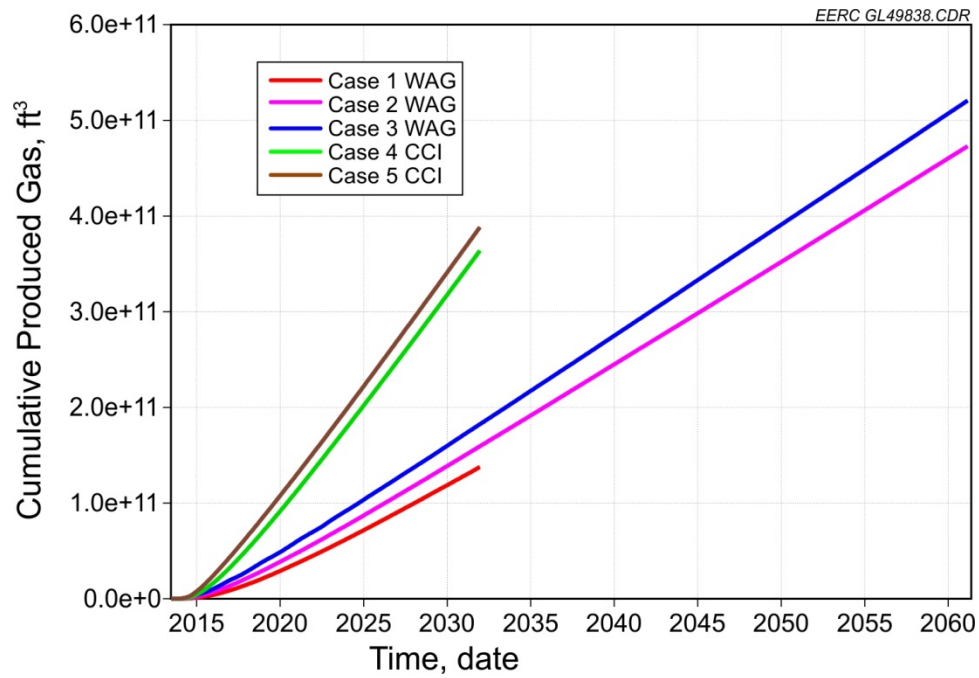


Figure A-10. Cumulative gas production for all five cases.

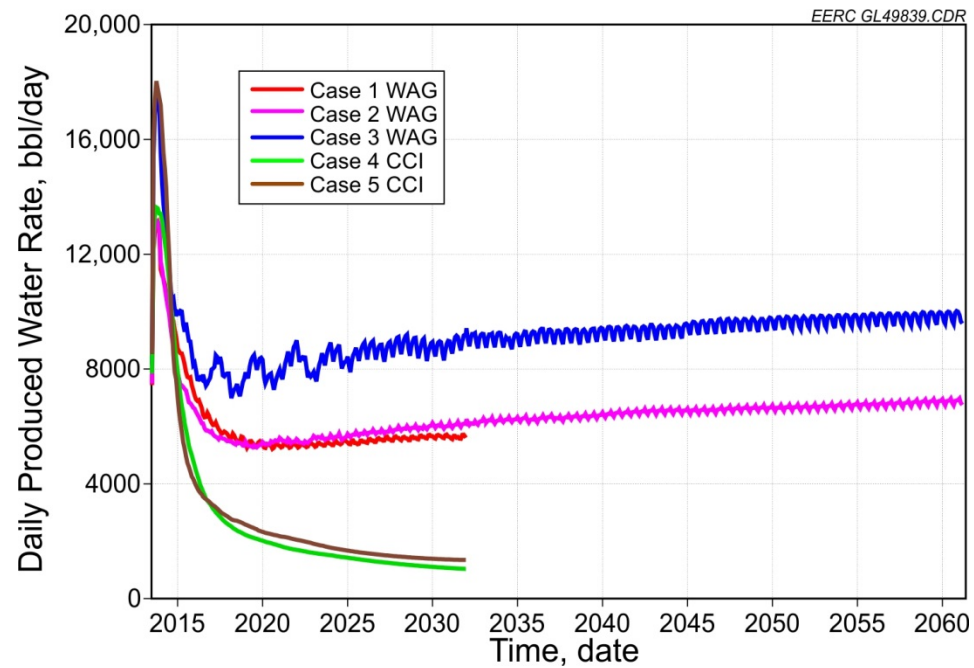


Figure A-11. Daily water production for all five cases.

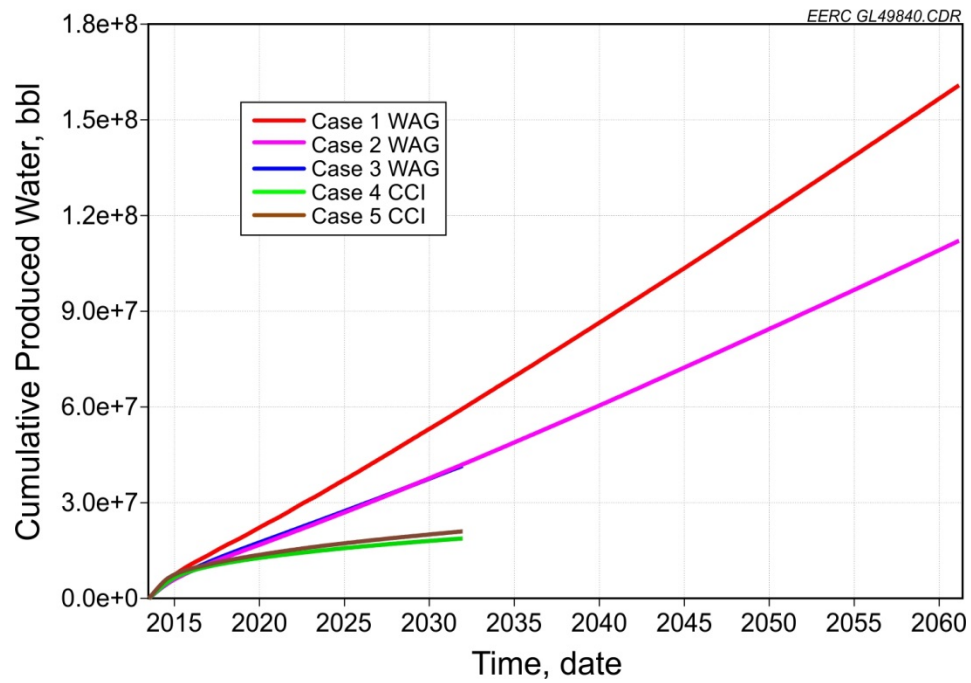


Figure A-12. Cumulative water production for all five cases.

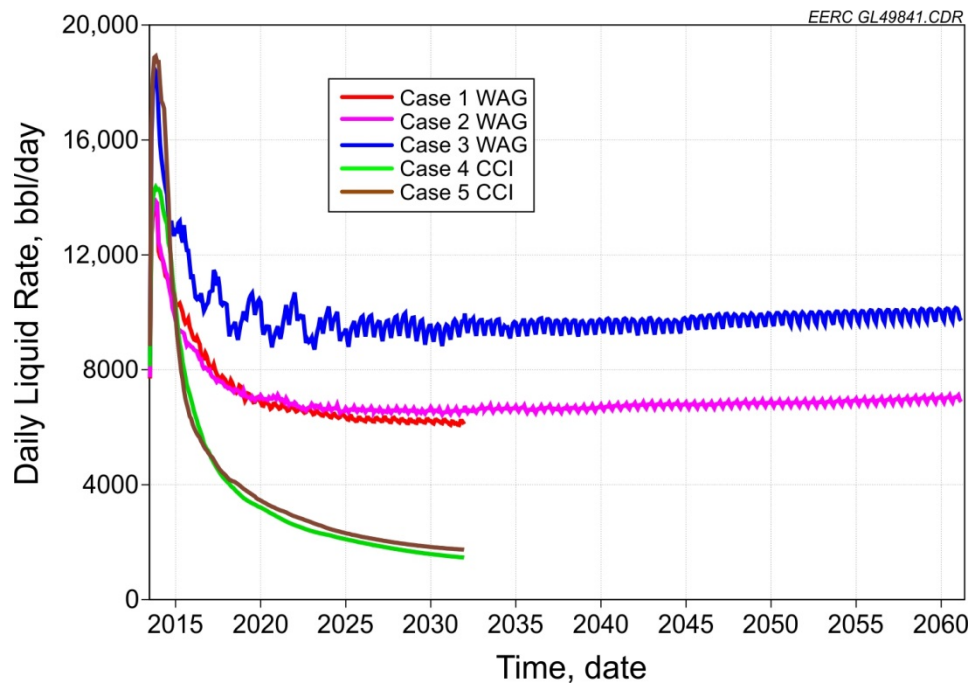


Figure A-13. Daily liquid production for all five cases.

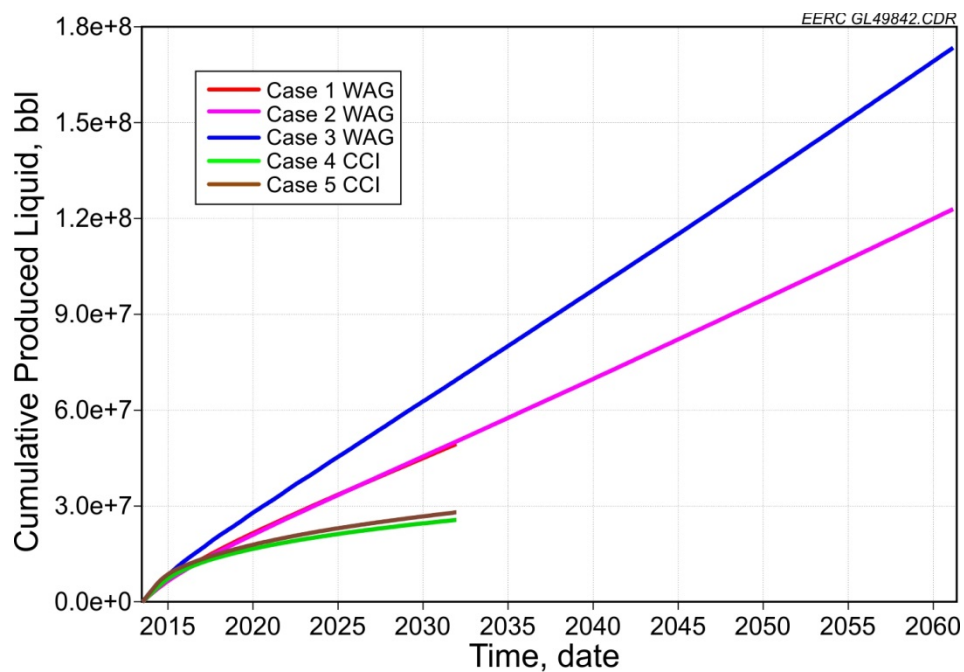


Figure A-14. Cumulative liquid production for all five cases.

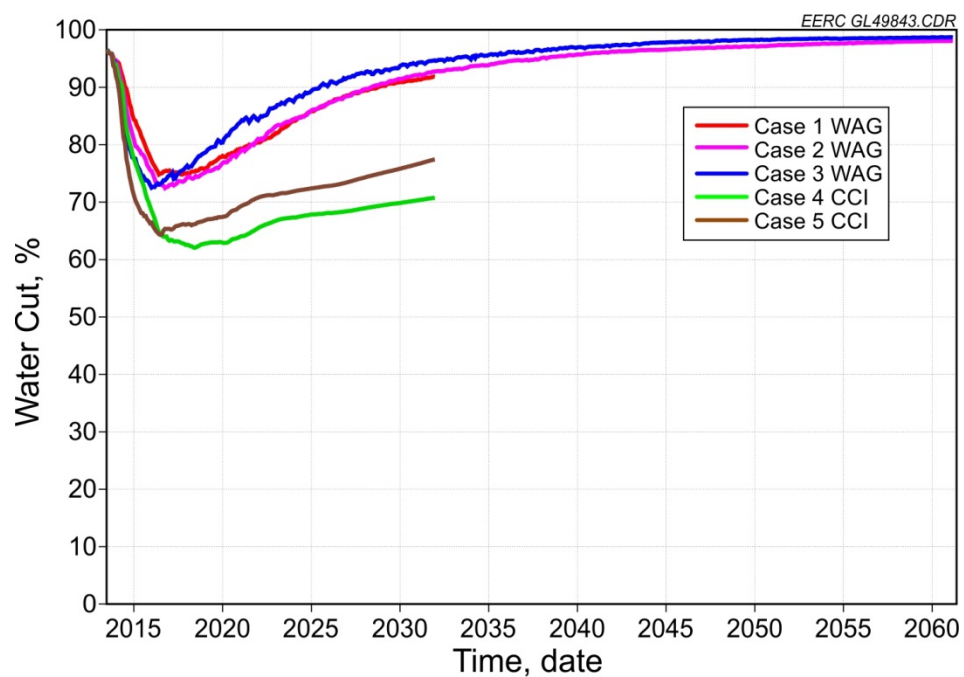


Figure A-15. Water cut for all five cases.

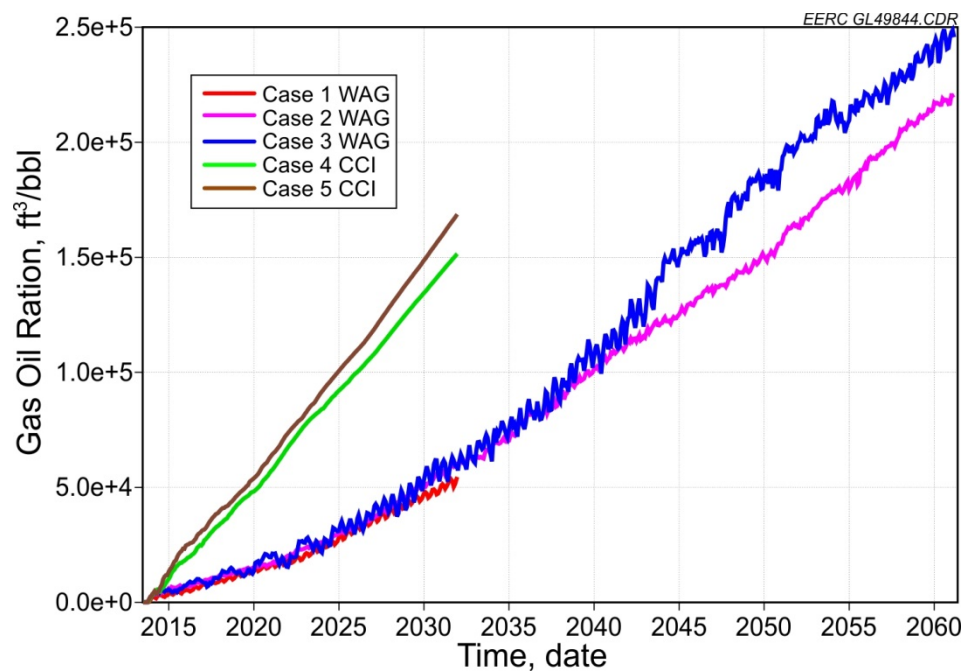


Figure A-16. GOR for all five cases.

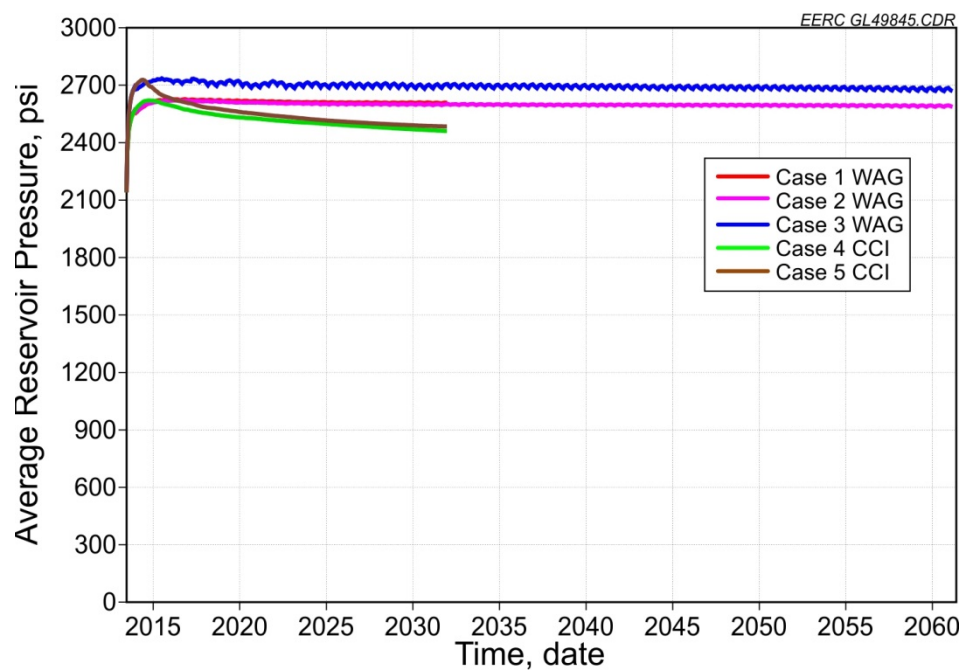


Figure A-17. Average reservoir pressure for all five cases.

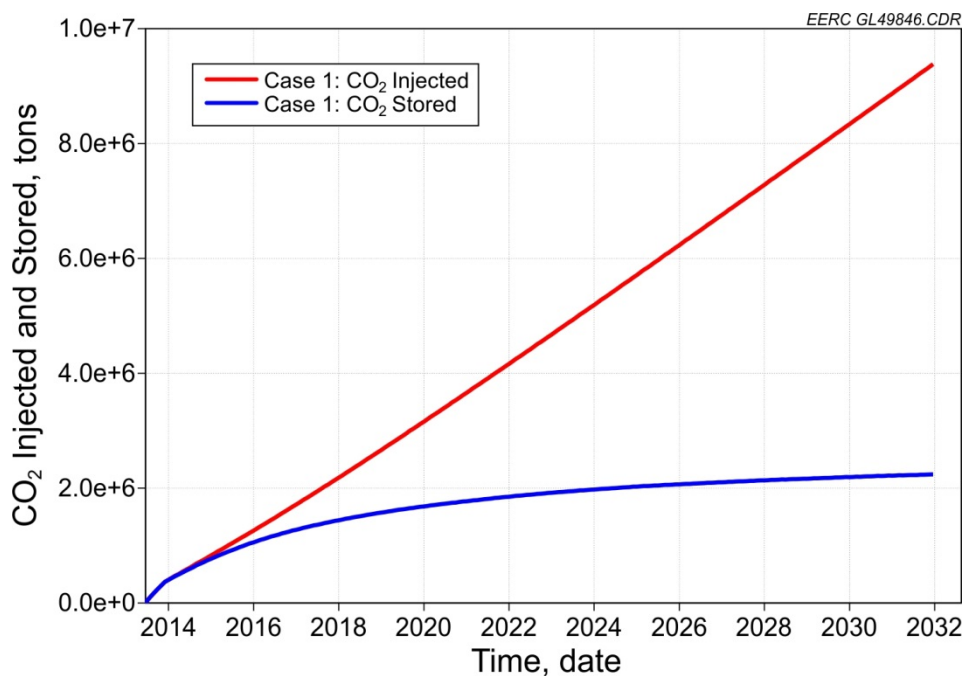


Figure A-18. Cumulative CO₂ injected and stored for Case 1 with WAG, injection pressure (IP) 2700 psi, production pressure (PP) 2300 psi, with hysteresis.

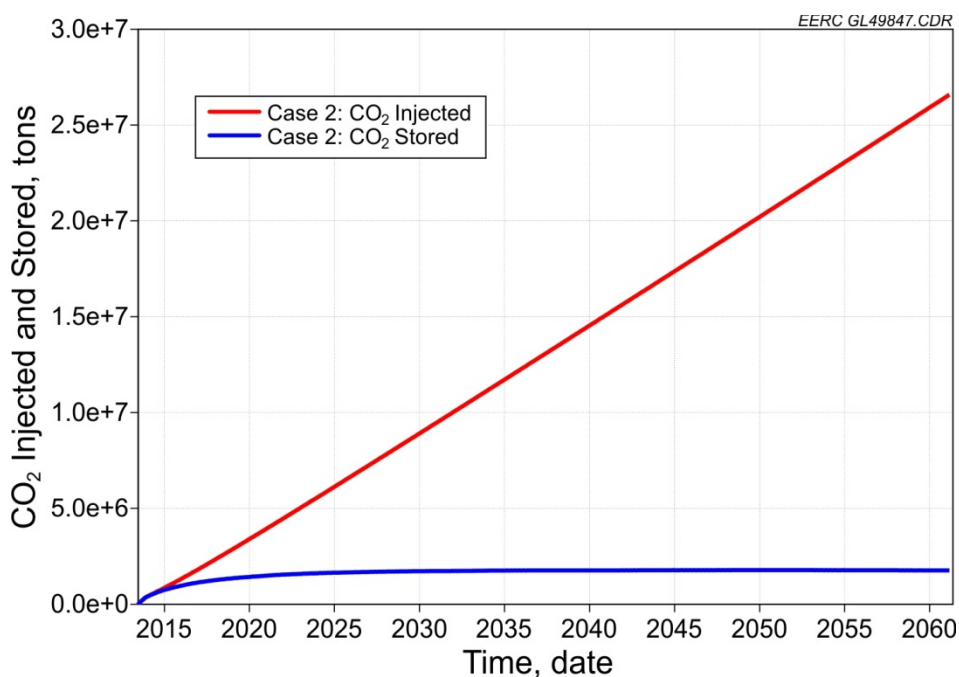


Figure A-19. Cumulative CO₂ injected and stored for Case 2 with WAG, IP 2700 psi, PP 2300 psi.

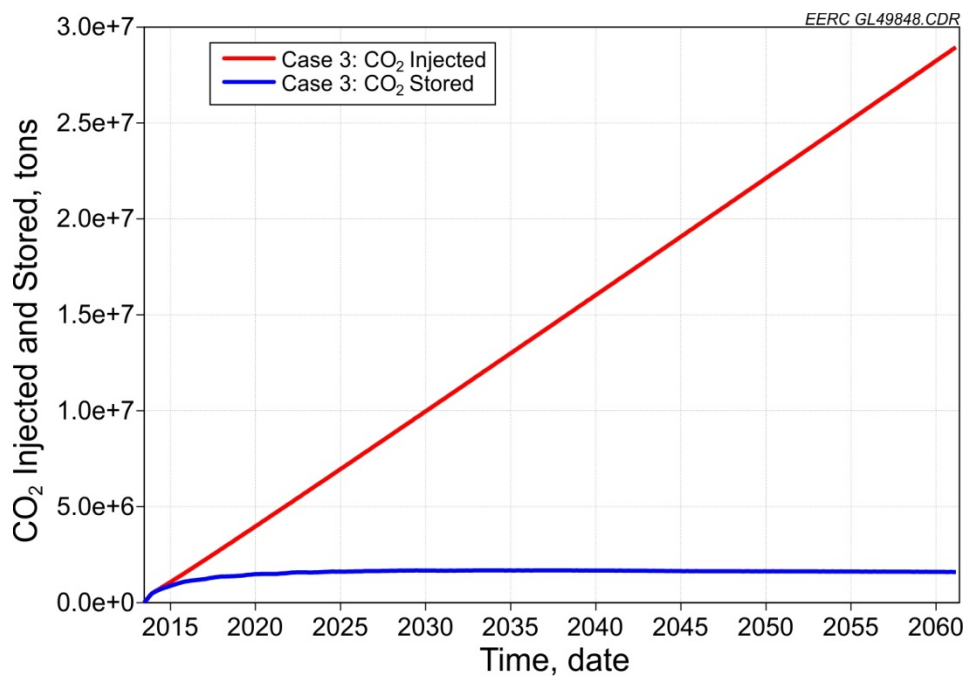


Figure A-20. Cumulative CO₂ injected and stored for Case 3 with WAG, IP 2900 psi, PP 2300 psi.

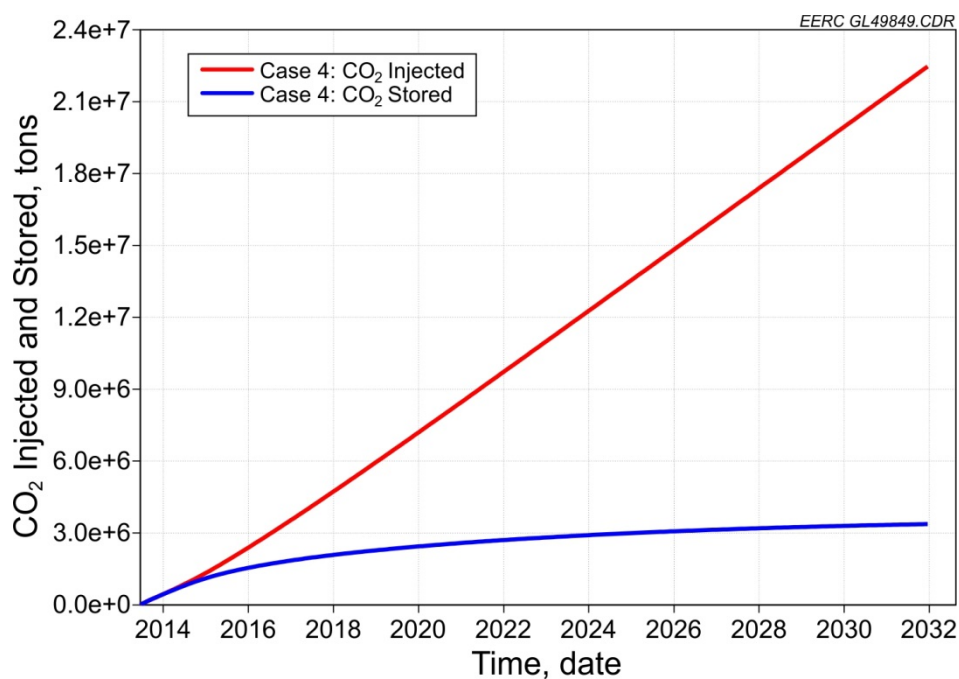


Figure A-21. Cumulative CO₂ injected and stored for Case 4 with CCI, IP 2700 psi, PP 2300 psi.

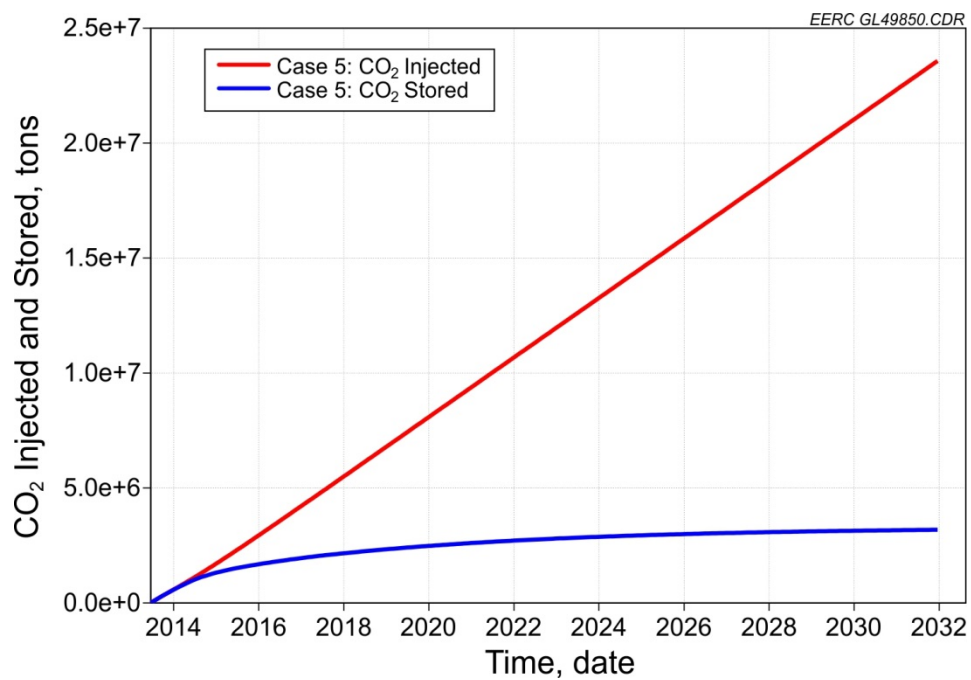


Figure A-22. Cumulative CO₂ injected and stored for Case 5 with CCI, IP 2900 psi, PP 2300 psi.

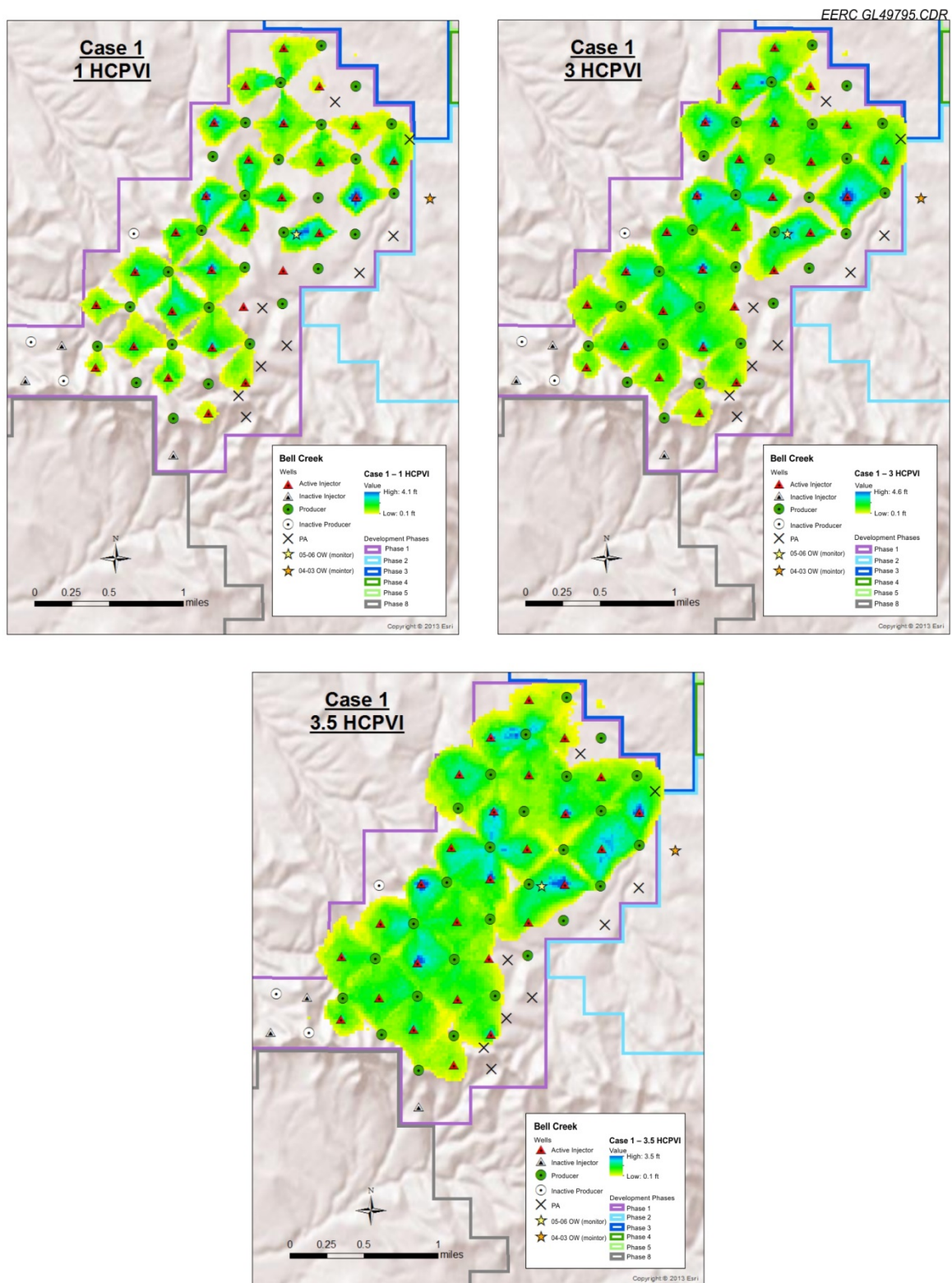


Figure A-23. Case 1 CO₂ plume at 1, 3, and 3.5 HCPVI.

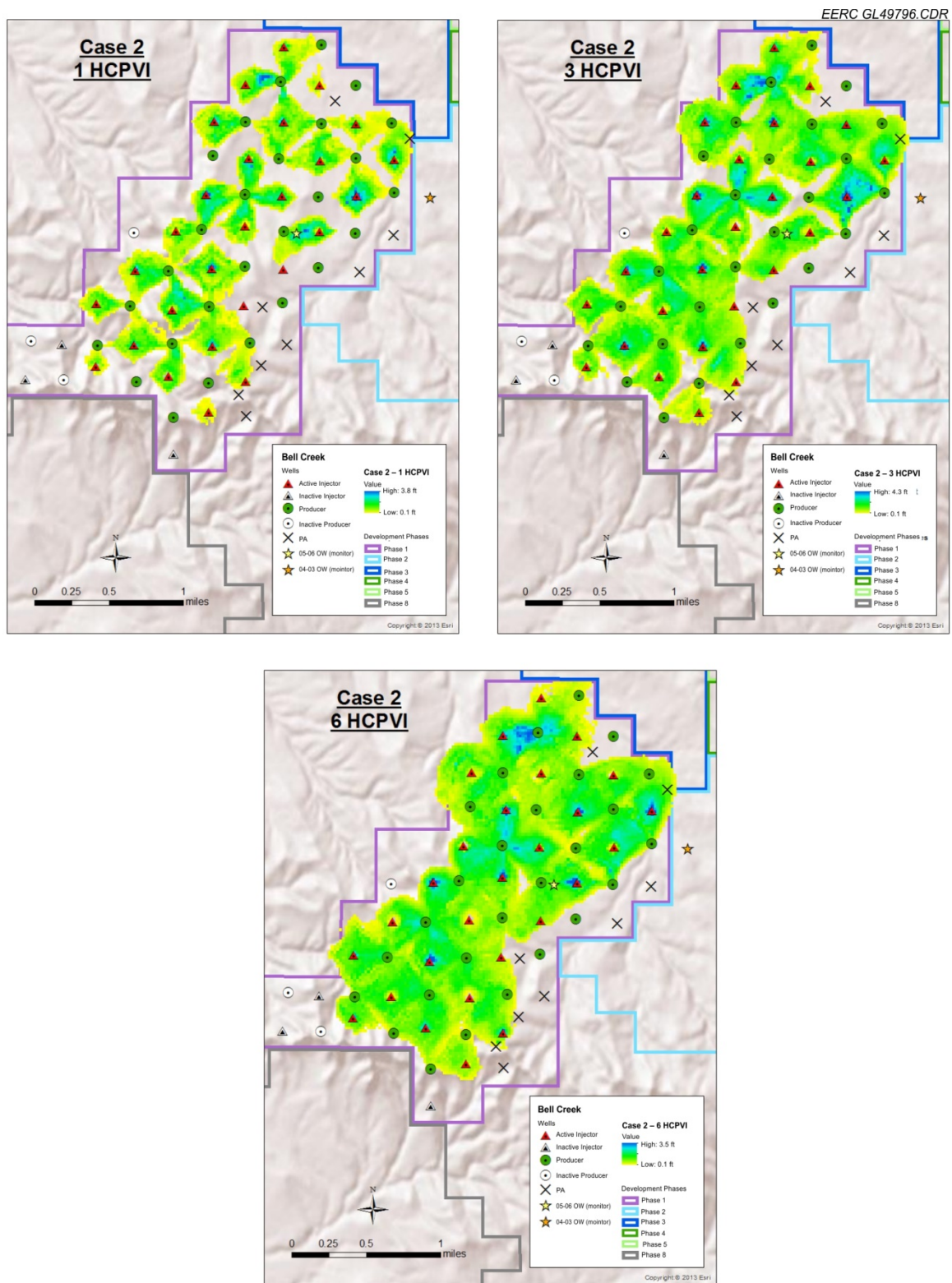
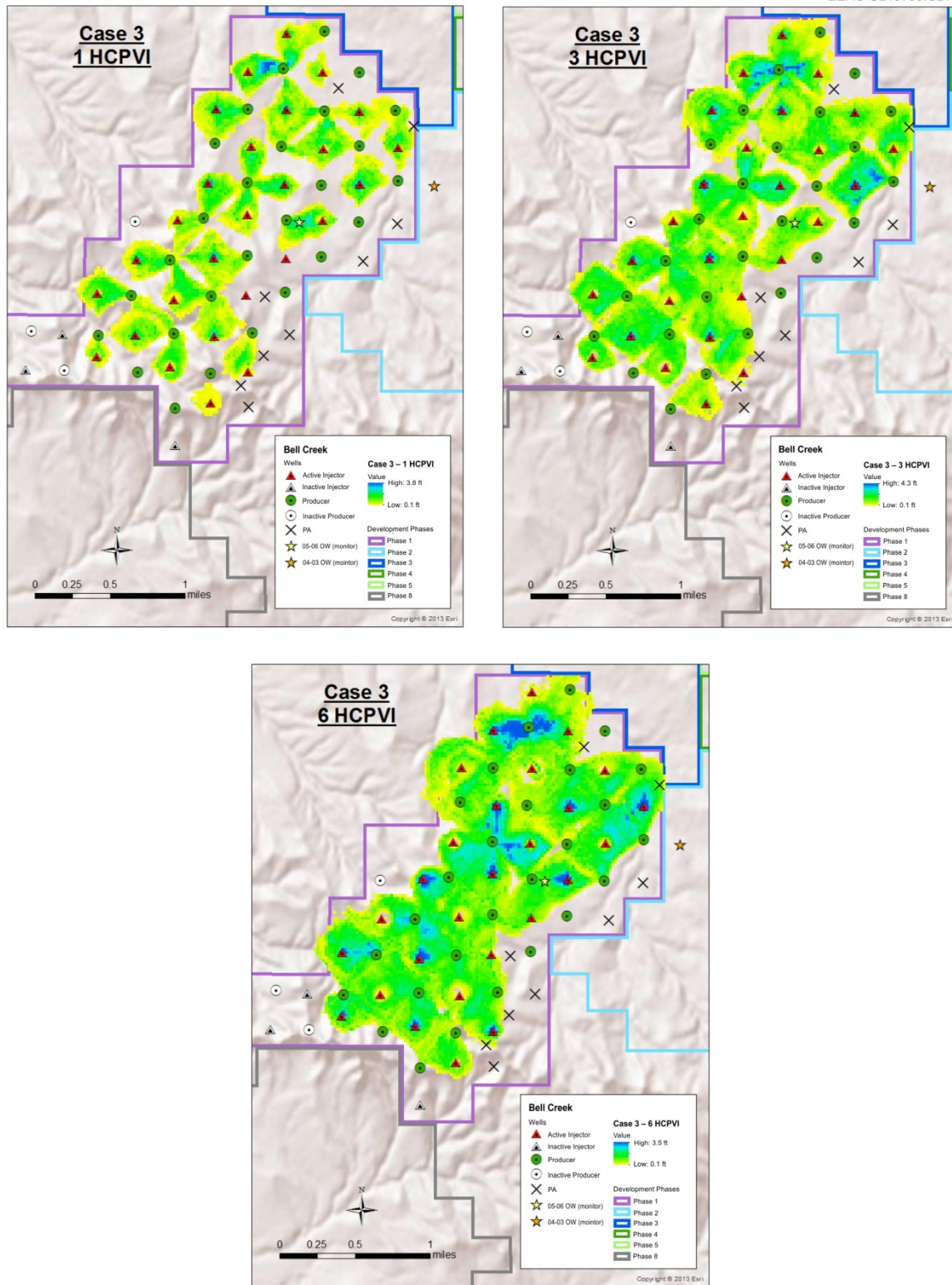


Figure A-24. Case 2 CO₂ plume at 1, 3, and 6 HCPVI.

Figure A-25. Case 3 CO₂ plume at 1, 3, and 6 HCPVI.

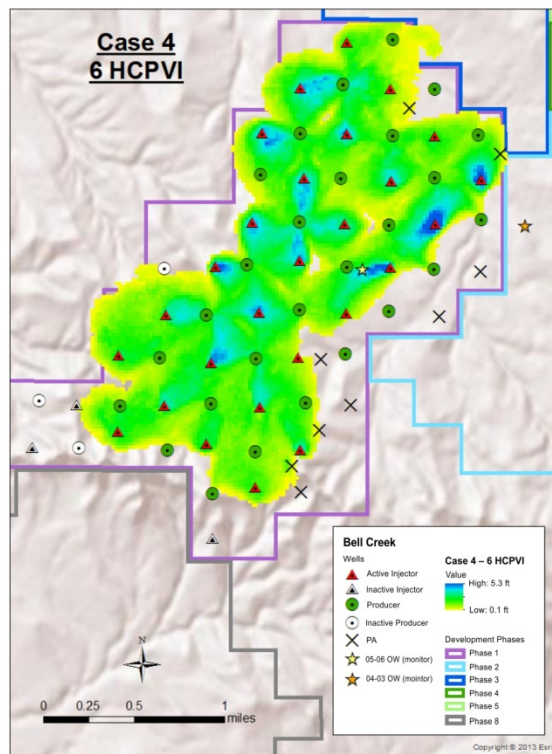
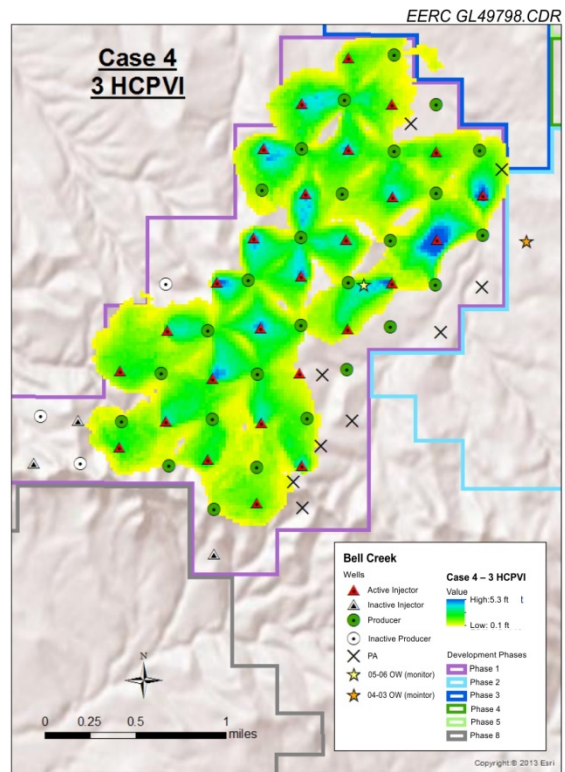
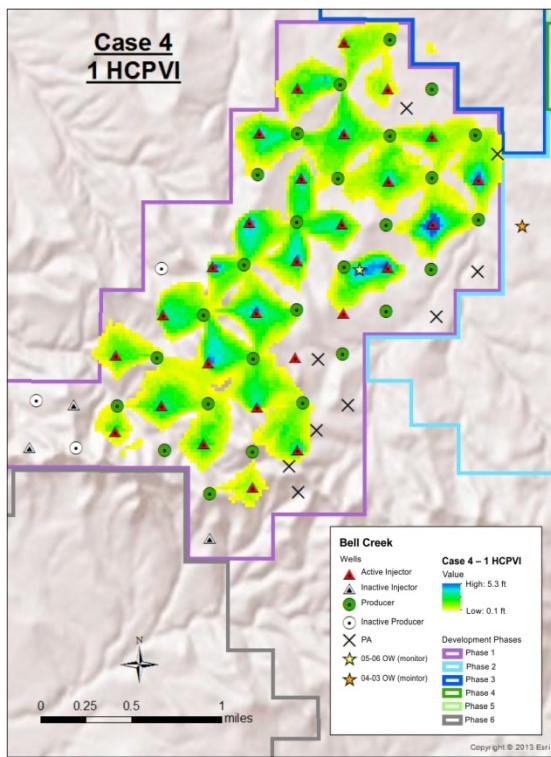


Figure A-26. Case 4 CO₂ plume at 1, 3, and 6 HCPVI.

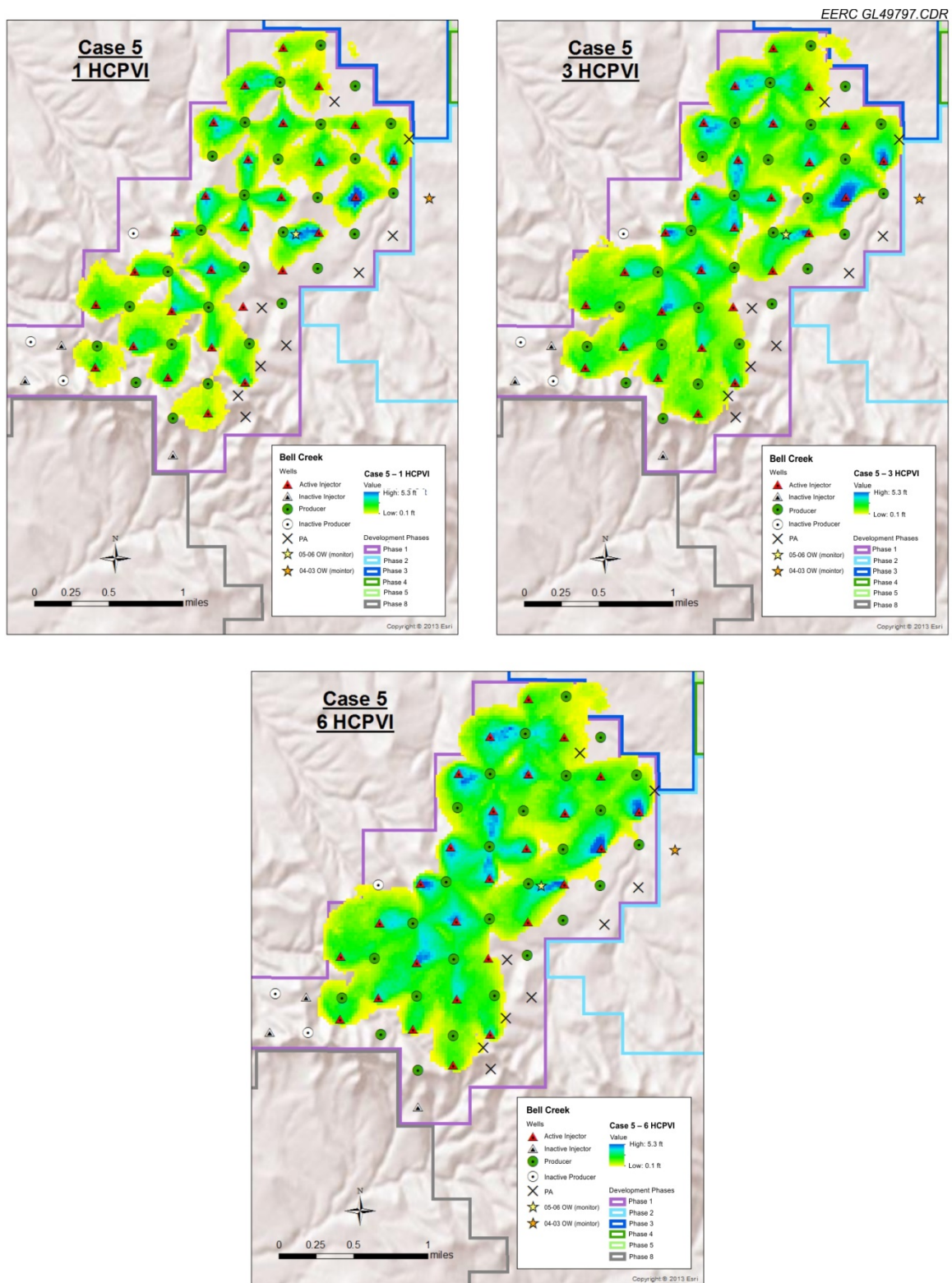


Figure A-27. Case 5 CO₂ plume at 1, 3, and 6 HCPVI.

APPENDIX B

RESERVOIR SIMULATION RESULTS: PHASE 2

RESERVOIR SIMULATION RESULTS: PHASE 2

This appendix contains the detailed results of Phase 2 history matching and five predictive simulations based on the dynamic simulation model, as shown in Figure B-1, which was clipped from the 3-D field model. History-matched results of oil and gas production, water cut, and average reservoir pressure for the Phase 2 are plotted in Figures B-2–B-5. The results in Figures B-6–B-11 show the water cut and oil production history matching for individual wells. Injected and produced oil, CO₂, and water over the simulation period vary with total amount of HCPV associated with water cut, gas-to-oil ratio (GOR), and average reservoir pressure profiles, shown in Figures B-12–B-27. Stored CO₂ for all five cases is plotted in Figures B-28–B-32 for storage comparison over the various conditions. The CO₂ plumes with 1, 3, and 6 HCPVI are tracked for each case to monitor the fluid movement during the WAG and continuous CO₂ injection (CCI) scenario in Figures B-33–B-37.

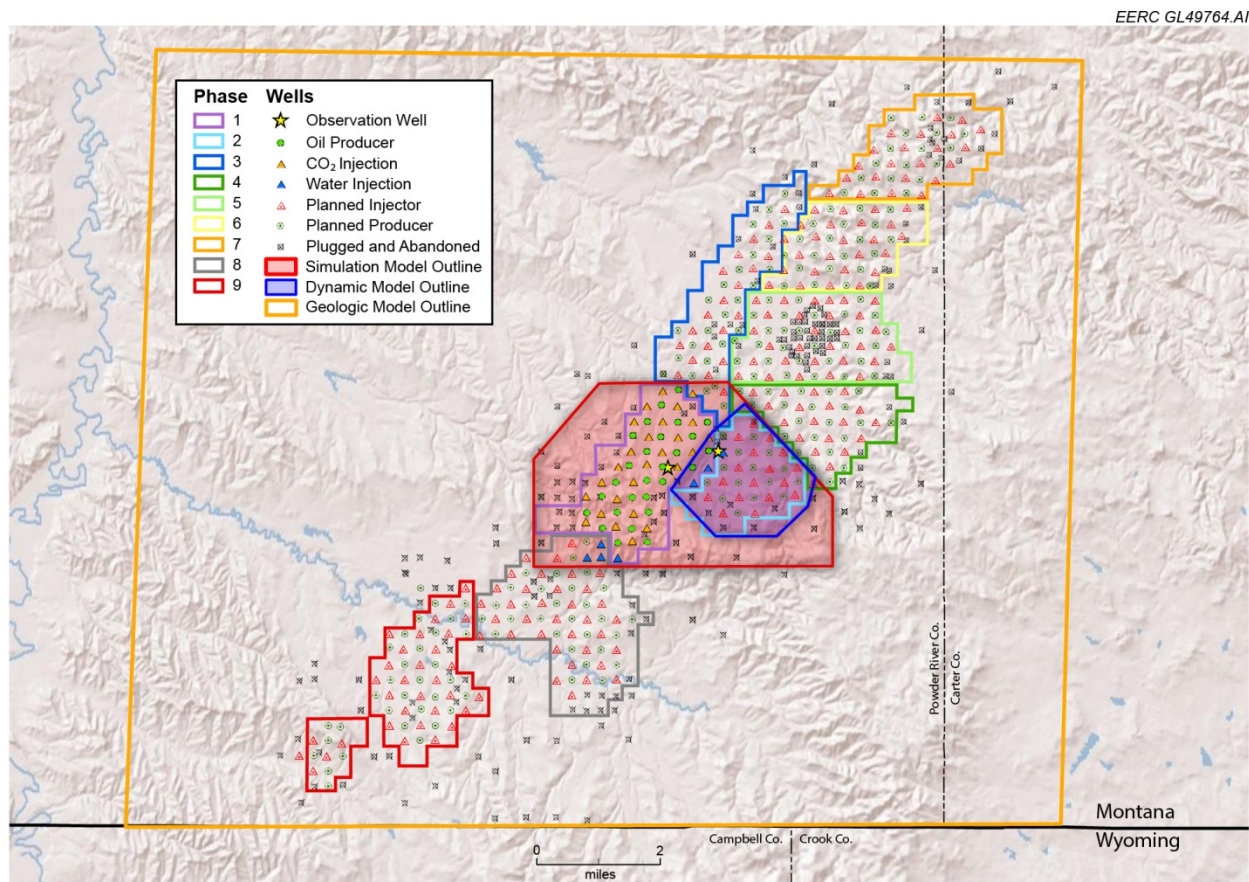


Figure B-1. Map showing the geologic model boundary (orange), the dynamic model boundary (blue), and their relation to the planned Bell Creek project development phases.

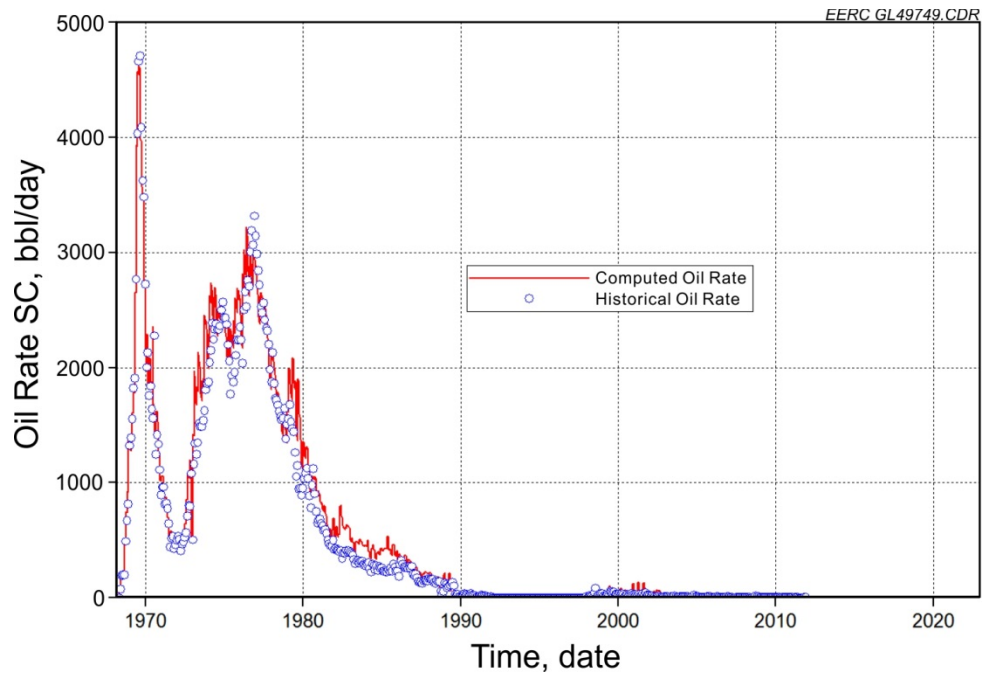


Figure B-2. History-matching results for Phase 2 oil rate, where the circles represent the field data and the solid line represents the simulation results.

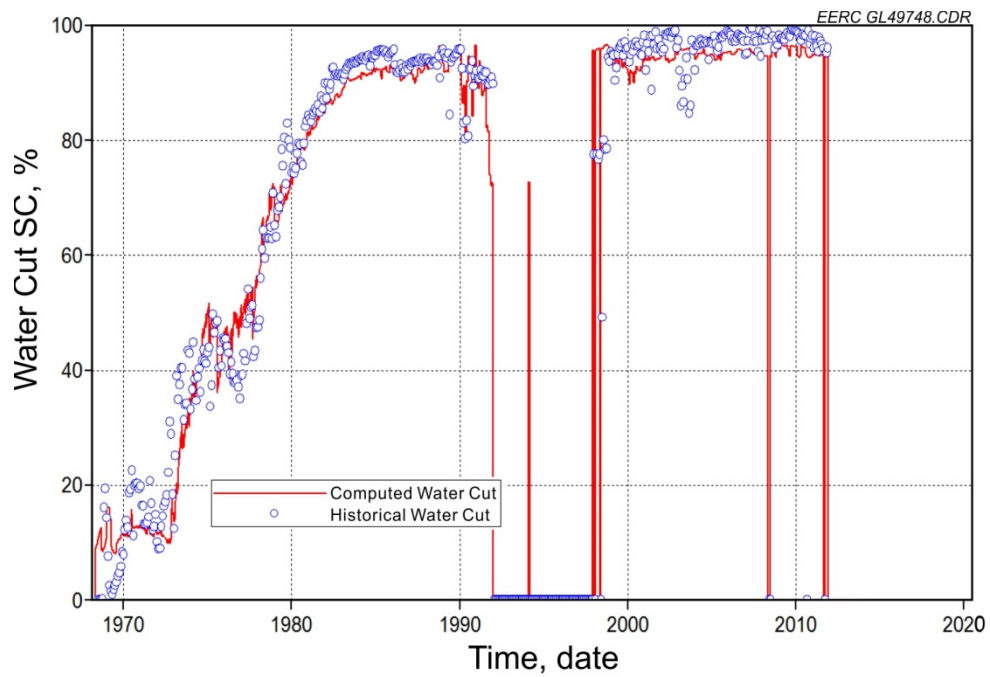


Figure B-3. History-matching results for Phase 2 water cut, where the circles represent the field data and the solid line represents the simulation results.

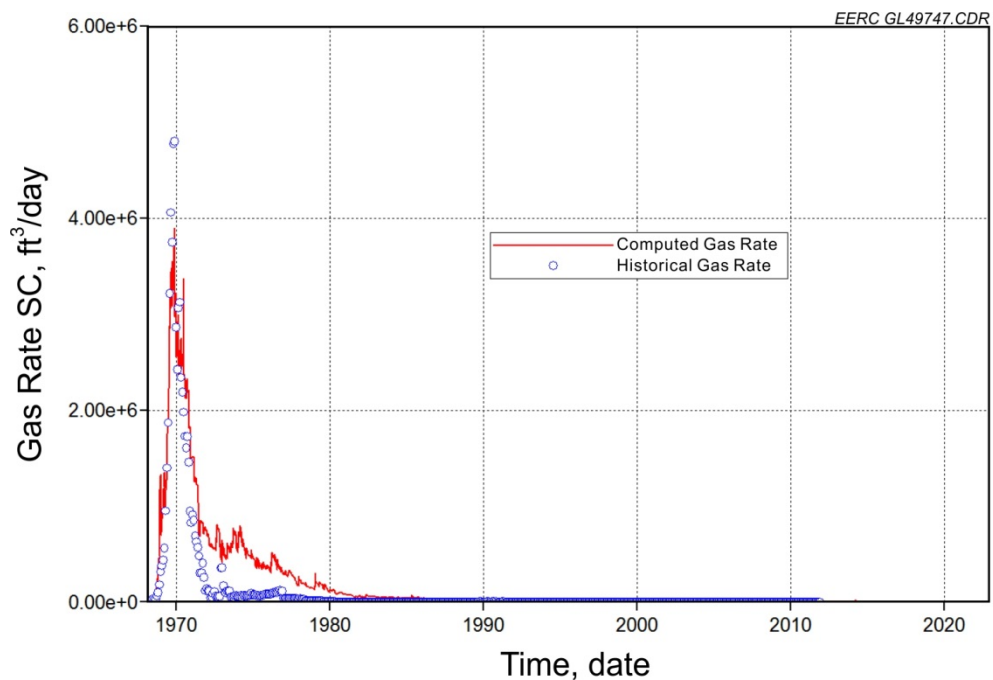


Figure B-4. History-matching results for Phase 2 gas production rate, where the circles represent the field data and the solid line represents the simulation results.

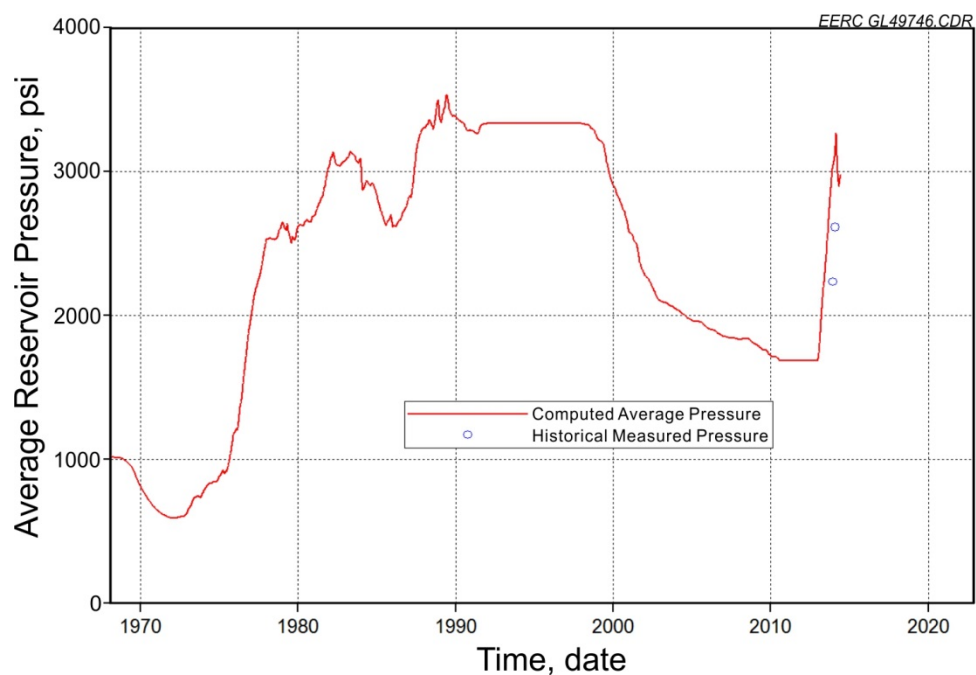


Figure B-5. Average reservoir pressure over the reservoir's history in Phase 2, where the circles represent the field data and the solid line represents the simulation results.

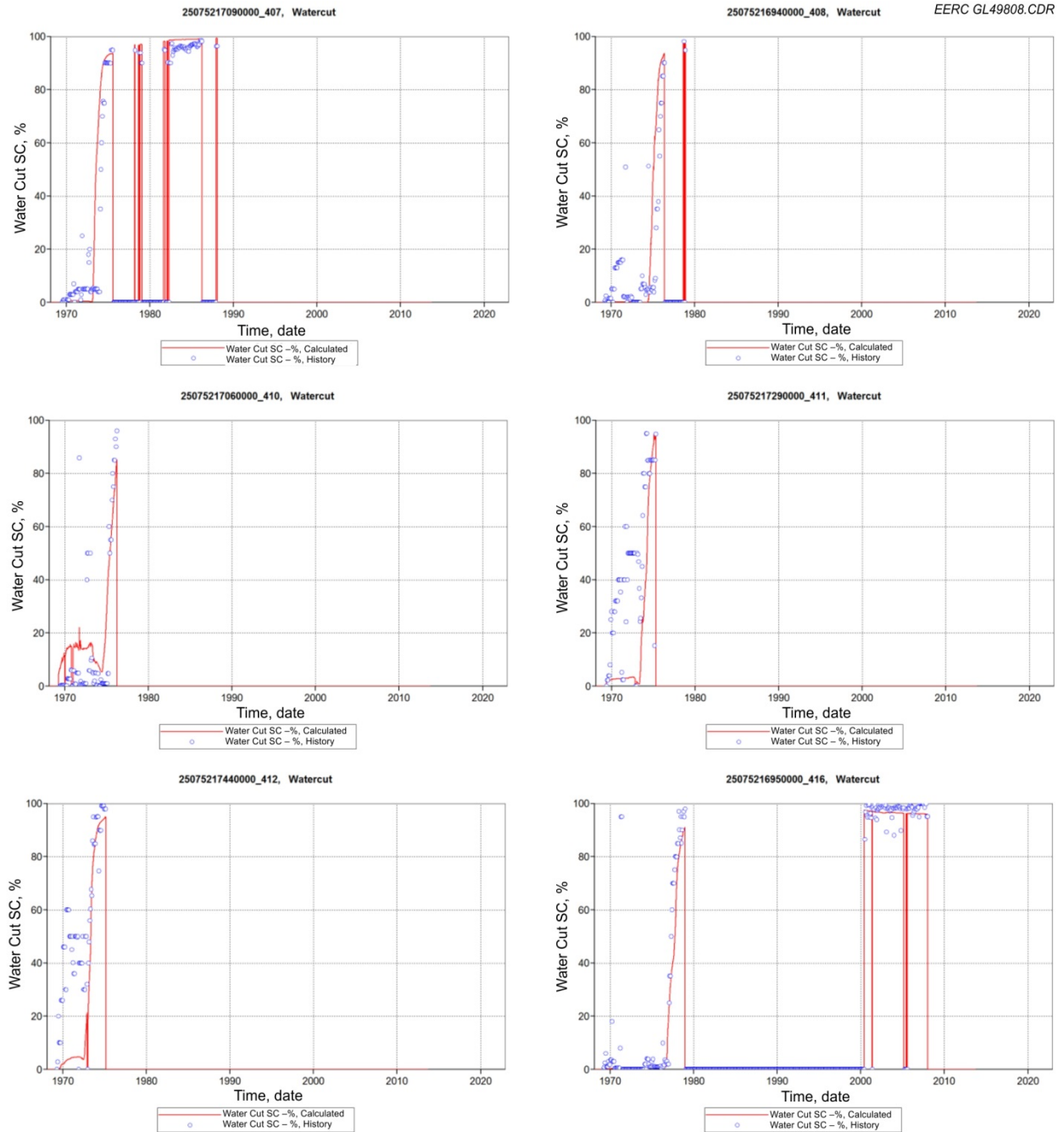


Figure B-6. Water cut matching for individual wells, where the circles represent the field data and the solid line represents the simulation results.

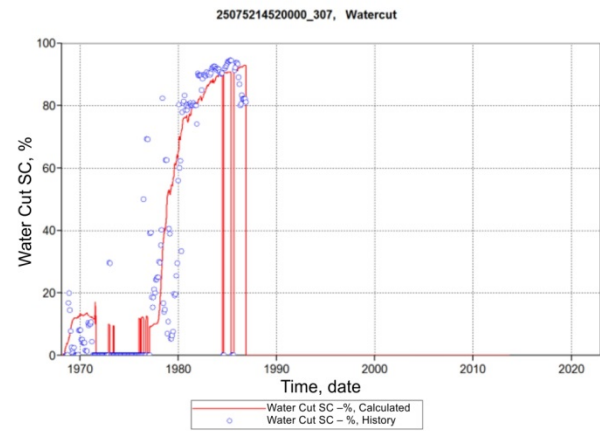
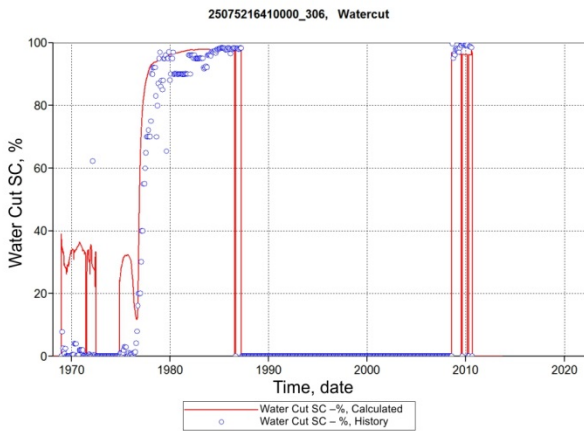
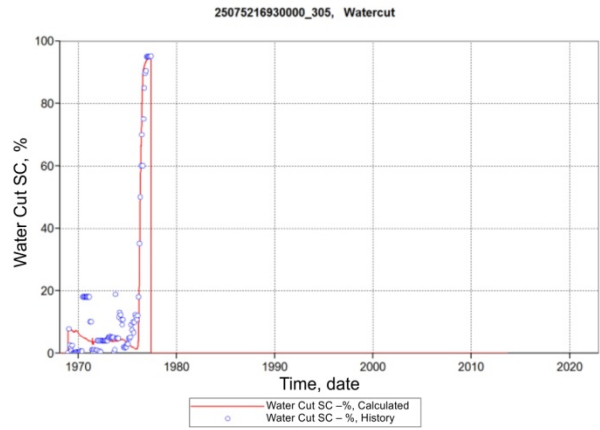
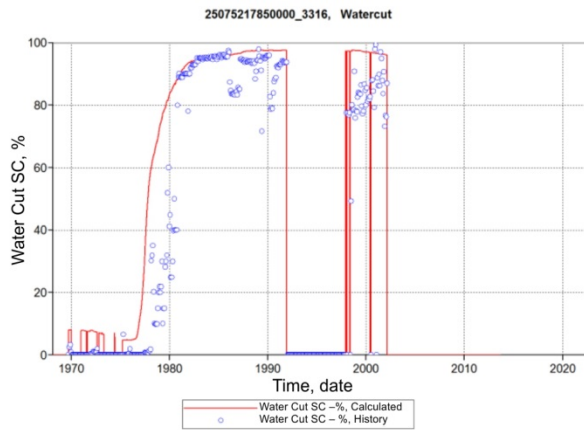
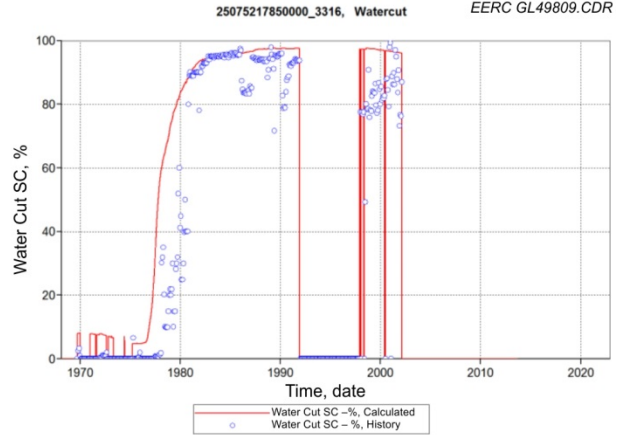
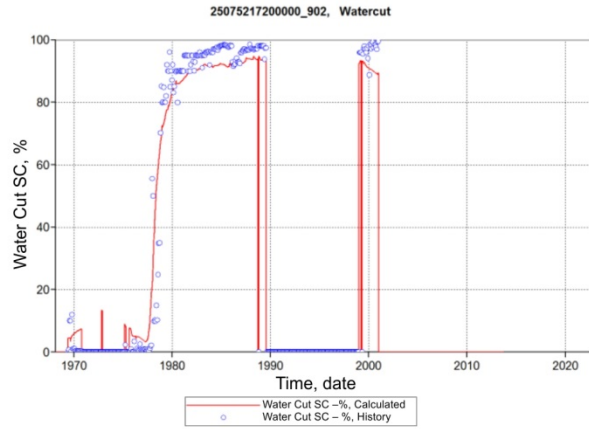


Figure B-7. Water cut matching for individual wells, where the circles represent the field data and the solid line represents the simulation results.

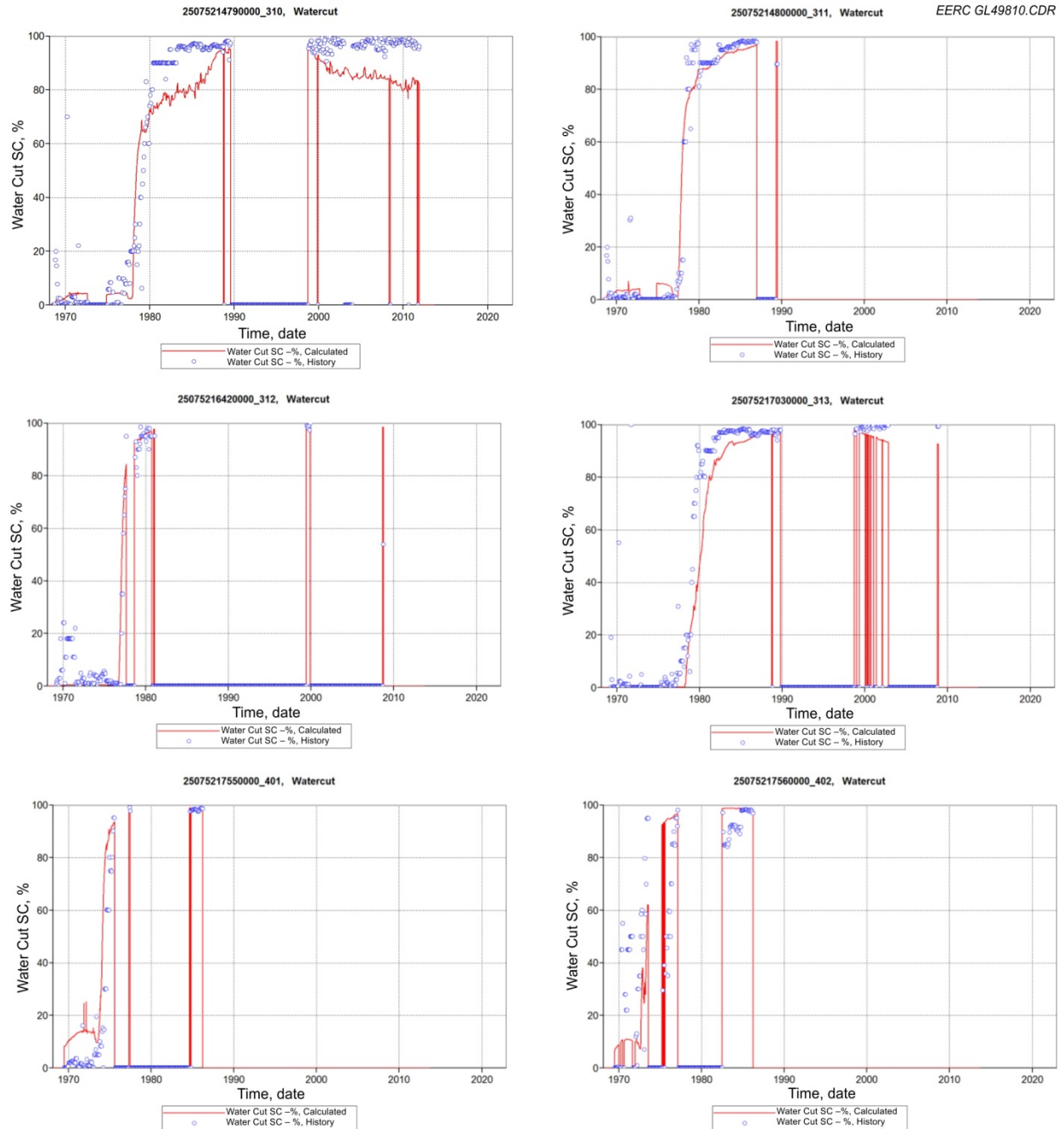


Figure B-8. Water cut matching for individual wells, where the circles represent the field data and the solid line represents the simulation results.

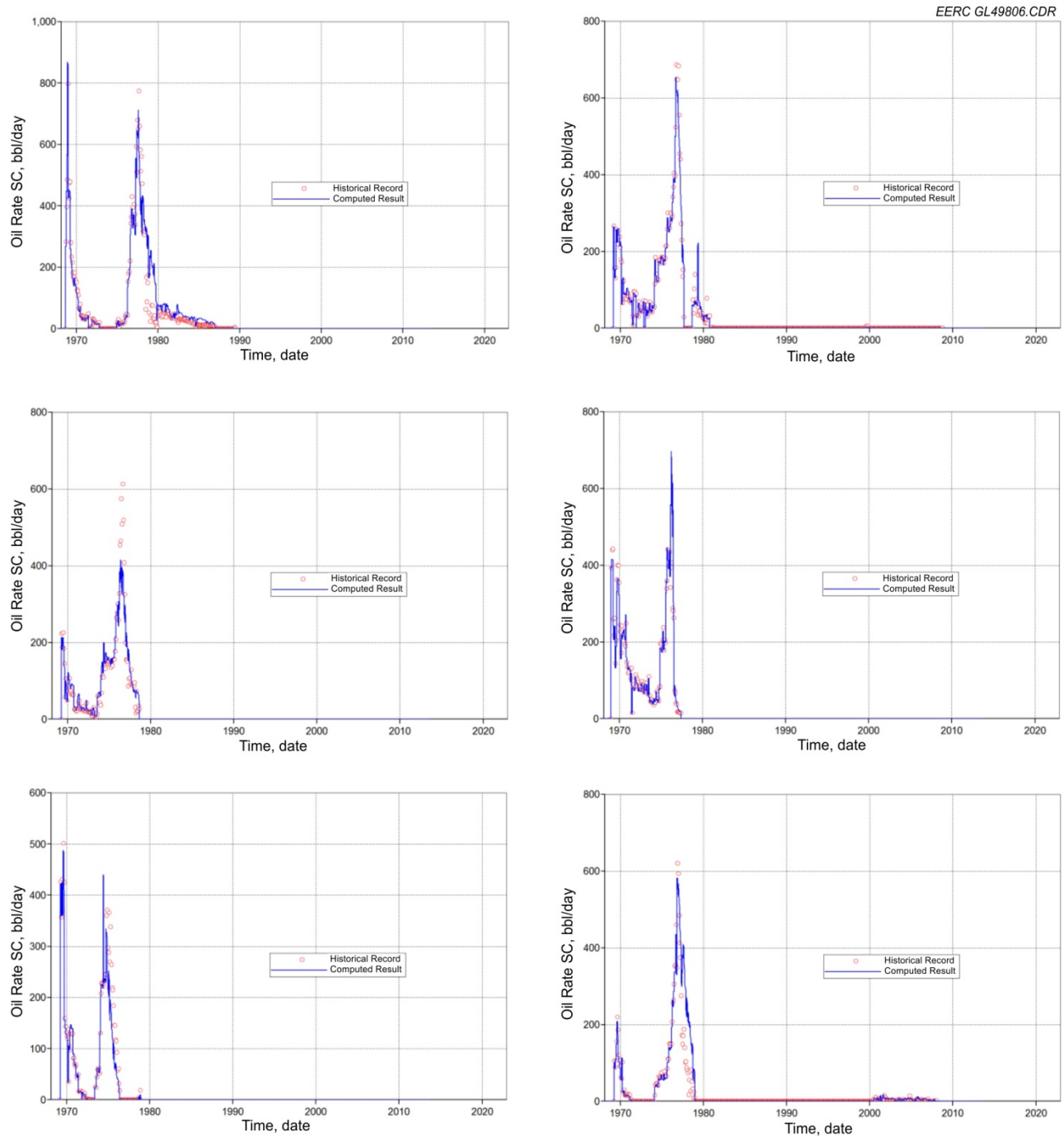


Figure B-9. Oil production rate matching for individual wells, where the circles represent the field data and the solid line represents the simulation results.

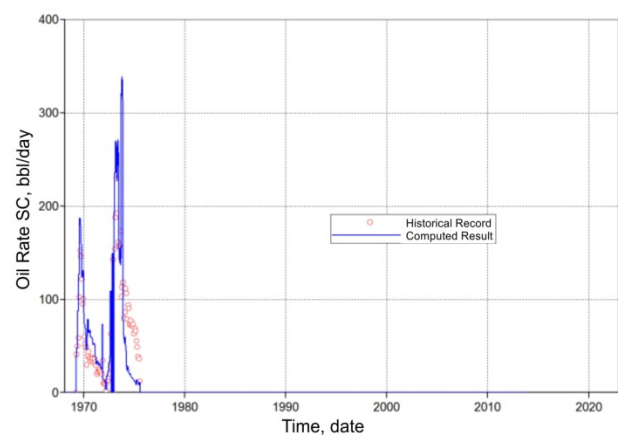
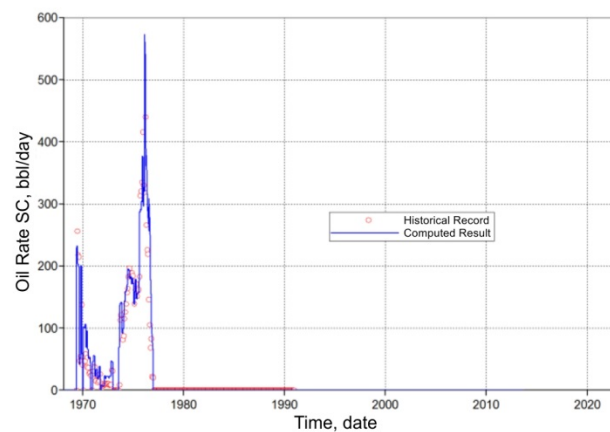
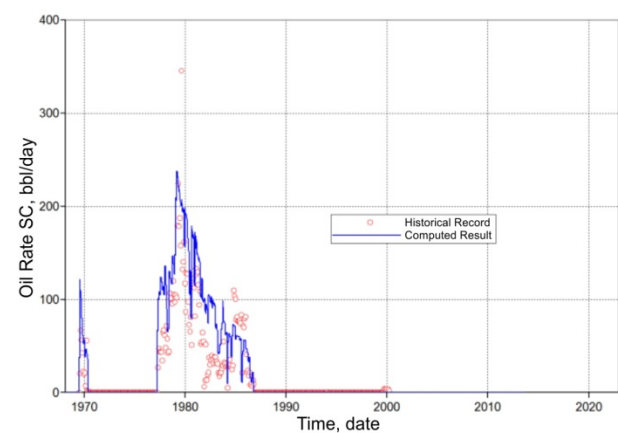
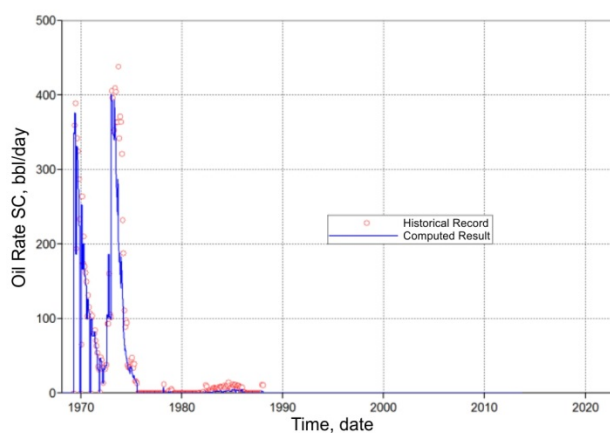
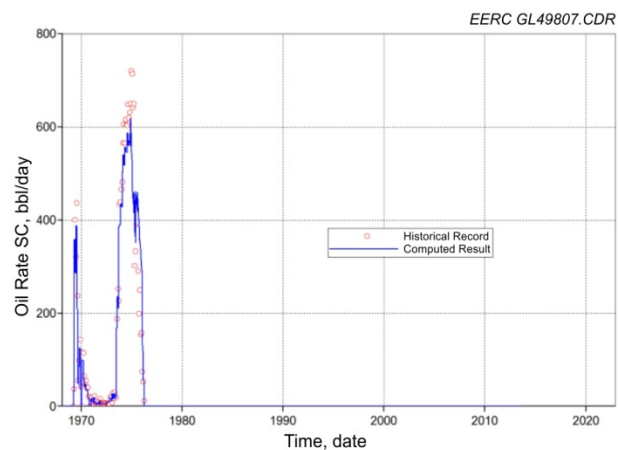
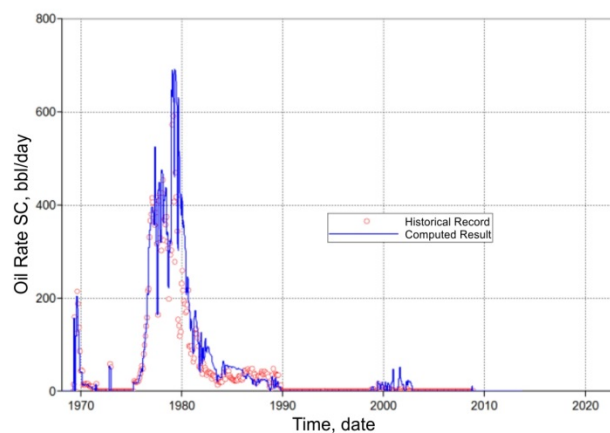


Figure B-10. Oil production rate matching for individual wells, where the circles represent the field data and the solid line represents the simulation results.

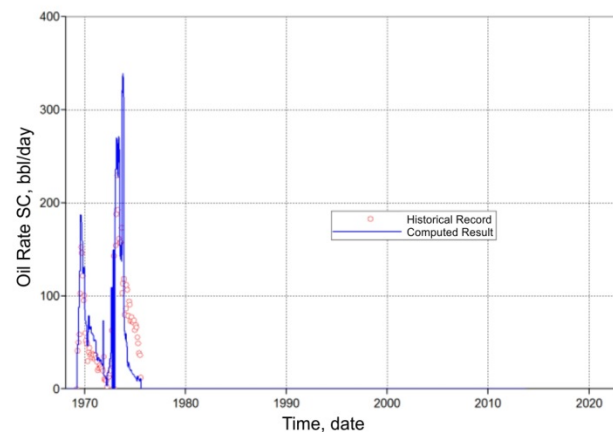
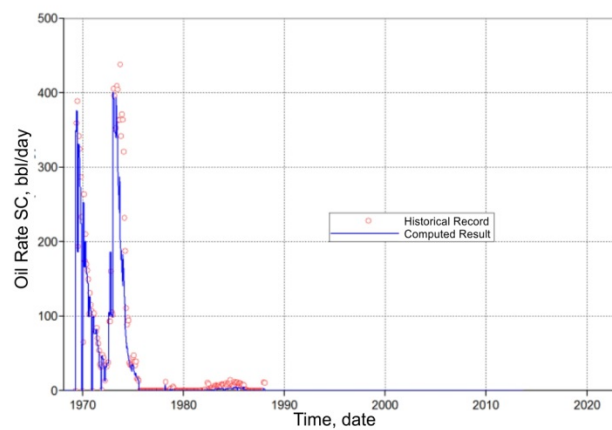
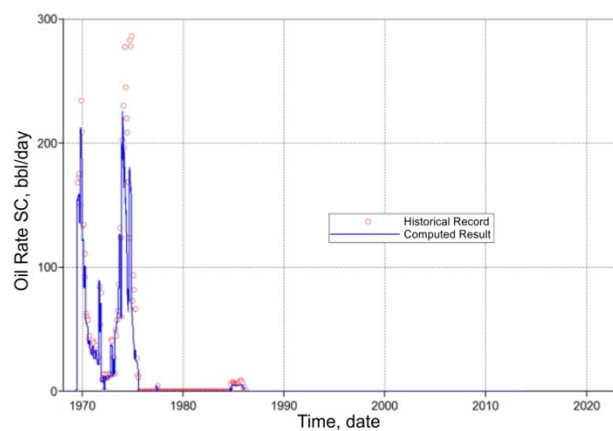
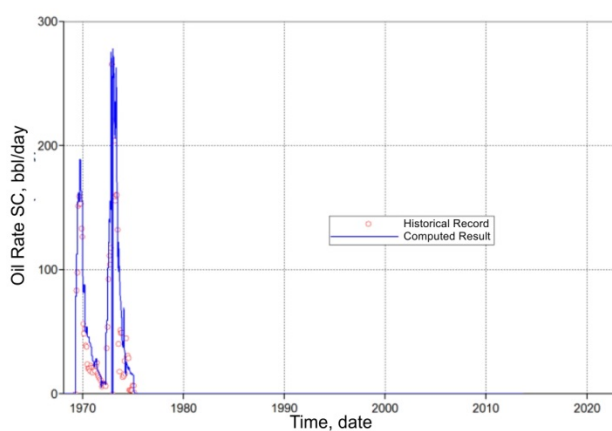
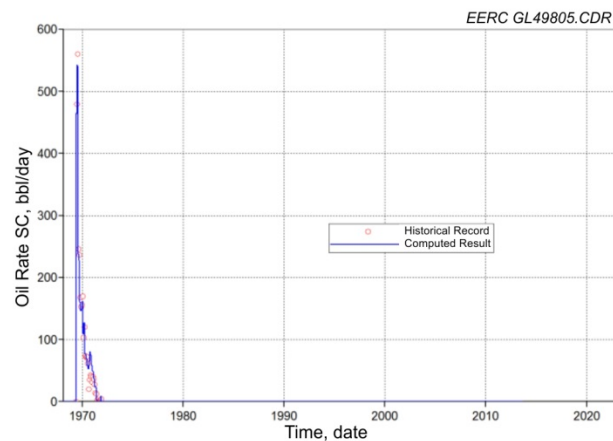
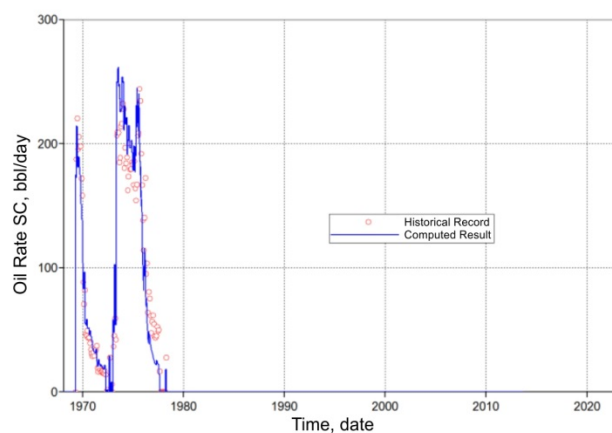


Figure B-11. Oil production rate matching for individual wells, where the circles represent the field data and the solid line represents the simulation results.

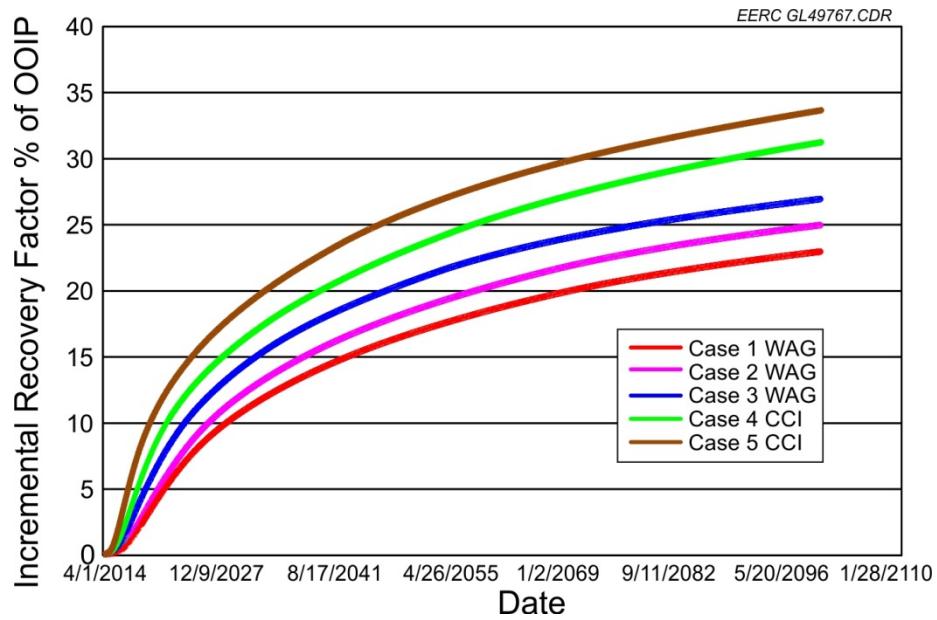


Figure B-12. Incremental oil recovery over time for all five cases.

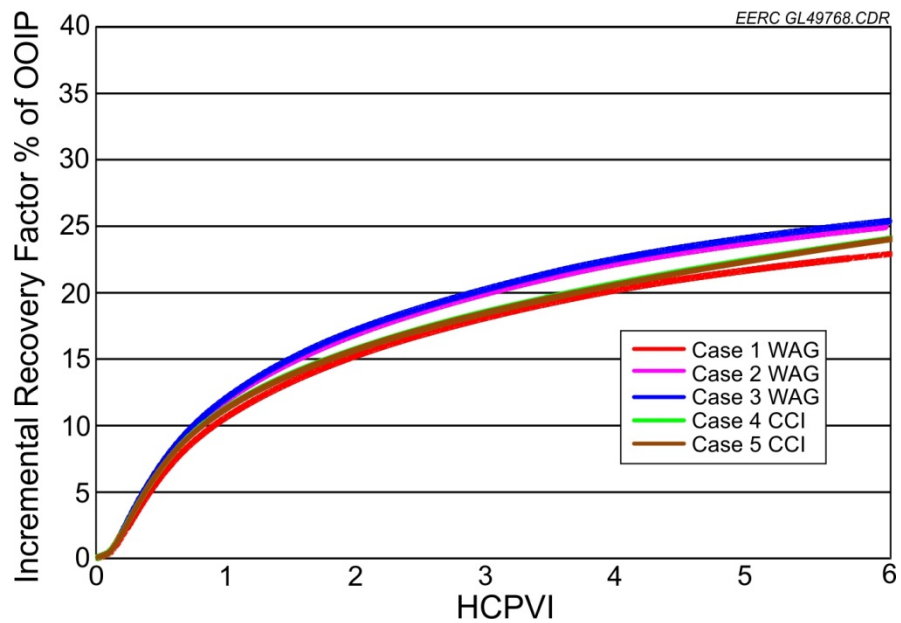


Figure B-13. Incremental oil recovery over HCPVI for all five cases.

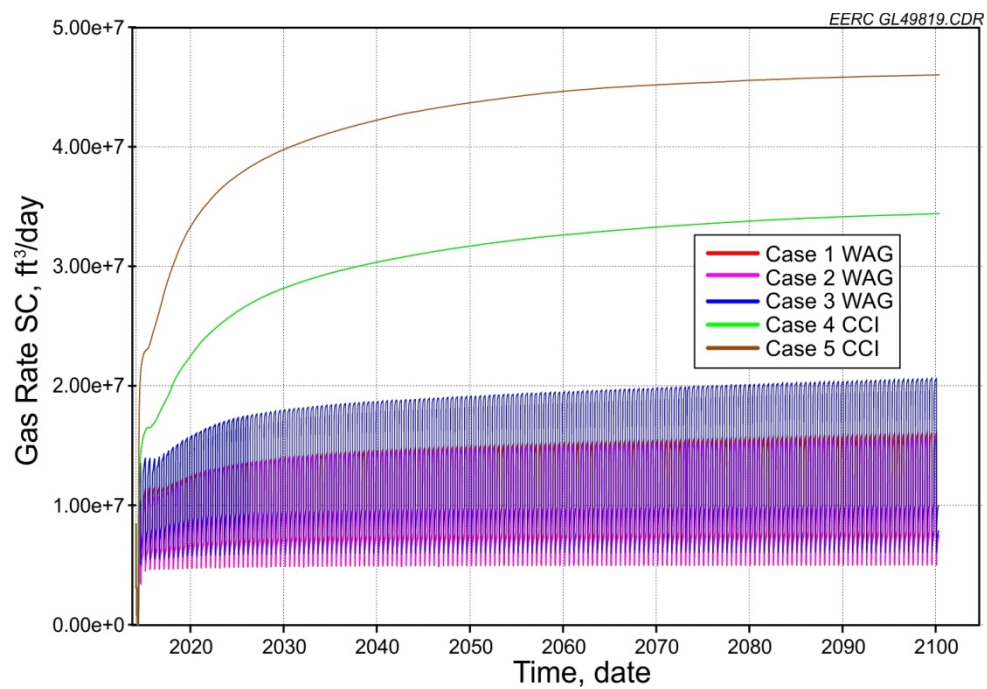


Figure B-14. Daily injected CO₂ for all five cases.

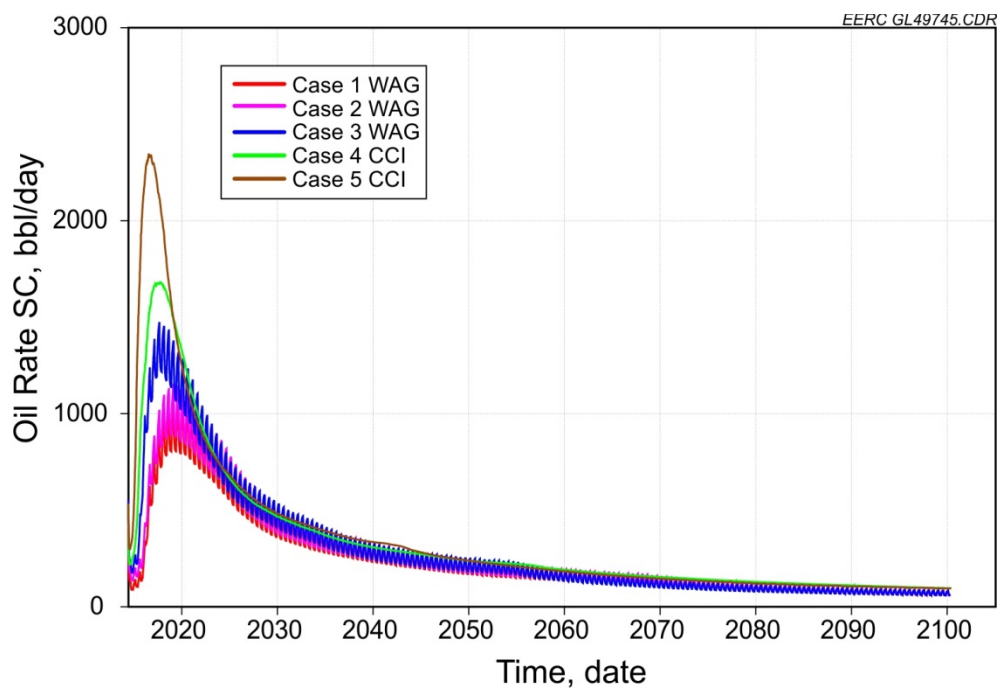


Figure B-15. Oil rates for all five cases.

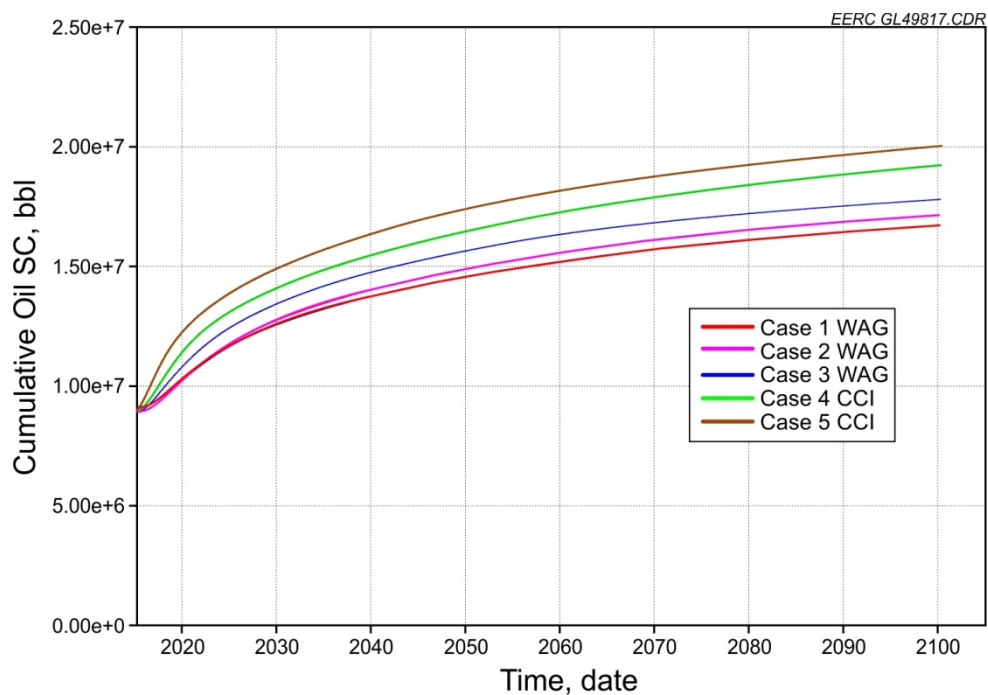


Figure B-16. Cumulative oil production for all five cases.

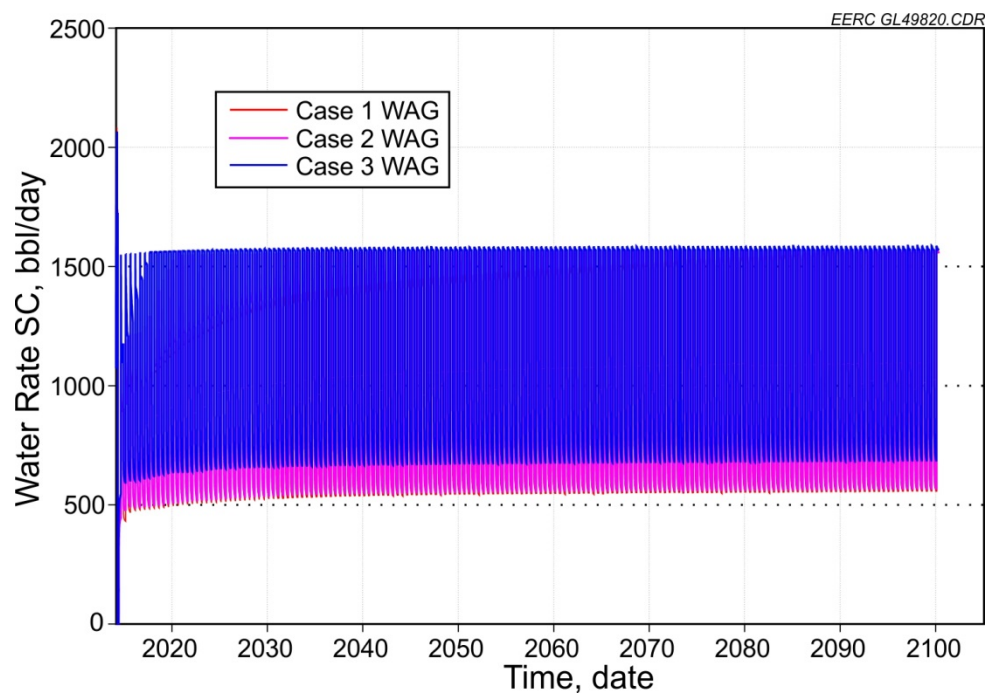


Figure B-17. Water injection rate for all WAG cases.

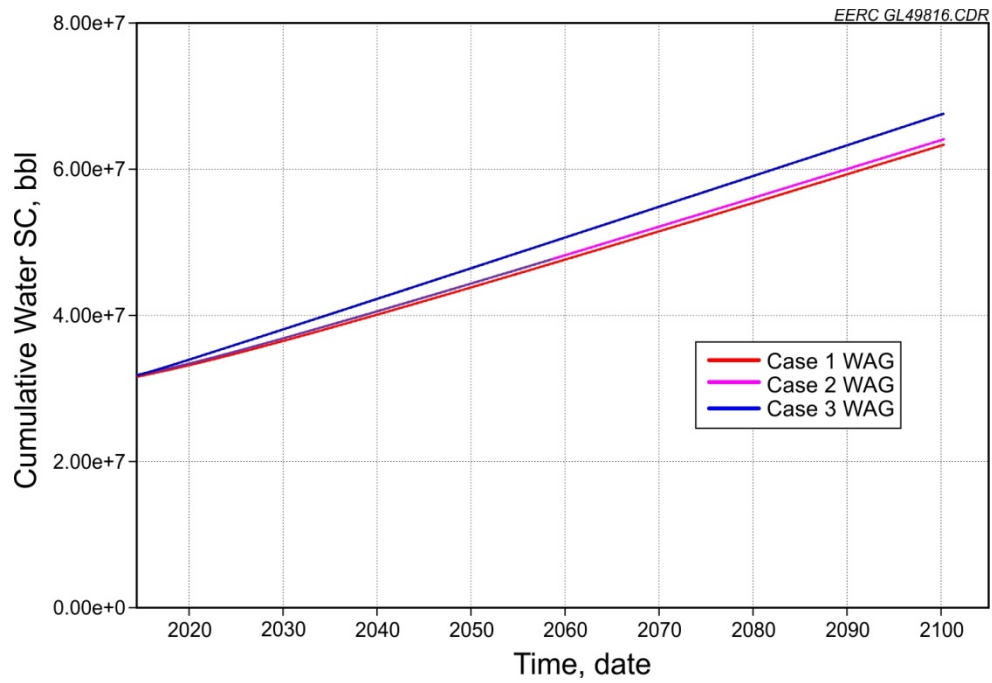


Figure B-18. Cumulative water injection for all WAG cases.

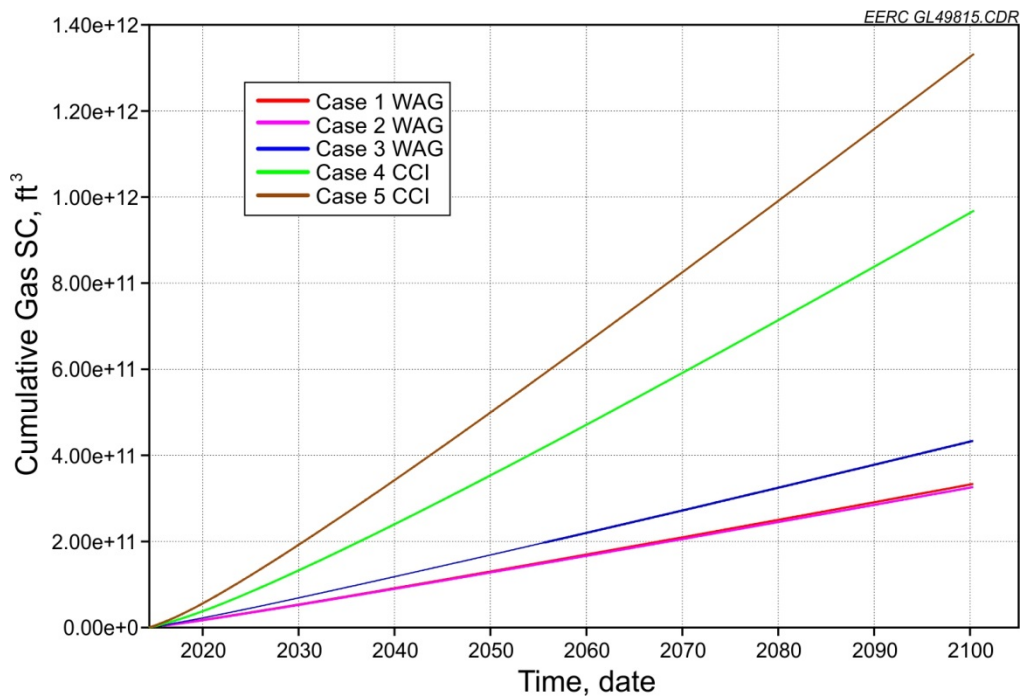


Figure B-19. Cumulative CO₂ injection for all five cases.

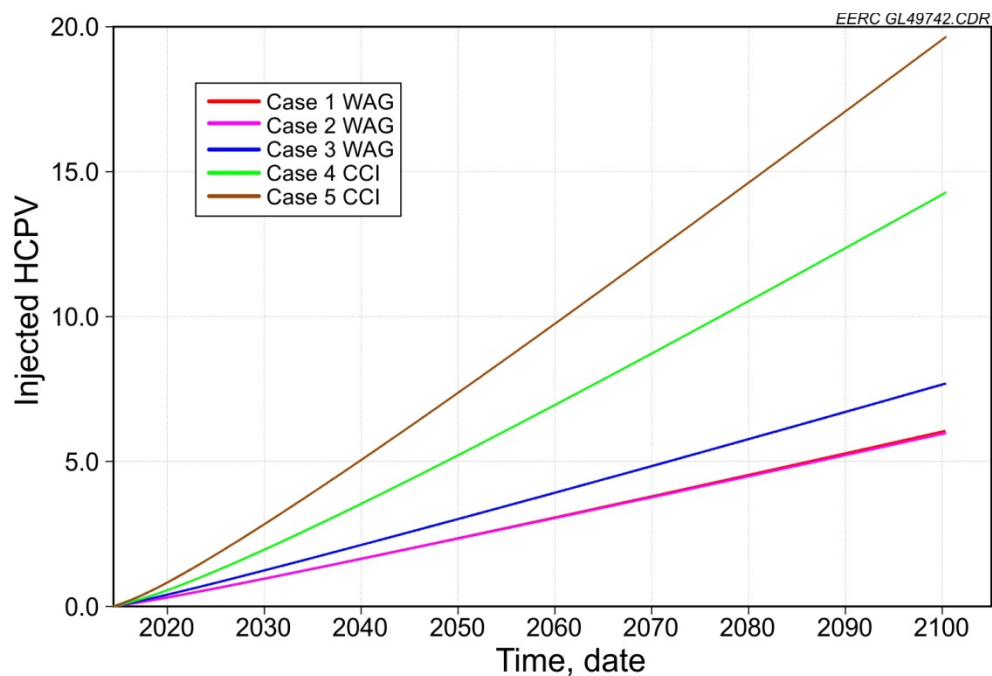


Figure B-20. Cumulative HCPVI (injected water and CO₂) for WAG and CCI scenarios for four cases.

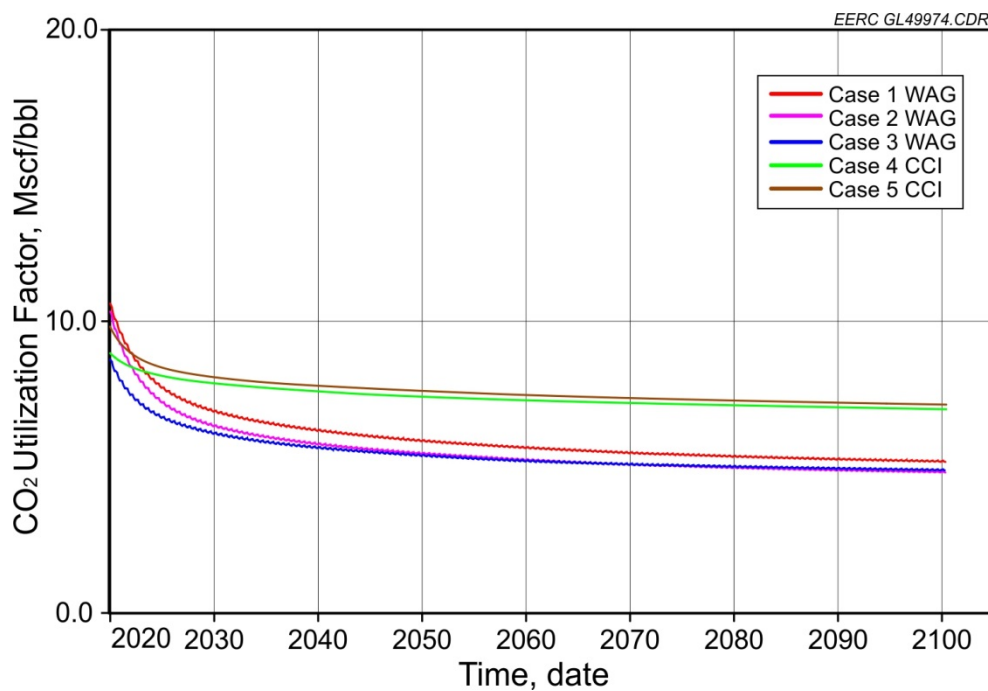


Figure B-21. Cumulative CO₂ utilization factors for all five cases.

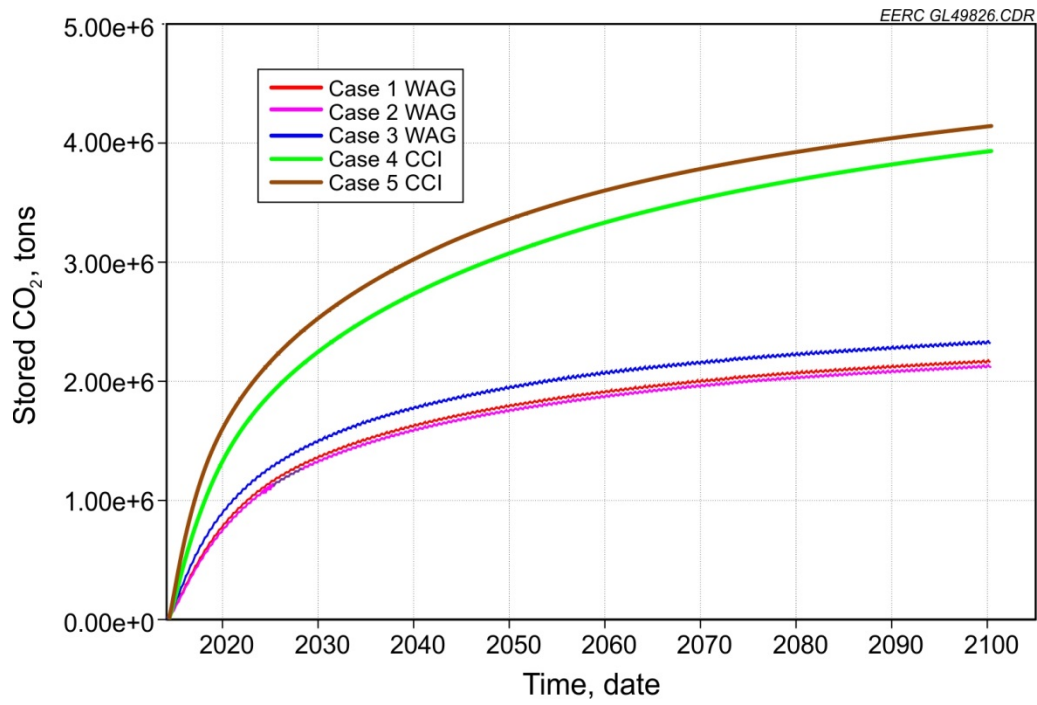


Figure B-22. CO₂ storage capacity for all five cases.

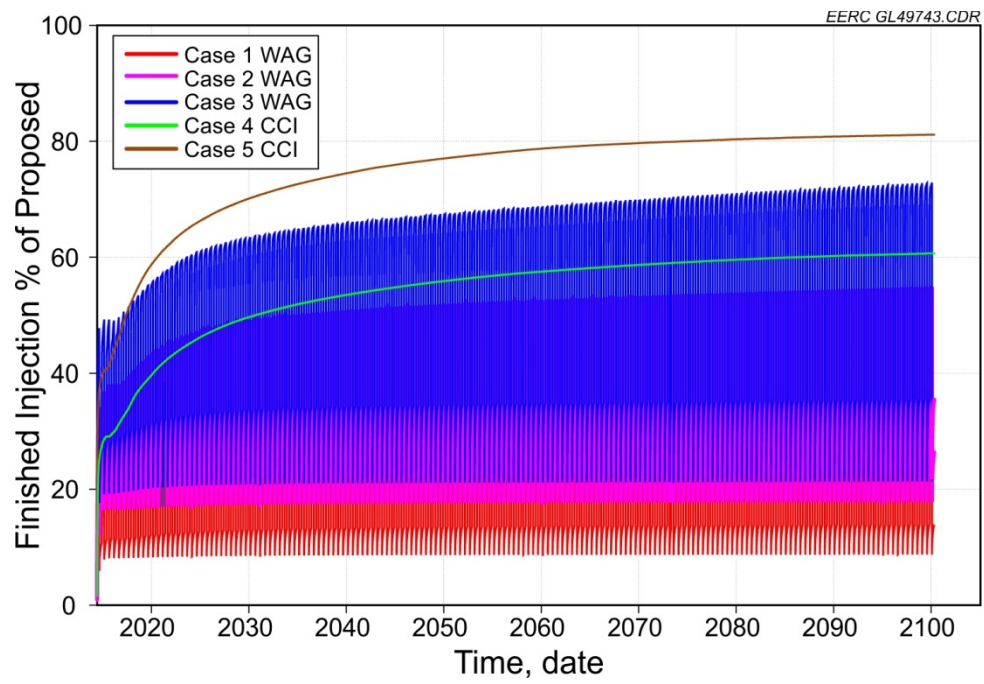


Figure B-23. Completion percentage for proposed CO₂ injection.

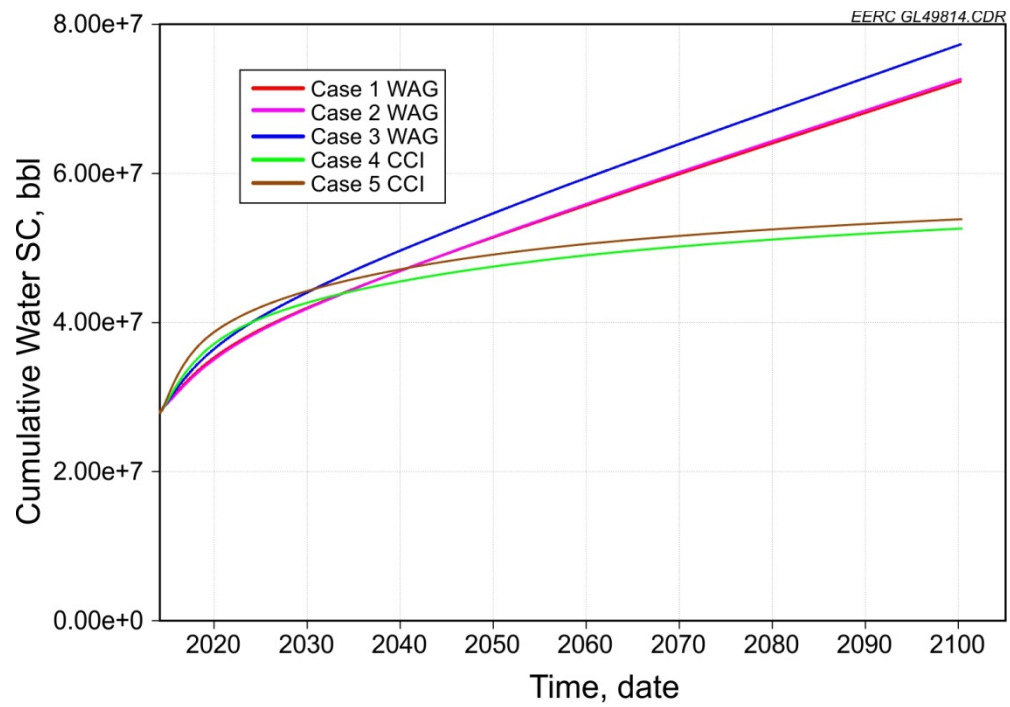


Figure B-24. Cumulative water production for all five cases.

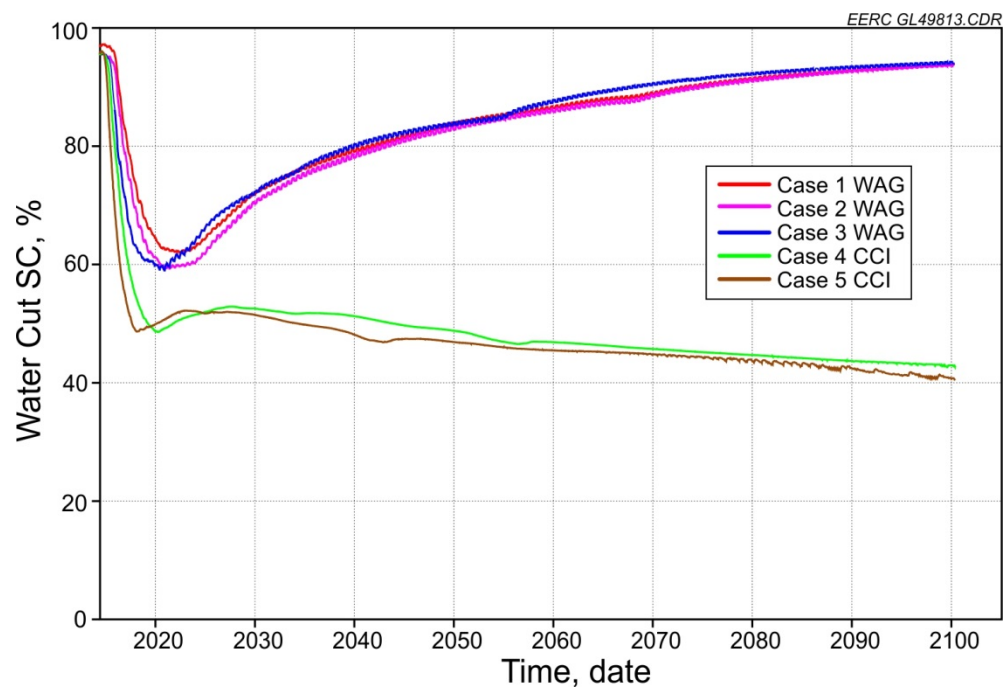


Figure B-25. Water cut for all five cases.

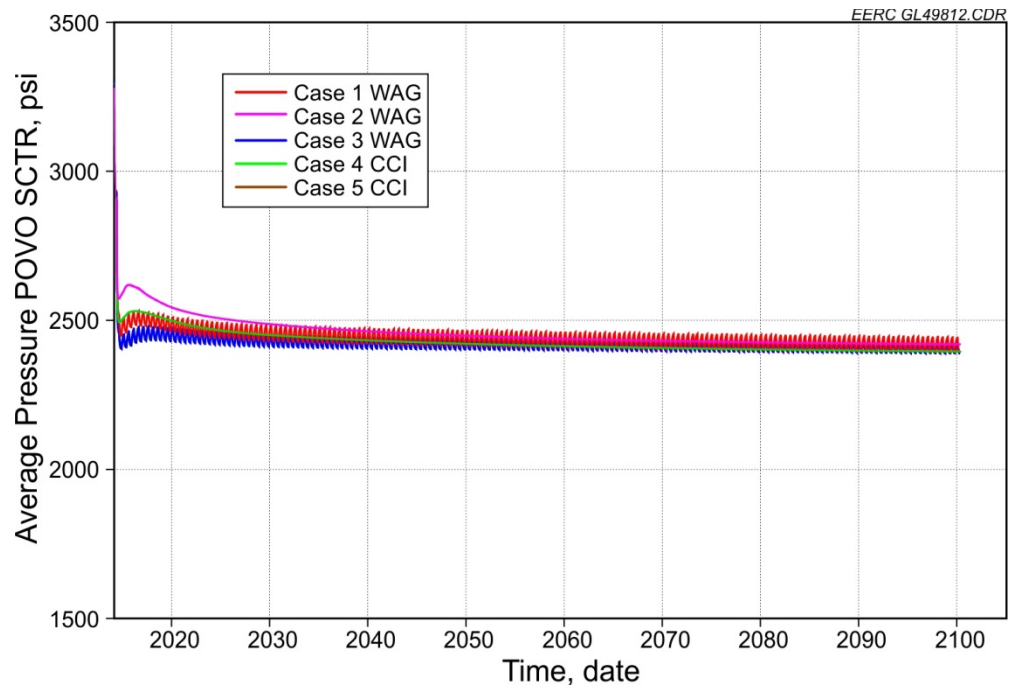


Figure B-26. Average reservoir pressure for all five cases.

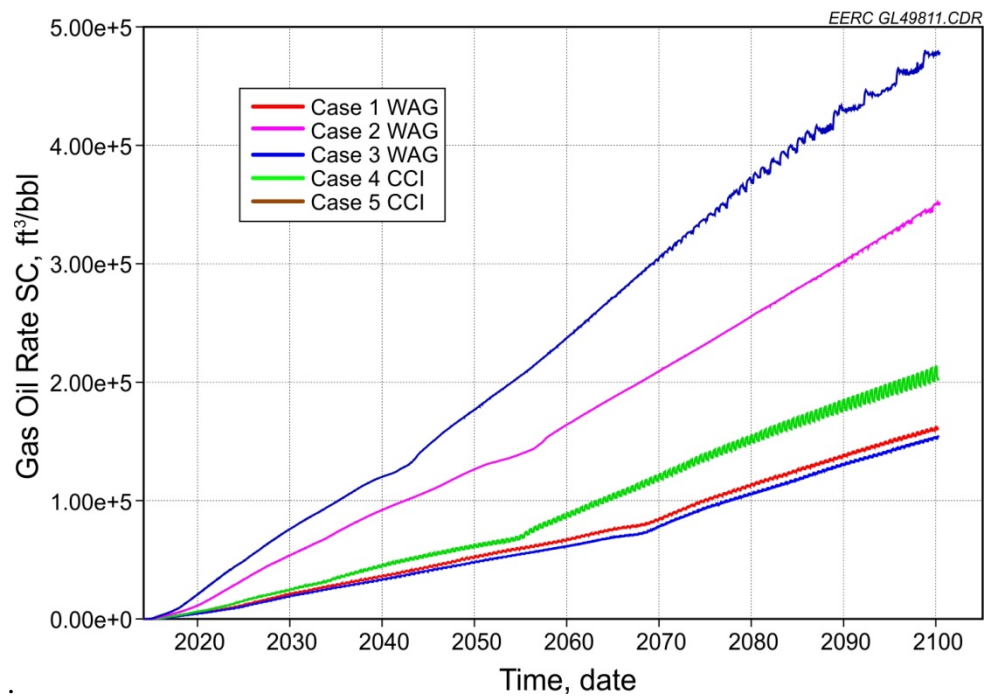


Figure B-27. GOR for all five cases.

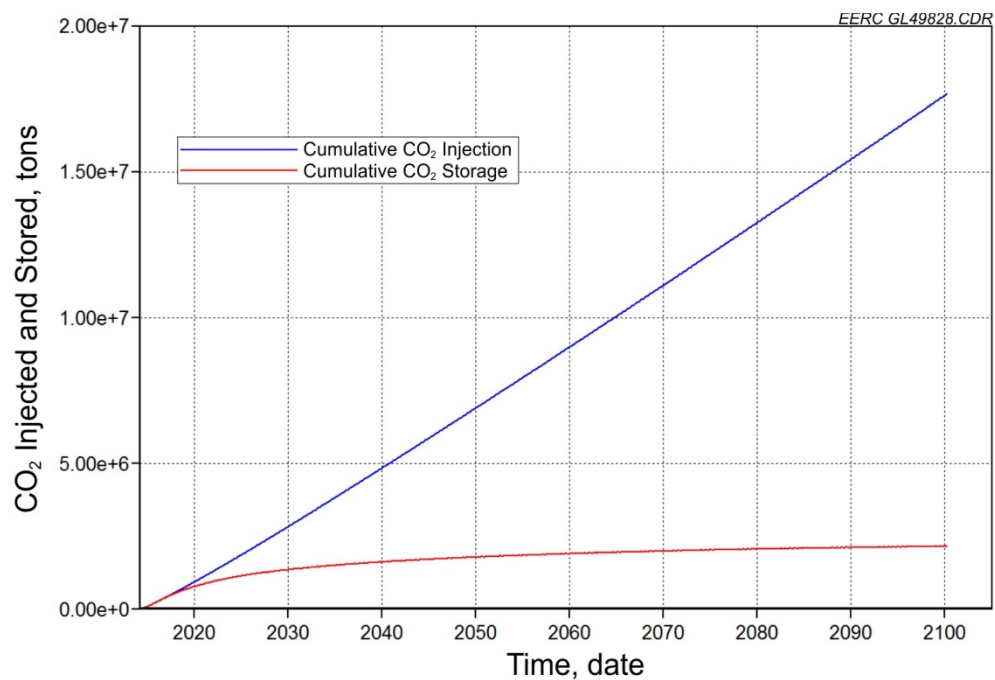


Figure B-28. Cumulative CO₂ injected and stored for Case 1.

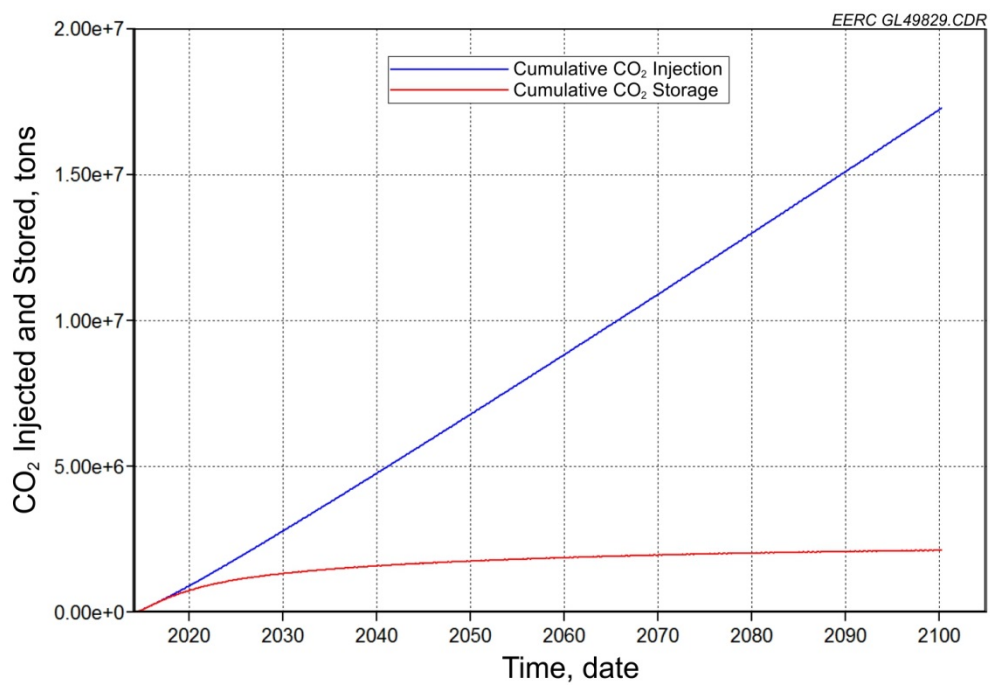


Figure B-29. Cumulative CO₂ injected and stored for Case 2.

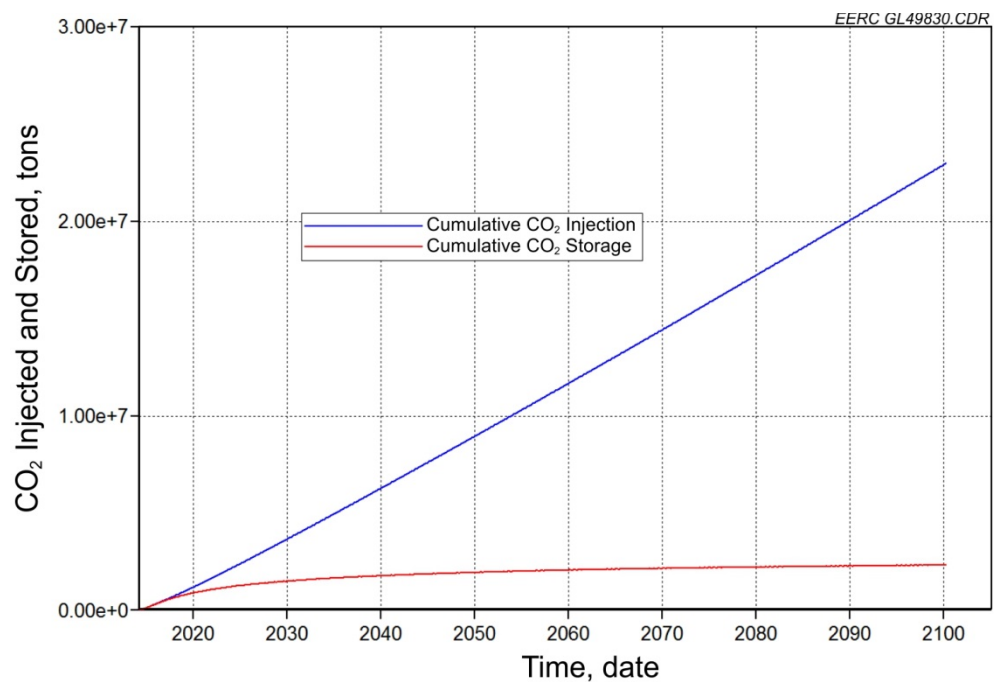


Figure B-30. Cumulative CO₂ injected and stored for Case 3.

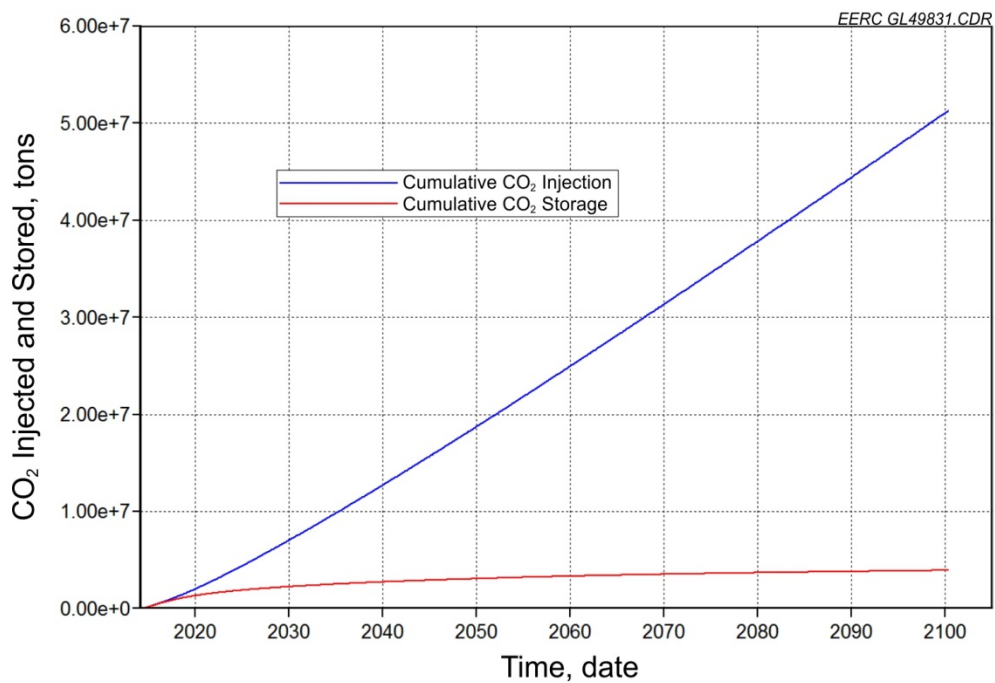


Figure B-31. Cumulative CO₂ injected and stored for Case 4.

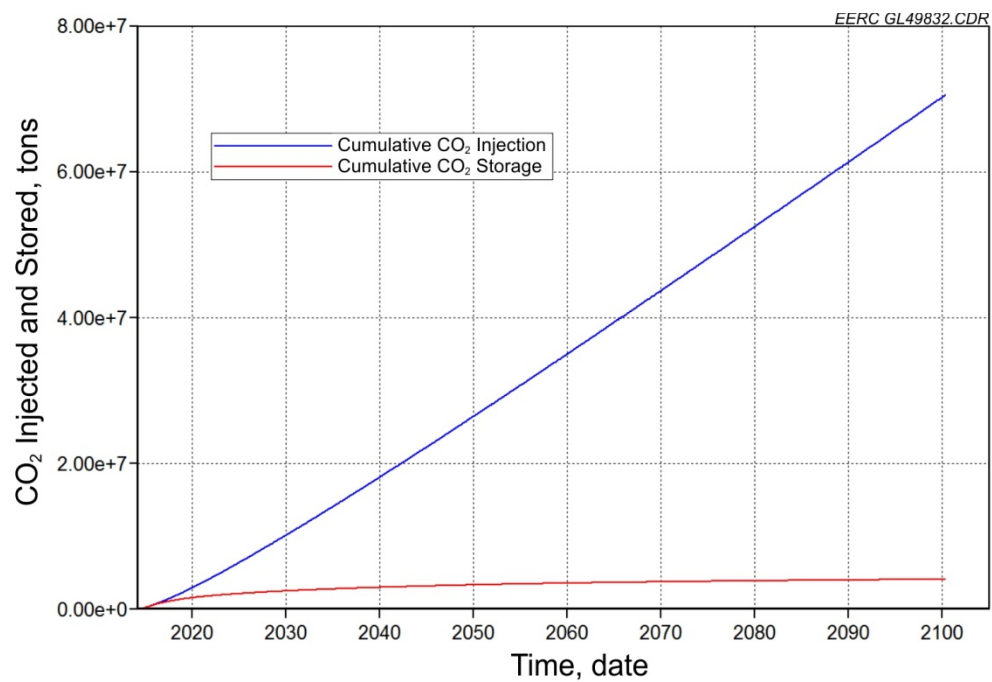


Figure B-32. Cumulative CO₂ injected and stored for Case 5.

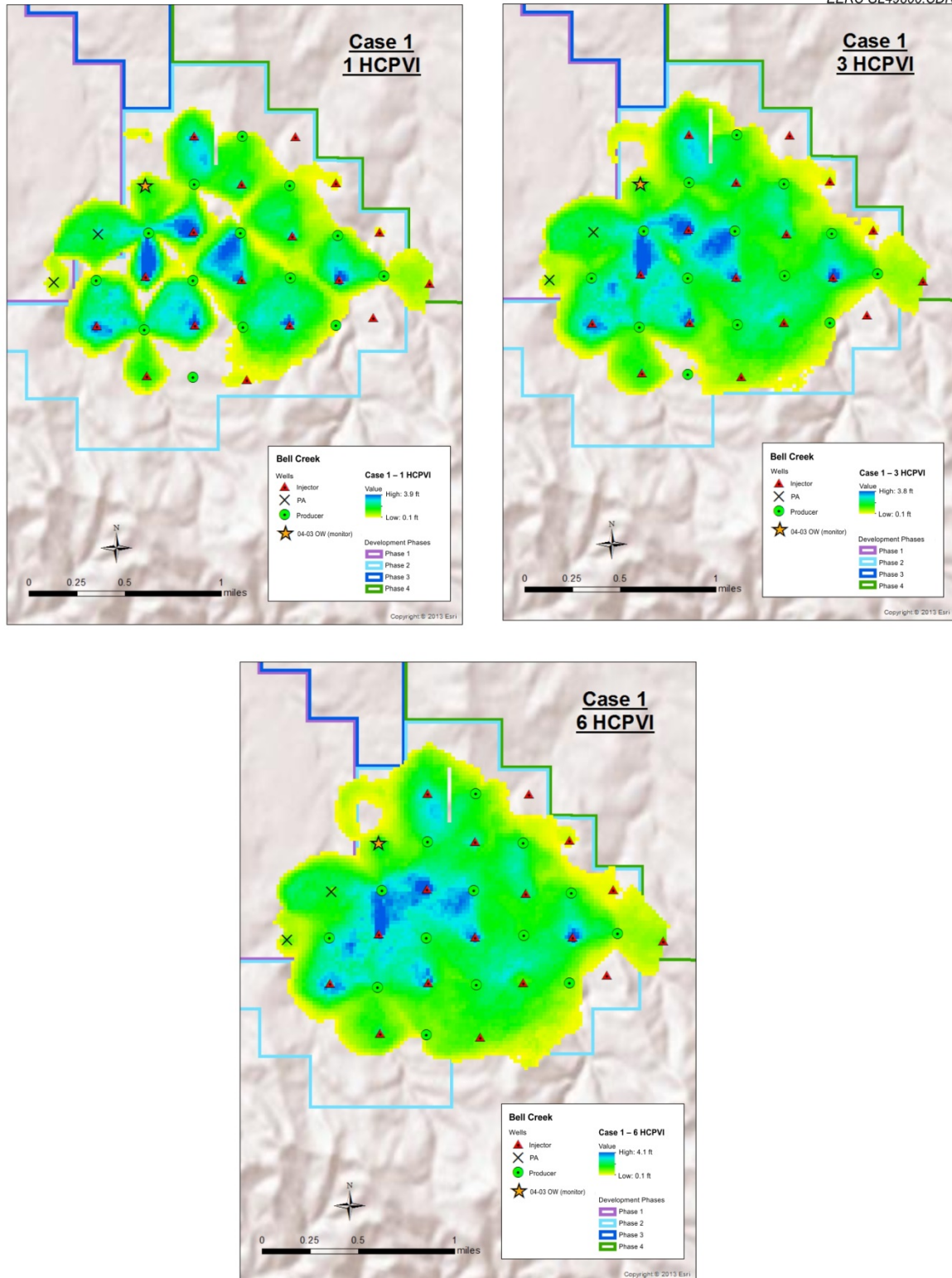


Figure B-33. Case 1 CO₂ plume at 1, 3, and 6 HCPVI.

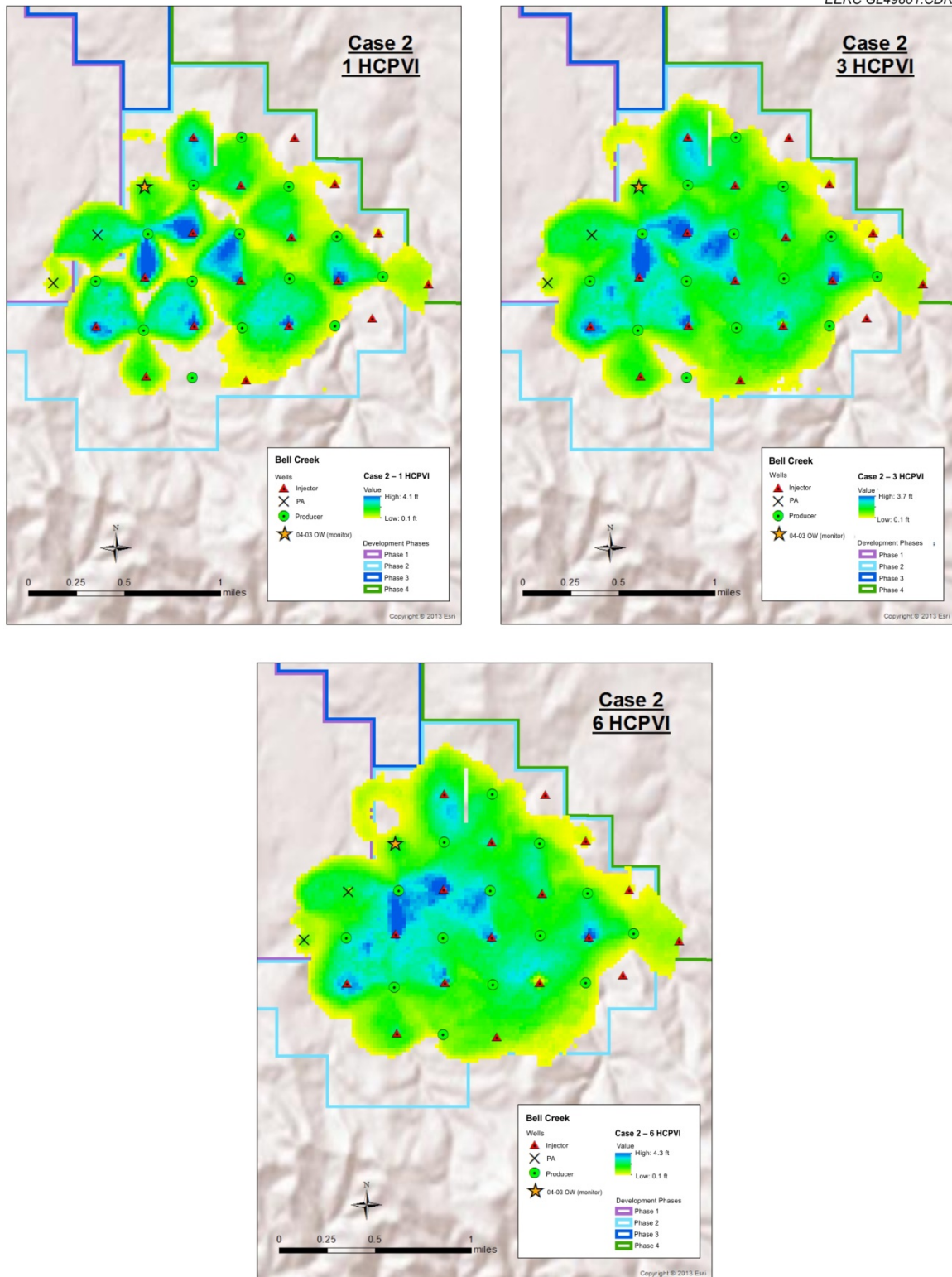


Figure B-34. Case 2 CO₂ plume at 1, 3, and 6 HCPVI.

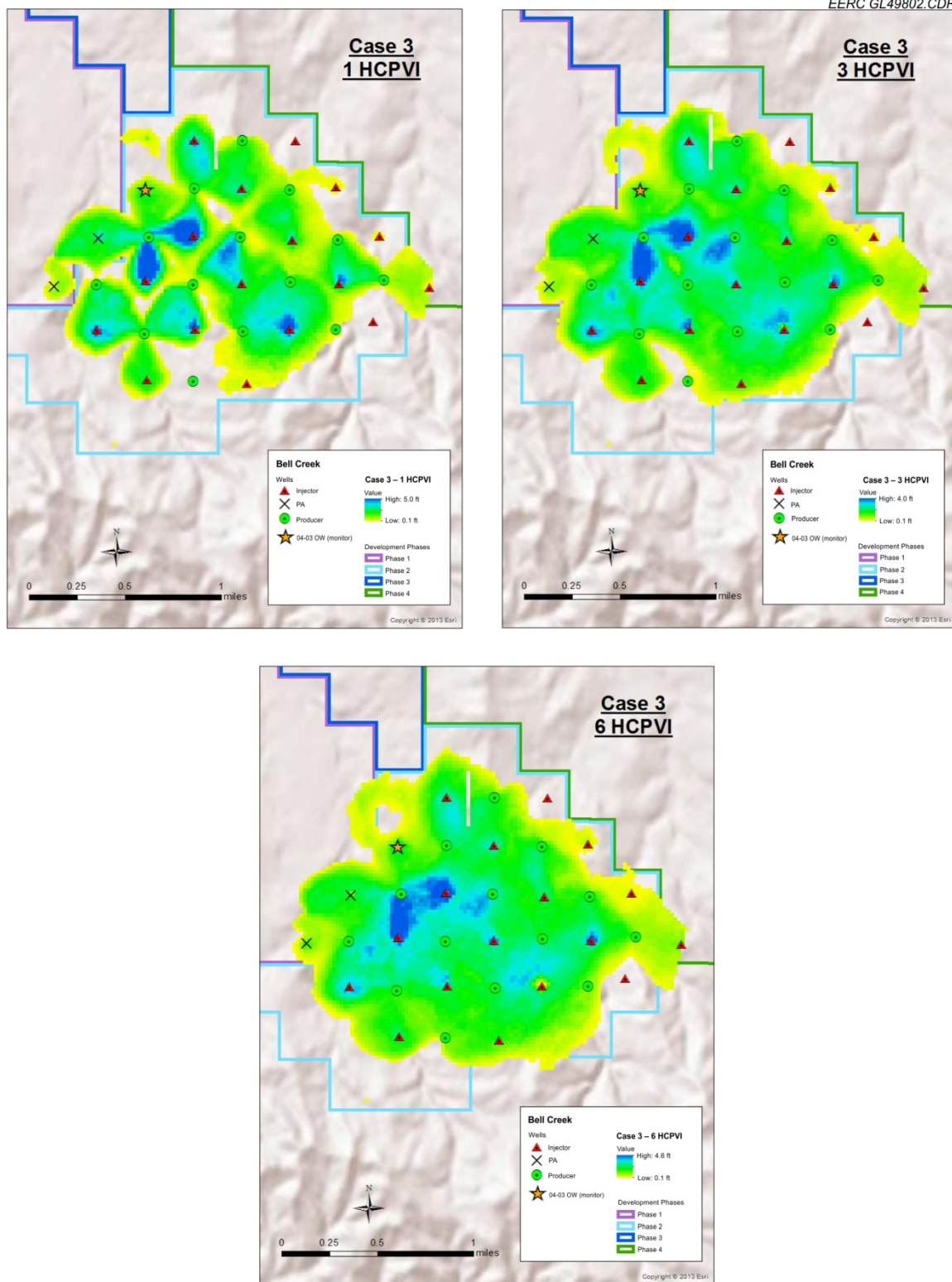


Figure B-35. Case 3 CO₂ plume at 1, 3, and 6 HCPVI.

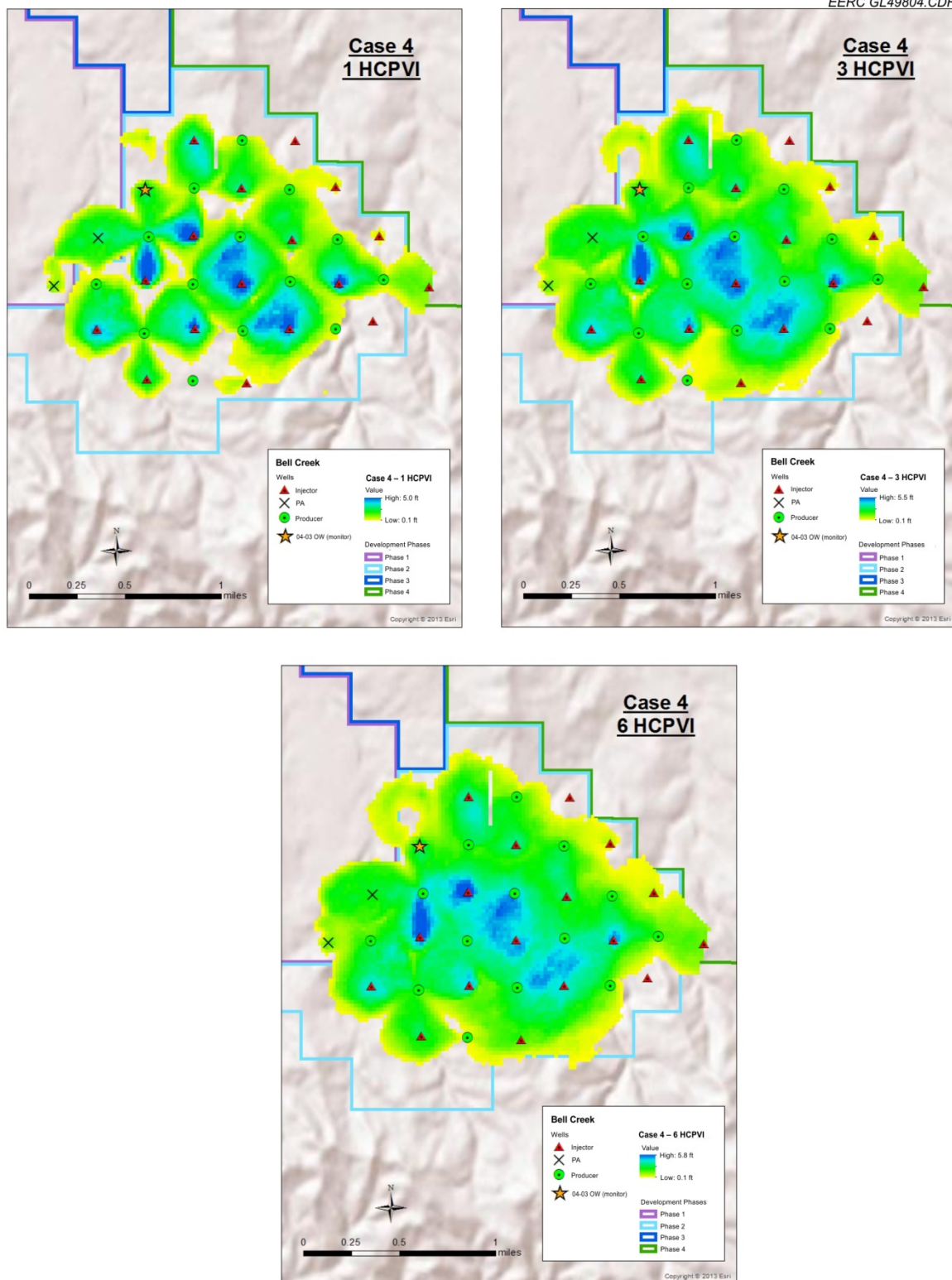
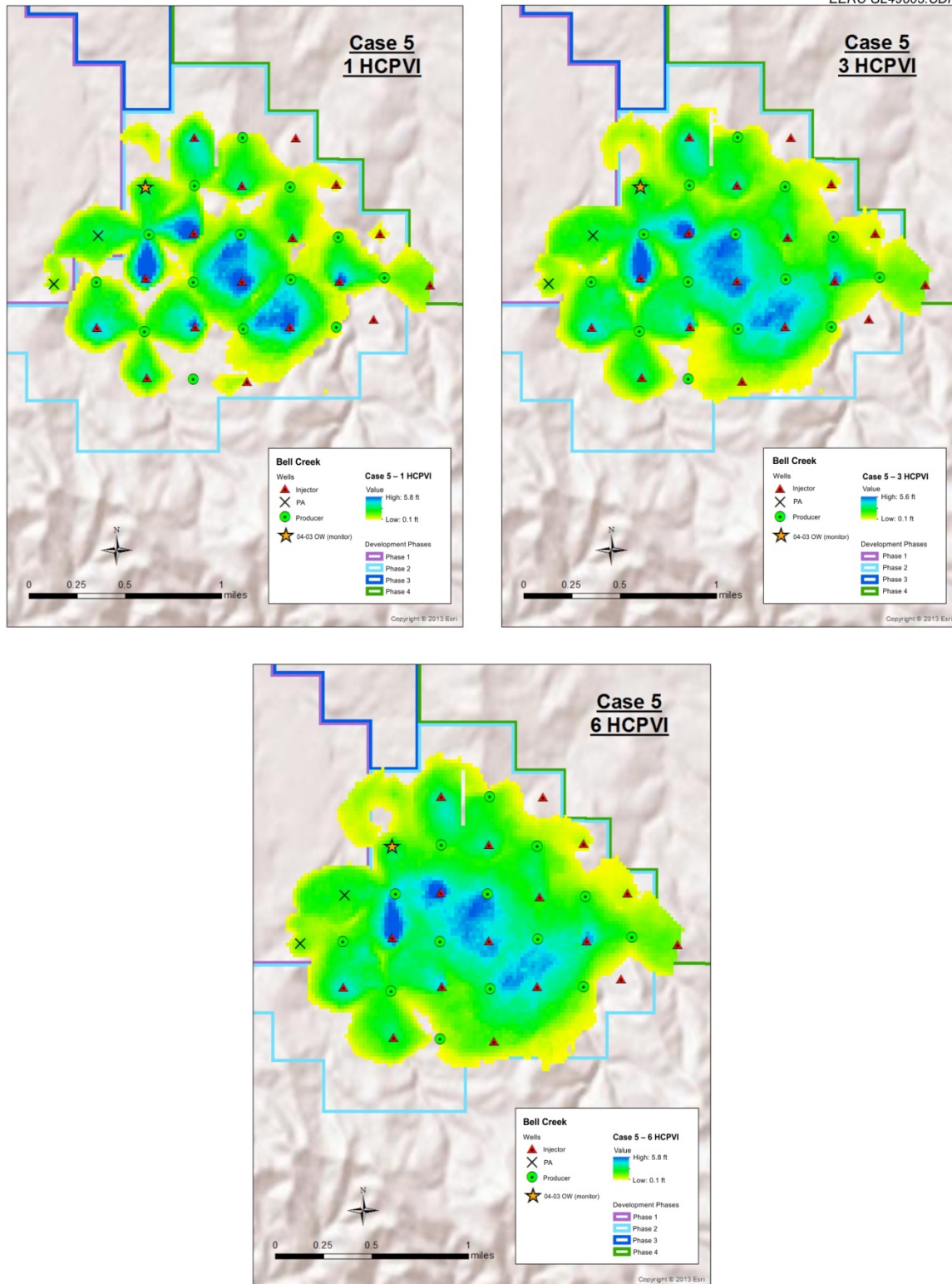


Figure B-36. Case 4 CO₂ plume at 1, 3, and 6 HCPVI.

Figure B-37. Case 5 CO₂ plume at 1, 3, and 6 HCPVI.